INTERNATIONAL ATOMIC ENERGY AGENCY
UNITED NATIONS EDUCATIONAL, SCIENTIFIC AND CULTURAL ORGANIZATION
INTERNATIONAL CENTRE FOR THEORETICAL PHYSICS
I.C.T.P., P.O. BOX 586, 34100 TRIESTE, ITALY, CABLE: CENTRATOM TRIESTE

SMR.550 - 34

SPRING COLLEGE IN MATERIALS SCIENCE ON

"NUCLEATION, GROWTH AND SEGREGATION IN MATERIALS SCIENCE AND ENGINEERING"

(6 May - 7 June 1991)

BACKGROUND MATERIAL FOR SEMINAR ON

"ORDERING OF VOIDS AND BUBBLES IN IRRADIATED METALS"

V. DUBINKO
Kharkov Institute of Physics & Technology
The Ukrainian Academy of Sciences
Kharkov 310 108
U.S.S.R.

ADDITIONAL MATERIAL TO LECTURE NOTES ON "ORDERING OF VOIDS AND BUBBLES IN IRRADIATED METALS"- V.I.DUBINKO

I N D E X

Nucleation, coarsening and ordering of cavities in metals under irradiation.

V.I. Dubinko
Institute of Physics & Technology
The Ministry of Atomic Energy & Industry
Kharkov 310108, USSR

ABSTRACT

This paper will summarise and update previous work in which the major features of formation and evolution of voids and gas bubbles in irradiated metals has been explained by taking into account elastic interaction of voids with point defects and dislocation loops. The former results in purely kinetic nucleation barrier and in a new mechanism of radiation-induced coarsening of voids which is qualitativly different from the well-known mechanism of Ostwald ripening. It limits the maximum number density and the minimum mean size of voids to values dependent only on the dislocation density and material constants. The interaction with loops is of great influence in those crystals where irradiation produces perfect interstitial loops which can glide and be absorbed by voids resulting in the shrinkage and mutual attraction of voids. Cooperation of the diffusion coarsening and dislocation interaction results under specific irradiation conditions in the swelling saturation and formation of the void lattice which has the symmetry determined by loop-gliding directions. The paper includes a discussion of other recent developments in this area including the gas bubble ordering under low temperature gas implantation and the recently proposed mechanism of bias-induced loop-punching from gas bubbles and precipitates at elevated temperatures. The latter may be a source of perfect interstitial loops which promotes void ordering and swelling saturation.

Nucleation, coarsening and ordering of cavities in metals under irradiation.

By V.I.DUBINKO
Kharkov Institute of Physics and Technology, Academicheskaya,1, Kharkov 310108, USSR.

CONTENTS

INTRODUCTION

Irradiation changes microstructure, microcomposition, and physical and mechanical properties of metals and alloys. Radiation effects is an important branch of material science for both the obvious technological need and the fundamental significance. The former is connected with a design of radiation-resistent materials, while the latter is due to the fact that irradiation is a useful tool for studying basic aspects of materials.

Materials under irradiation are examples of open dissipative systems far away from thermal equilibrium. The continuous production of point defects (PD) by irradiation and their annihilation by diffusion-and dislocation-controlled, non-linear reactions fulfill the conditions for an open and dissipative system which must be described in the framework of kinetics rather than thermodynamics. This is evident also from many experimental verifications of radiation-induced formation of periodic structures , such as void and gas bubble lattices, periodic dislocation arrangements etc. Although the basic theoretical tools for treating non-linear systems can be found in the classical lecture book by Nicolis and Prigogine [1] these are of little help without knowledge of physical mechanisms underlying the evolution of microstructure in radiation environments. As an example there have been a great number of unsuccessful attempts to explain the void lattice formation in the framework of formal kinetic approach based on oversimplified (though conventional) conceptions about reactions between voids and other lattice defects. The present paper is aimed at providing a description of the void ensemble evolution under irradiation based upon recent insights on the radiation-induced reactions between crystal defects.

In contrast to previous theories on void evolution, the present one takes into careful consideration elastic interaction of voids with PD and dislocation loops, which is shown to play a very important role under irradiation. This is due to the fact that by production of self-interstitial atoms (SIA) and their clusters (E.g. SIA-loops) the irradiation induces a new class of reactions with the microstructure which can be neglected under thermal conditions. Consequently, the microstructural evolution is governed by the difference between influxes of vacances and SIA which arises as a result of the asymmetry in elastic interaction between sinks and PD, and the boundary kinetics at the sink surfaces.

According to the conventional theory [2-5] void growth during irradiation must be attributed to the stronger attraction which SIA experience in the stress field of a dislocation. This produces an asymmetry in the flow of SIA and vacancies: the former are biased towards dislocations whereas the latter condense in excess at voids. The voids also have a bias for SIA , which is however small compared to that of dislocations in the case of large voids. For this reason, the void bias is either neglected or, at most, its effect is subsumed into the dislocation bias. As will be shown in this paper, the conventional approach greatly underestimates an important role of the void bias in the evolution of microstructire under irradiation.

In section 2, a complete set of equations describing the diffusion-induced evolution of voids is derived in the mean field approximation with account of finite sizes of sinks [9] , their elastic interaction with PD [10] and finite rates of reactions at sink surfaces [11] .

All this factors are shown to influence the void bias for SIA, which is inversly proportional to the void size in the diffusion-limited approximation assumed for subsequent calculations in this paper.

In section 3, the void nucleation during irradiation is described within the framework of the "classical" theory of precipitate nucleation of solute clusters in a solvent . The modification accounts for the fact that under irradiation precipitation of both the "solute" (vacancy) and the "antisolute" (SIA) determines the nucleation rate 6-8 . As a result, the nucleation rate equation may be made superficially similar to the equation of the classical theory, in involving a Boltzmann-type factor , but the activation barrier is kinetic in nature rather than being thermodynamic. It is determined by the difference in the arrival rates of vacancies and SIA, which makes their elastic interaction with nuclei a factor of key importance, resulting in the void bias for SIA, which is stronger than the dislocation bias in the case of sufficiently small voids. This creates the kinetic barrier for the transition of the nuclei into larger sizes which, along with the thermodinamic barrier, determines the void nucleation rate 8 . At sufficiently high PD production rate (or at low temperatures) thermal emission of PD is negligible and the nucleation rate is shown to be independent of irradiation conditions and to be determined by the constants of interaction of PD with voids and dislocations. In this limit the theory predicts higher nucleation rates for bcc metals as compared to fcc ones which is in agreement with experimental observations.

In section 4, the diffusion-controlled coarsening of the void ensemble at a postnucleation stage is described, which is

based upon two different physical mechanisms. The first one is the well known mechanism of Ostvald ripening, i.e. thermally-induced coarsening (TIC), driven by a difference in thermal emission rates of vacancies from voids of different sizes allowing larger voids grow at the expense of smaller ones 12 . The TIC rate is determined by the surface energy constant, PD diffusivities and temperature. The second mechanism of "radiation-induced coarsening" (RIC) 13,14 originates from the inversely proportional size dependence of the void bias according to which smaller voids absorb an excess of radiation-produced SIA and shrink, while larger voids absorb an excess of vacancies and grow. The RIC rate is determined by the bias constant and PD generation rate. Thus, the RIC is the direct response of the void ensemble to irradiation which induces the competition between voids of different sizes, if their number density exceeds a certain critical value determined by the dislocation density and the dislocation-to-void bias ratio. As a result of this competition the size distribution function of voids takes the universal form that does not depend on the nucleation mechanism. And besides , the void mean size and number density may not only rize under irradiation but be reduced as well depending on the evolution of the dislocation structure. This radiation-induced void shrinkage is indeed observed experimentally and can not be explained without taking into account the void bias for SIA. A comparison with experimental data shows that the coarsening mechanisms control the void evolution over a wide range of irradiation conditions.

An important consequence of the coarsening mechanisms is the impossibility of a stationary state of a void ensemble under irradiation of a purely diffusion origin. Indeed, in the presence of dislocations biased for SIA the mean size of voids grows with

time, and swelling increases. On the other hand, even the absense of other sinks ensures only the conservation of the void total volume (i.e. swelling), whereas the void number density decreases and the mean size encreases due to the RIC mechanism. It has been shown (by both the theory and experiment) to be strong enough to make 90% of voids shrink out in less than 5 dpa (displacements per atom) [14]. And this may seem to be in contrust with the most spectacular phenomenon encountered in the study of radiation effects in metals: the alignment of voids into regular superlattices stable up to the doses as high as 400 dpa [17-19]. Striking features are that voids in the superlattices neither grow nor shrink, and the superlattices possess the same structure and orientation as their host lattices. Thus, a mechanism of void ordering must impede the disordering effect of the coarsening mechanisms without letting the voids grow.

Many theories have been proposed to explain void lattice formation, the relative merits of which have been discussed by various authors [20-29]. The greatest number attempts undertaken have attributed the driving force for ordering to the interaction between voids [15]. However, static-energy considerations cannot provide an adequate description of kinetic processes in open system such as a crystal under irradiation. Another group of models is based on phase-instability mechanisms [19,20], which may induce spatial fluctuations in the vacancy concentration, gioing rise to the possibility of a periodic structure. This approach does not specify the underlying atomistic mechanisms and can not explain the observed correlation between the void and the host lattices, and the superlattice stability against coarsening.

A considerable progress has been achieved recently in works by Evans [21,22], Woo and Frank [23,24] and Dubinko et al [26-29], where a role of the crystal structure in the void ordering process has been taken into account. These theories combine synergetics with SIA-transfer anisotropy which is essential for the explanation of both symmetry and stability of void lattices.

The first two of the theories are based on the strong assumption of anisotropic diffusion of SIA-Foreman's proposal [16] on one-dimentionally propagating crowdions and Evans' model on two-dimentionally diffusing dumbbells. Their basic idea is that the difference in the anisotropy of diffusion of vacansies and SIA leads to the process analogous to that of a Darwinian selection: only the aligned voids survive, while the random ones shrink due to excessive SIA influxes. The relative merits of these models have been discussed in [22,24], however their main assumption is a controversial area and seems to be at variance with established knowledge of the dimensionality of SIA migration in either fcc, bcc, or hcp metals. Besides, this approach fails to explain the ordering of helium bubbles and precipitates observed during the low temperature implantation of noble gas ions into metals [18,25]: the bubbles and precipitates, in contrast to voids, are unable to shrink as required by 1D or 2D-SIA models. In order to align they have to move, and it has to be proved if the anisotropic SIA diffusion is able to move them in the required directions.

The main peculiarity of the model by Dubinko et al [26-29] presented in sections 5 and 6, is the dislocation mechanism of anisotropic SIA transfer which assumes that diffusion of isolated SIA is isotropic (contrary to the basic assumptions made in refs. [21-24]) but SIA clusters having converted into perfect dislocation loops, can glide along certain crystallographic directions

under elastic stress exceeding the Peierls stress. In the case of highly overpressurized gas bubbles SIA-loops are formed at the bubble surfaces and then are punched out due to the bubble-loop repulsion induced by the gas pressure [27]. On the other hand, vacancy voids absorb SIA-loops from the matrix due to the void-loop elastic attraction [29]. Obviously, neighbouring cavities lying along the same loop-gliding direction punch out or absorb a smaller number of loops as compared to isolated ones. As a result, a new type of dissipative interaction (reffered to as the dislocation interaction) arises between cavities where SIA-loops rather than SIA play the role of quanta. This interaction influences both the size and position of cavities in the matrix and leads under specific conditions to ordering of the cavities.

In the case of voids the dislocation interaction is attractive and, together with the diffusion repulsion, it results in the formation of locally ordered configurations of voids which then grow at the expense of random voids that shrink due to the diffusion coarsening mechanisms. In this way the void lattice emerges, wherein voids have immediate neighbours along the loop-gliding directions; and besides, they neither grow nor shrink since the excessive vacancy influxes are exactly compensated by the SIA-loop influxes.

In the case of gas bubbles the dislocation interaction is repulsive and, together with the isotropic diffusion attraction (due to the absorption of isolated SIA), it induces instability in a random distribution of bubbles that transforms into a lattice where the bubbles have immediate neighbours along the loop-punching directions. The observed copying of the matrix host by the lattices of voids and bubbles is explained by the coincidence of the loop-gliding directions with close-packed directions of

the matrix.

Thus, in contrast to previous theories, the present one explains all assential observations on both void and bubble lattices and gives simple analitical expressions for their parameters, being in good agreement with experimental data. In addition it explains why the void lattice is formed more readily in bcc than in fcc metals, the important difference between them being that in the latter case the majority of SIA-loops produced by irradiation remain sessile until they intersect to form a network, whereas in bcc metals they become glissile well before this stage including the dislocation interaction between voids. This also explaines higher swelling resistance of bcc as compared to fcc metals and offers a recommendation for strengthening of fcc metals against swelling by adding impurities stimulating the formation of perfect SIA-loops instead of faulted ones. It is a difficult task since the type of SIA-loops formed by the aggregation of SIA is controlled by a stacking fault energy γ_{SFA} that is one of the fundamental lattice parameters. In fcc metals is almost an order of magnitude lower than in bcc metals [29], and it is unclear if it is possible to increase γ_{SFA} by alloying additions to such an extent. There exists, however, an alternative way of formation of perfect SIA-loops - the bias-induced loop-punching from gas bubbles and precipitates at elevated temperatures which is considered in section 7.

The effect of gaseous impurities on swelling are of particular interest in the theory because of very significant effects observed experimentally. The insoluble rare gas helium is of primary concern. It is produced at levels of tens of parts per million (p.p.m.) in fast reactors, and levels of thousands of

2. DIFFUSION FLUXES OF POINT DEFECTS TO SINKS.

2.1. Effective Medium Concept.

In materials under irradiation PD are generated in spatially and temporally discrete cascades and are lost to spatially localized sinks or in atomictically discrete recombination events. However, the kinetic theory generally follows continuum descriptions, wherein irradiation is assumed to produce PD continuously in time and space at a doze rate K in displacements per atom per second ($dpas^{-1}$). Assuming further the recombination to be characterized by the effective parametre β_r, the exact value of PD concentration at any point $\vec{r}$ and time t is given by the diffusion equation

$$\frac{\partial C_n}{\partial t} = -\,div\vec{j}_n + K - \beta_r(\mathcal{D}_v+\mathcal{D}_i)C_vC_i\,, \quad n=i,v \qquad (1)$$

$$\vec{j}_n = -\frac{\mathcal{D}_n}{\omega}\nabla C_n - \frac{\mathcal{D}_n C_n}{\omega}\nabla V_n\,, \quad V_n \equiv \frac{E_n}{kT}\,, \qquad (2)$$

with appropriate boundary conditions at all ID sinks, where the subscript n=i,v designates SIA and vacancies, respectively, $\mathcal{D}_n$ the PD diffusivity, K is the PD generation rate, k is the Boltzmann constant, E_n is the energy of interaction between PD and the elastic strain field, T is the temperature, ω the atomic volume.

In the mean field approximation one is interested in the PD flux into a given sink (such as a void of radius R) averaged over all possible positions of other sinks. To carry out the averaging procedure Brailsford et al [2,3] described the real material with discrete sinks as an effective lossy medium containing a homogeneous distribution of these same sinks, with strengthes determined self-consistently. A macrodefect of interest should be surrounded by a sink-free region before being placed in the effective medium. However, the size of this region appeared to be a free parameter and, to avoid the ambiguity, the effective medium was extended up to the sink surface [2,3]. Another approach have been developed by Glezov et al [9-11], who have defined a supply region of the sink which is free of other sinks and can be determined self-consistently. According to this approach the total PD flux in the vicinity of a given sink of s-type $\vec{j}_n^{\,s}$ is presented as a sum of two components $\vec{j}_n^{\,s} = \vec{j}_n^{\,(0)s} + \vec{j}_n^{\,(1)s}$. The physical meaning of this division is to distinguish explicity between the "thermal" flux $\vec{j}_n^{\,(0)s}$ which is due to an exchange of thermally emitted PD between different macrodefects, and the "radiation" flux $\vec{j}_n^{\,(1)s}$ which is due to radiation-produced PD that are absorbed from the supply region $r < R_n^s$ of the macrodefect. The supply region is then defined self-consistently by a requirement of the zero "radiation" flux across the boundary of the region:

$$\left(\vec{j}_n^{\,(1)s}\vec{e}_r\right)\Big|_{r=R_n^s} = 0\,, \quad \vec{e} = \frac{\vec{r}}{r} \qquad (3)$$

where $\vec{r}$ is the radius vector directed outwards the sink centre, and R_n^s is the radius of the supply region which is assumed to be spherical for a cavity ($s=c$) and cylindrical for a dislocation ($s=d$). The concentration of radiation-produced PD $C_n^{(1)s}$ changes only inside the supply region, while outside we have $C_n^{(1)s} = C_n^*$, $r > R_n^s$, which is the same for all macrodefects as a result of the averaging. C_n^* is sustained by the balance between irradiation and sinks, and it is determined by the condition that the total volume of supply regions should make up the crystal bulk. If cavities and dislocations are the dominant sinks for PD, then the condition takes the explicit form

$$\frac{4\pi}{3}N\overline{(R_n^c)^3} + \pi\rho_d\,(R_n^d)^2 = 1\,, \qquad (4)$$

where ρ_d is the dislocation density, N the cavity number density.

Thus, the diffusion problem for radiation-produced PD in the absence of the bulk recombination is given by [11]

$$-\omega\, div\, j_n^{(1)s}(r) + K = 0\ ,\quad r < R_n^s;\quad j_n^{(1)s}\big|_{r \geq R_n^s} = 0\ , \tag{5}$$

$$j_n^{(1)s}\big|_{r=r^s} = -\frac{\gamma_n^s}{\omega} c_n^{(1)}\big|_{r=r^s}, \qquad (c_n^{(1)} e^{V_n^s})\big|_{r=R_n^s} = c_n^* \tag{6,7}$$

where r^s is the radius of the sink surface, while γ_n^s/ω is the rate of PD crossing the unit surface of the sink. The solution of eq. (5-7) for a cavity of a radius r^c is given by

$$c_n^* = \frac{K (R_n^c)^3}{3\mathcal{D}_n R_n^*}\left[1 - \frac{R_n^*}{(R_n^c)^3}\int_{r^c}^{R_n^c} r e^{V_n^c} dr\right] + \frac{K (R_n^c)^3}{3(r^c)^2}\frac{e^{V_n(r^c)}}{\gamma_n^c} \tag{8a}$$

$$\times\left(1 - \left(\frac{r^c}{R_n^c}\right)^3\right);\quad j_n^{(1)c} = -\frac{K}{3\omega (r^c)^2}\left[(R_n^c)^3 - (r^c)^3\right];\quad R_n^* \equiv \left[\int_{r^c}^{R_n^c} e^{V_n^c}\frac{dr}{r^2}\right]^{-1} \tag{8b}$$

For a dislocation we have

$$c_n^* = \frac{K (R_n^d)^2 r^d}{2\mathcal{D}_n r_n^*}\left[1 - \frac{r_n^*}{r^d (R_n^d)^2}\int_{r^d}^{R_n^d} r e^{V_n^d} dr\right] + \frac{K (R_n^d)^2 e^{V_n^d(r^d)}}{2 r^d \gamma_n^d}\left(1 - \left(\frac{r^d}{R_n^d}\right)^2\right) \tag{9a}$$

$$j_n^{(1)d} = -\frac{K}{2\omega r^d}\left[(R_n^d)^2 - (r^d)^2\right],\quad \frac{r_n^*}{r} \equiv \left[\int_{r^d}^{R_n^d} e^{V_n^d}\frac{dr}{r}\right]^{-1} \tag{9b}$$

where r^d is the dislocation core radius. To obtain R_n^s in explicit form one should express them in terms of c_n^* using eqs. (8a),(9a) and, substituting into eq.(4) solve the problem. Thus, we have derived the complete set of equations, (4),(8)-(9), that describes radiation-induced PD fluxes to cavities and dislocations.

In contrast to $j_n^{(1)s}$, the thermal PD fluxes $j_n^{(0)s}$ do not vanish at the supply region boundaries because of thermal PD exchange between macrodefects. The diffusion equation for $j_n^{(0)s}$ and its solution has been derived in refs. [9-10]. In this paper we are interested mainly in the radiation-induced evolution of voids and dislocations which is governed by the difference between $j_i^{(1)s}$ and $j_v^{(1)s}$, i.e. between R_i^s and R_v^s. This difference arises as a result of two factors, namely, the elastic interaction with PD and the boundary kinetic at the sink surfaces; and it depends on the volume fraction of sinks.

2.2. Bias of a Spherical Sink.

The interaction energy of PD with strain fields is composed of various contributions, each of which can be associated with a particular physical aspect of PD. From elastostatic consideration the PD is viewed as an inclusion and as an elastic inhomogeneity. The interaction between a spherical cavity and a nearby PD is induced then by the image distortion field of the PD (the size effect) and by the distortion field of the cavity due to the forces applied to the cavity surface (the modulus effect) [37]:

$$V_n^c = \left(\frac{\alpha_n}{r^c}\right)^3\left[\left(\frac{r}{r^c} - 1\right)^3 + \frac{7-5\nu}{30}\left(\frac{r}{r^c} - 1\right)^6\right]^{-1} + \frac{3}{2}\frac{\alpha_n^\mu}{kT\mu^2}\left(P^* + \sigma_H\right)^2\left(\frac{r^c}{r}\right)^6 \tag{10}$$

$$\alpha_n \equiv \left[\frac{(1+\nu)/\pi\omega}{36kT\pi}\right]^{\frac{1}{3}} b\left(\frac{\Omega_n}{\omega}\right)^{2/3},\quad P^* \equiv P - \frac{2\gamma}{r^c},$$

where P is the gas pressure, γ the surface energy, $\sigma_H = \frac{1}{3}(\sigma_{11} + \sigma_{22} + \sigma_{33})$ is the hydrostatic part of the external stress tensor, μ the shear modulus, ν the Poisson ratio, Ω_n is the PD relaxation volume which characterizes the intensity of the size interaction, α_n^μ is the PD shear polarizability which determines the modulus effect, b is the interatomic spacing. Characteristic values of these parameters are presented in Table 1.

In the zero approximation of the cavity volume fraction $r^c/R_n^c \to 0$ eq. (8) reduces to the following one:

$$J_n^{(1)} = 4\pi (r^c)^2 j_n^{(1)} = \frac{4\pi}{\omega}\mathcal{D}_n c_n^* r^c Z_n^c \tag{11}$$

$$Z_n^c \simeq \left[1 - \frac{\alpha_n}{r^c} + \frac{3}{56}\frac{\alpha_n}{kT}\left(\frac{P^* + \sigma_H}{\mu}\right)^2 + \mathcal{D}_n \frac{e^{V_n^c(r^c)}}{\gamma_n r^c}\right]^{-1} \tag{12}$$

Note that the product $r^c z_n^c$ plays the role of the cavity effective capture radius resulting from the cavity interaction with PD and boundary kinetics. If $V_n^c \to 0$, $\gamma_n \to \infty$ then $r^c z_n^c \to r^c$. If the last PD jump into the cavity is not substentially different from defect jumps within the matrix then $\gamma_n \sim D_n/b$, so that for a cavity of any significant size $D_n/\gamma_n r^c \sim b/r^c \ll 1$. It means that the last term of the sum (12) may be neglected which corresponds to the diffusion-controlled approximation:

$$z_n^c \simeq 1 + \frac{\alpha_n}{r^c} - \frac{3}{56}\frac{\alpha_n^4}{kT}\left(\frac{p^+ + \sigma_H}{\mu}\right)^2 \qquad (13)$$

which will be assumed for subsequent derivations in this paper. The difference $\delta_c \equiv z_i^c - z_v^c$ is the void bias factor, which plays the central role in the mechanism of radiation-induced coarsening (section 4) and in the formation of the bimodal size distribution of cavities (section 7).

2.3. Dislocation Bias.

The dislocation bias for SIA is the driving force of irradiation swelling originating from the size effect interaction with PD 38, 39 :

$$V_n^d = \frac{\mu b \Omega_n (1+\nu)}{3\pi kT(1-\nu)}\frac{\sin\theta}{r} \qquad (14)$$

where θ is the angle between the position of PD $\vec{r}$ and the Burgers vector, $\vec{b}$. The previous analysis 38, 39 has shown that the greatest contribution to the diffusion current comes from the cylindrically symmetric part of the interaction. Accordingly, we shall use the conventional substitution for eq. (14):

$$V_n^d = -\frac{L_n}{r}, \quad L_n \equiv \frac{\mu b(1+\nu)}{3\pi kT(1-\nu)}|\Omega_n| \qquad (15)$$

Substituting (15) into eq.(9) it is possible to obtain the PD flux to dislocation precisely. In the lowest order of

one comes to

$$J_{n1}(r^d) = \frac{z_n^0 D_n C_n^*}{\omega} \qquad (16)$$

$$z_n^0 \simeq 2\pi / \left\{E_1(L_n/R_n^d) - E_1\left(\frac{L_n}{r^d}\right) + \frac{D_n e^{-\frac{L_n}{r^d}}}{\gamma_n^d r^d}\right\} \qquad (17)$$

where $E_1(x)$ is the integral exponential function of x. In the diffusion-controlled approximation ($D_n/\gamma_n^d r^d \to 0$) eq.(17) reduces to the result of 38, 39 which can be expressed in the following form:

$$z_n^0 \simeq \begin{cases} 2\pi/\ln\{R_n^d/r^d\}, & r^d \gg L_n \qquad (18a) \\ 2\pi/\ln\{2R_n^d/L_n\}, & r^d \ll L_n \ll R_n^d \qquad (18b) \end{cases}$$

which has a simple interpretation: the elastic interaction, if strong enough, leads to a new effective capture radius that is larger for SIA than for vacancies since $\Omega_i > \Omega_v$.

If an external stress-field is superimposed, then the nonlinear inhomogeneity interaction gives rize to induced changes which are in the lowest order linear in the external stress : $z_n^0(\sigma) = z_n^0(0) + \delta z_n^0$. In general, δz_n^0 contains terms which depend on the orientation of the Burgers vector. These terms have been shown to lead to the mechanism of stress-induced preference absorption (SIPA), i.e. to the irradiation creep 40 . However, swelling rate is affected only by other terms which depend on σ_H and do not on orientation 41 :

$$\delta z_n^0(\sigma_H) = -\frac{b/4r^d}{\ln(R^d/r^d)}\left[\frac{1-2\nu}{2\pi kT(1-\nu)}\right]^2 \alpha_n^K \Omega_n \sigma_H \qquad (19)$$

where α_n^K is the PD bulk polarizability.

To derive (17),(18), one has to assume that dislocations are homogeneously distributed in a crystal. Only this case admits the consideration of a dislocation structure as an ensemble of "isolated" dislocations interacting only with the single self-consistent diffusion field. The bias of an isolated dislocation is given by the difference $\delta_0 = z_i^0 - z_v^0$ that is essentially deter-

mined by the $\Omega_i/|\Omega_v|$ ratio and is independent of irradiation conditions as distinct from the mean dislocation bias $\bar{\delta}$, which is observed to increase with the temperature rise and to decrease with irradiation dose 42.

This discripancy may be understood taking into account that the dislocation structure is generally very inhomogeneous and involves dislocation pile-ups, rafts, dipoles, networks, etc. The arrangement of dislocations in such substructures can not be considered as a random one. Accordingly, in the mean-field approximation it is not correct to single out one dislocation from the pile and to perform the overaging over all other ones. Instead, one has to single out the pile as a hole, place it into the effective medium and solve the diffusion problem with account of the pile geometry. In some cases a symmetry of the dislocation arrangement within a pile helps to obtain an analytical solution of the problem. A characteristic example of such arrangement is a pile of dislocation loops (one-dimentional periodic structure of loops) which has been investigated by Dubinko et al 33. They have shown that if the loop density within the pile exeeds a certain critical value then the pile absorbs PD as a single "superdislocation" with effective capture radius that depends on the ratio of the loop radius to their spacing. Accordingly, the pile bias is less than that of an isolated dislocation and diminishes with growth of pile radius untill it reaches the mean bias of all the sinks present. This is a stable point where currents of vacancies and SIA to the pile compensate each other so that the pile becomes sessile. A stability criterion for intersitial piles has been found in 34 to be in a good agreement with experimental observations.

The above example shows that bias should be different for different substructures resulting in a complex nature of the mean dislocation bias $\bar{\delta} = \sum_m \rho_m \delta_m / \bar{\rho}$, where $\rho_m/\bar{\rho}$ is the relative fraction of dislocations with the bias δ_m, $\bar{\rho} = \sum_m \rho_m$ is the mean dislocation density. The existence of the bias spectrum is confirmed by experimental observations of the radiation-induced evolution of the dislocation structure in the absence of voids 1,8,26 which requires, at least, two components with different biases δ_1 and δ_2.

Below we distinguish two structural components, namely, "isolated" and "sessile" ones with densities ρ_c and ρ_s, respectively. The isolated dislocations have the standard bias δ_0, whereas the bias of the sessile dislocations is such as to compensate the biases of voids and isolated dislocations, thereby equalizing the influxes of SIA and vacancies to the sessile dislocations.

Generally, we believe that any sufficiently dense dislocation substructure may become sessile, since its bias should decrease as the dislocations draw together shadowing each other against PD fluxes. Another possible reason of the sessile dislocation formation resides in impurity atoms and precipitates which may impede the dislocation glide and climb.

The role of sessile dislocations consists in the enhancement of the PD recombination rate which reduces the supersaturation. Besides, it acts as a sink for the isolated dislocations whose density ρ_c is determined by the equilibrium between the dislocation sources (SIA-loop nucleation, etc.) and sinks (mutual annihilation, escape to the grain boundary or integration with a sessible component). The mean dislocation bias $\bar{\delta} = (\delta_0\rho_c + \delta_s\rho_s)/\bar{\rho}$ is close to δ_0 at an initial stage, when the isolated SIA loops are the main components of the dislocation structure, so that $\rho_c \gg \rho_s$

As the loops grow to form the dislocation network, the inequality becomes reverse $\rho_s >> \rho_0$, resulting in the mean bias decrease $\bar{\delta}(t) \to \delta_s \ll \delta_0$, even if the mean dislocation density $\bar{\rho} = \rho_0 + \rho_s$ remains constant. At higher temperatures the sessile structures become unstable 34 and do not form, hence $\bar{\delta}(T)$ increases up to the δ_0 value, which is in agreement with the experimental data 42 .

The main advantage of this phenomenological model of the dislocation structure is its ability to describe the observed evolution of $\bar{\delta}(t)$ in terms of physically transparent parameters ρ_0 and ρ_s which can be measured from experiment.

2.4. The Boundary Concentrations of Point Defects.

A crystal under irradiation is a nonequilibrium system, though quasi-equilibrium PD concentrations are sustained near the macrodefect boundaries if the rate of the boundary kinetics is higher than the rate of PD arrival from the matrix 9 . In this diffusion-limited approximation, the boundary conditions for cavities and dislocations are given by

$$C_n^c = C_n^e \exp\left\{\frac{\Omega}{kT}\left(\frac{\Sigma_n}{\omega}\sigma_H \mp p^*\right) - V_n^c(r)\right\} \qquad (20)$$

$$C_n^d = C_n^e \exp\left\{\frac{\omega}{kT}\left(\frac{\Sigma_n}{\omega}\sigma_H \pm \sigma_{em}\frac{b_e b_m}{b^2}\right) - V_n^d(r)\right\} \qquad (21)$$

$$C_n^e = \exp\left\{-E_n^f/kT\right\} \qquad (22)$$

where the plus and minus signs correspond to vacancies (n=v) and SIA (n=i), respectively; C_n^e is the equilibrium PD concentration at the flat surface, E_n^f is the PD formation energy. Since PD boundary concentrations at different macrodefects differ they exchange thermal PD between themselves. Hence, there is no supply region for thermal PD. However, R_n^s which has been defined for radiation-produced PD, may be used as the sink-free region radius in the effective medium approach.

2.5. The Rate Equations.

So far we have not considered the intrinsic recombination of vacancies and SIA which may be characterised by the mean path of PD before the recombination:

$$\ell_n^r \simeq \left\{\frac{\mathcal{D}_i \mathcal{D}_v}{(\mathcal{D}_i + \mathcal{D}_v)\beta_r \mathcal{D}_n \bar{C}_n}\right\}^{\frac{1}{2}} \qquad (23)$$

where β_r is the recombination constant. If $\ell_n^r >> R_n^s$ then the recombination may be neglected. In general, recombination reduces the supersaturation which should be accounted for in the rate equations for PD since corrections to the sink strengths due to recombination are usually small 36 . At a given PD generation rate K , the rate equations have the following form:

$$\frac{d\bar{C}_n}{dt} = K - \omega N \overline{J_n(r^c)} - \omega J_n(r^d)\rho_0 - \omega J_n^s \rho_s - \beta_r(\mathcal{D}_i + \mathcal{D}_v)\bar{C}_i \bar{C}_v \qquad (24)$$

where the total PD fluxes to sinks are obtained by summing up the thermal and radiation fluxes. In the lowest approximation of defect volume fraction $r^s/R_n^s \to 0$ one has

$$J_n(r^c) = \frac{4\pi}{\omega}\mathcal{D}_n z_n^c(\bar{C}_n - C_n^c); \quad J_n(r^d) = \frac{z_n^c}{\omega}\mathcal{D}_n(\bar{C}_n - C_n^d), \qquad (25)$$

where C_n^c and C_n^d are given by eqs. (20-22) at $V_n^s = 0$. For a cavity z_n^c does not depend on the supply region in the approximation under consideration (eq.(13)), whereas z_n^o for dislocation does (see eq.(18)). At $R_n^d \to 0$ R_n^d is given by

$$R_n^d = \sqrt{z_v^o/\pi(\rho_0 z_n^o + 4\pi N \overline{z_n^c r^c})} \qquad (26)$$

The fluxes to the sessile dislocations do not depend on the PD type by definition:

$$\omega J_s = z_v^s \mathcal{D}_v(\bar{C}_v - C_v^d) = z_i^s \mathcal{D}_i(\bar{C}_i - C_i^d) \qquad (27)$$

equations (27) may be expressed in terms of the well known sink strengths 36 :

$$\frac{d\bar{C}_n}{dt} = K - k_n^2 \mathcal{D}_n \bar{C}_n - \rho_s J_s - \beta_r(\mathcal{D}_v + \mathcal{D}_i)\bar{C}_i \bar{C}_v - \kappa e \qquad (28)$$

where k_n^2 is the sum of void and isolated dislocation sink strengths for PD:

$$k_n^2 = 4\pi N \overline{Z_n^c r_c} + Z_n^o \rho_o \qquad (29)$$

K_n^e is the PD emission rate from voids and isolated dislocations:

$$K_n^e = k_n^2 D_n \overline{C_n^e} \qquad (30)$$

$$\overline{C_n^e} = \left(4\pi N \overline{Z_n^c r_c C_n^c} + Z_n^o \rho_o C_n^d\right) / k_n^2 \qquad (31)$$

where $\overline{C_n^e}$ is the mean concentration of thermal PD in the crystal.

Equations (24)-(31) make a complete set describing the diffusion fluxes to cavities and dislocations for the given irradiation conditions K, T, the dislocation parameters ρ_o , ρ_s and the bias factors Z_n^o, Z_n^c , in the lowest order of the defect volume fraction. This approximation will be used in the following description of the microstructural evolution under irradiation.

REFERENCES

1. G.Nicolis and I.Prigogine, Self-Organization in Non-Equilibrium Systems (Wiley-Interscience, 1977).
2. R.Bullough, R.S.Nelson, Phys.Technol. 5(1974)29.
3. R.Bullough, M.H.Wood, in: Physics of Radiation Effects in Crystals (Elsevier, Amsterdam, 1986) p.189.
4. W.G.Wolfer, J.Nucl.Mater. 122/123 (1984) 367.
5. L.K.Mansur, in: Kinetics of Nonhomogeneous Processes (John Wiley and Sons, Inc.,1987) p.377.
6. J.L.Katz, H.Wiedersich, J.Chem.Phys. 55(1971)1414.
7. K.C.Russell, Acta Met. 19(1971)753.
8. V.I.Dubinko, in Proc.Int.Conf. on Radiat.Mater.Science, Alushta, USSR, 1990,v.2, Kharkov-1990, p.10.
9. V.V.Slezov, Fiz.Tverd.Tela 31(1989)1289 Sov.Phys.Solid State 31(1989) N 8 .
10. V.V.Slezov, P.N.Ostapchuk, Fiz.Tverd.Tela 327(1990)193. Sov.Phys.Solid State 327(1990) .
11. V.I.Dubinko, P.N.Ostapchuk, V.V.Slezov, in: Proc.Int.Conf. on Radiat.Mater.Science, Alushta, USSR, 1990, v.5, Kharkov-1990, p.112.
12. I.M.Lifshits, V.V.Slezov, Zh.Ehksp.Teor.Fiz. 35(1958)479, Sov.Phys. JETP 8(1959)331 .
13. V.I.Dubinko, P.N.Ostapchuk, V.V.Slezov, Fiz.Met.Metalloved. 65(1988)32 Sov.Phys.Met.Metall. 65(1988) .
14. V.I.Dubinko, P.N.Ostapchuk, V.V.Slezov, J.Nucl.Mater. 161(1989)239.
15. A.M.Stoneham, J.Phys. F 4(1974)1335.
16. A.J.E.Foreman, AERE-R-7135, Harwell(1972).
17. J.H.Evans, Nature, 229(1971), 403.

18. S.L.Gess, B.L.Eyre, Phil.Mag. 27(1973)1447.
19. L.Krishan, Radiat.Eff. 66(1982)121.
20. C.Abromeit, Int.J.Mod.Phys.B, 3(1989)1301.
21. J.H.Evans, J.Nucl.Mater. 119(1983)180.
22. J.H.Evans, Mater.Science Forum. 15-18(1987)869.
23. C.H.Woo, W.Frank, J.Nucl.Mater. 137(1985)7.
24. W.Frank Solid State Phenom. 3/4(1988) 315.
25. D.J.Mazey, J.H.Evans, J.Nucl.Mater. 138(1986)16.
26. V.I.Dubinko, V.V.Slezov, A.V.Tur, V.V.Yanovsky, Preprint, Space Research Institute N922 (Moscow,1984).
27. V.I.Dubinko, A.V.Tur, A.A.Turkin, V.V.Yanovsky, Vopr. At. Nauki Teh., Ser.: Fiz.Rad.Povrezd. i Rad. Materialoved. 1(39)(1987)40.
28. V.I.Dubinko, V.V.Slezov, A.V.Tur, V.V.Yanovsky. Radit.Eff. 100(1986)85.
29. V.I.Dubinko, A.V.Tur, A.A.Turkin, V.V.Yanovsky. Nucl.Mater. 161(1989)57.
30. V.I.Dubinko, in:Proc.Int.Conf. on Radiat.Mater.Science, Alushta, USSR, 1990, v.2. Kharkov-1990, p.149.
31. K Farrell. Radiat.Eff. 53(1980)175.
32. B.A.Loomis, J.Nucl.Mater. 141/143(1986)690.
33. V.I.Dubinko, A.A.Turkin, V.V.Yanovsky, Fiz.Met.Metalloved. 59(1985)291 Sov.Phys.Met.Metall. 59(1985)No2 .
34. V.I.Dubinko, A.A.Turkin, V.V.Yanovsky, Fiz.Met.Metalloved. 59(1985)686 Sov.Phys.Met.Metall. 59(1985)No4 .
35. F.S.Ham. J.Phys.Chem.Solids. 6(1958)335.
36. A.D.Brailsford and R.Bullough, Philos.Trans.Roy.Soc. (London) A 302 (1981) 87.
37. W.G.Wolfer, in: Proc. Int. Conf. on Fundamental Aspects of Radiation Damage in Metals, Gatlinburg, Tennessee, USA,
38. F.S.Ham, J.Appl.Phys. 30(1959)915.
39. I.G.Margvelashvili and Z.K.Saralidze, Fiz. Tverd. Tela 15(1973)2665 Sov.Phys.Solid State 15(1973) .
40. P.T.Heald and M.V.Speight, Philos Mag. 29(1974)1075.
41. W.G.Wolfer, M.A.Shkin, J.Appl.Phys. 47(1976)791.
42. N.A.Demin, Yu.V.Konobeev and O.V.Tolstikova, Fiz. Met. Metalloved. 58(1984)98 Sov.Phys.Met.Metall. 58(1984) .

Proc. Int. Conf.: Radiation Materials Science, Alushta, 1990, V. 5, Kharkov 1990 PP. 112-120.

UDC 539.219.2

THEORY OF THE VOID NUCLEATION IN CRYSTALS UNDER INTENSIVE IRRADIATION

V.I.Dubinko

Institute of Physics and Technology, Kharkov

1. Introduction

Irradiation produces vacancies and self-interstitial atoms (SIA) in excess of their respective thermal equilibrium concentrations, i.e. both types of point defects (PD) are supersaturated. At the same time, vacancies and SIA are produced in essentially the same numbers. It means that formation of defect clusters of various types (such as voids and SIA dislocation loops) needs a mechanism of PD segregation. The latter is based on the difference in elastic interaction of voids and dislocations with PD resulting in their bias for SIA absorption. The dislocation bias has been first considered by Hamilton and it is thought to be the driving force of the irradiation swelling of materials [2,3]. The void bias has been shown [4,5] to result in the radiation-induced coarsening, i.e. competition between voids which limits their stationary number density N_s to the value dependent only on the dislocation density and material constants and independent of the void nucleation rate. The latter, however, determines the time it takes to reach N_s. Katz and Wiedersich [6] and, independently, Russell [7] have shown that under irradiation the nucleation rate equation is superficially similar to the equation of classical nucleation theory, in involving a Boltzmann-type factor, but the activation barrier is partially kinetic in nature, rather than being strictly thermodynamic. In fact, they have taken into account the dislocation bias for SIA, owing to which the arrival rate ratio of SIA and vacancies to any void is less than unity. The nucleation activation barrier is then a result of the competition between this constant arrival ratio and a thermally activated emission of PD from voids which is size dependent. In this paper the void bias resulting from image interaction with PD will be accounted for within the mathematical framework of classical nucleation theory. This bias is inverselyproportional to the void size, resulting in the nucleation barrier which is strictly kinetic in nature in the limit of infinite supersaturation, i.e. when thermal emission of PD is negligible.

2. General theory of homogeneous void nucleation

Nucleation is homogeneous when it does not need distinguished centres, so that any cluster containing x vacancies may be considered as a nucleus beginning from $x = 1$. If $f(x,t)$ is the number density of voids of x vacancies at time t and it is changed only by capture or emission of single PD then the master equation is given by [6,7].

$$\frac{\partial f(x,t)}{\partial t} = J_{x-1,x} - J_{x,x+1}, \tag{1}$$

$$J_{x-1,x} = W^{+}(x-1)f(x-1,t) - W^{-}(x)f(x,t) \tag{2}$$

where $W^{+}(x)$ and $W^{-}(x)$ are the frequencies with which an x-mer becomes an $(x+1)$-mer or an $(x-1)$-mer, respectively. $J_{x-1,x}$ is the net flow of void embryos, that is, the rate at which $(x-1)$ mers grow to x-mers minus the rate for the inverse process.

A steady state solution of eq. (1) is given by

$$f_s(x) = f_o(x) - \frac{J^s}{W^{+}(x)} \sum_{j=0}^{x-2} \prod_{m=x-j}^{x} \frac{W^{+}(m)}{W^{-}(m)}, \tag{3}$$

where $J^s = \text{const}$ is the steady state nucleation rate, $f_o(x)$ is the constrained equilibrium distribution of x-mers which obeys a recursive equation $J_{x-1,x}[f_o(x)] = 0$. Following the standard procedures of nucleation theory, this equation can be solved and J^s be determined, if the following boundary conditions are satisfied:

$$\frac{f_s(x)}{f_o(x)} \xrightarrow[x \to 1]{} 1, \qquad \frac{f_s(x)}{f_o(x)} \xrightarrow[x \to \infty]{} 0 \tag{4}$$

which means that (i) J^s is small enough so that the concentration of vacancies ($x = 1$) is close to the constrained equilibrium value, and (ii) the concentration of extremely large voids is negligibly small compared to that for the constrained distribution. Using this limits one obtains

$$W^+(x) f_0(x) = f_0(1) W^+(1) \exp\left\{\sum_{m=2}^{x} \ln \frac{W^+(m)}{W^-(m)}\right\}, \qquad (5)$$

$$J^s = \left\{\sum_{m=1}^{\infty} \frac{1}{W^+(m) f_0(m)}\right\}^{-1}. \qquad (6)$$

Thus, the steady state nucleation rate can be evaluated if the constrained equilibrium distribution of voids $f_0(x)$ is known.

3. The constrained equilibrium distribution of voids

Consider a system which contains only vacancies and their clusters, i.e. voids. Then the equilibrium distribution of voids is given by [6,7]

$$f_0(x) = N \exp\left\{-\frac{\Delta G_v(x)}{T}\right\} \qquad (7)$$

where N is the number of nucleation sites per unit volume, $\Delta G_v(x)$ is the free energy change on forming a void of x vacancies T is the temperature. The usual capillarity model gives

$$\Delta G_v(x) = -x T \ln S_v + \left(\frac{4x}{\omega}\right)^{1/3} \alpha_\gamma x^{2/3}, \quad \alpha_\gamma \equiv \frac{2\gamma\omega}{T}, \qquad (8)$$

where $S_v = \bar{C}_v / C_v^e$ is the vacancy supersaturation, i.e. the ratio of the mean concentration of vacancies $\bar{C}_v$ to the equilibrium one C_v^e, γ is the surface free energy per unit area, ω the atomic volume.

The presence of excess SIA under irradiation does not allow one to define uniquely "free energy of void formation" [7], as a void of x vacancies may be formed from $x+m$ vacancies and m SIA, where m is any number. However, it is possible to evaluate $f_0(x)$ according to eq. (5), if the frequencies $W^+(x)$ and $W^-(x)$ are known. This is the case in the limit of infinite supersaturations $S_n = \bar{C}_n / C_n^e \to \infty$ (index $n = v$ designates vacancies, while n = i - SIA) when thermal emission of PD may be neglected. Then $W^+(x)$ and $W^-(x)$ are simply the rates of arrival of vacancies and SIA at a void, respectively. Solution of diffusion equation with account of image interaction of void with PD gives [4,5]:

$$W^+(x) = \frac{4\pi}{\omega} \mathcal{D}_v \bar{C}_v (R(x)+\alpha_v), \quad W^-(x) = \frac{4\pi}{\omega} \mathcal{D}_i \bar{C}_i (R(x)+\alpha_i); \tag{9}$$

$$\alpha_n \approx b \left(\frac{\Omega_n}{\omega}\right)^{2/3}, \qquad R(x) = (3\omega/4\pi)^{1/3} x^{1/3} \tag{10}$$

where Ω_n is the PD relaxation volume, b is the interatomic spacing, $R(x)$ is the void radius, while $R(x)+\alpha_n$ is the void effective capture radius resulting from the image interaction with PD. Substituting expressions (9) into (5) one obtains

$$W^+(x) f_o(x) = W^+(1) f_o(1) \exp\left\{\sum_{m=2}^{x} \ln\left[\frac{\mathcal{D}_v \bar{C}_v}{\mathcal{D}_i C_i} \frac{1+\alpha_v/R(m)}{1+\alpha_i/R(m)}\right]\right\}. \tag{11}$$

Note that at $\alpha_n/R \ll 1$ $\ln\left[(1+\alpha_v/R)/(1+\alpha_i/R)\right] \approx (\alpha_i - \alpha_v)/R$. Then for mathematical convenience one approximates the summation in eq. (11) by the integration with the result ($x \gg 1$)

$$W^+(x) f_o(x) = W^+(1) f_o(1) \exp\left\{x \ln S_{iv} - \frac{3}{2}\left(\frac{4\pi}{3\omega}\right)^{1/3} \alpha_{iv} x^{2/3}\right\}, \tag{12}$$

$$S_{iv} = \mathcal{D}_v \bar{C}_v / \mathcal{D}_i \bar{C}_i, \quad \alpha_{iv} = \alpha_i - \alpha_v > 0, \tag{13}$$

where index "iv" underlines the two-component nature of parameters S_{iv} and α_{iv}. As for the rest, exponents of eqs. (7) and (12) are alike which reveals an interesting analogy between nucleation in materials with finite vacancy supersaturation S_v and nucleation in materials with infinite supersaturation of vacancies and SIA. In the latter case the ratio S_{iv} plays the role of the supersaturation, while the difference between the constants of void interaction with SIA and vacancies, α_{iv}, substitutes for the surface energy constant α_γ. Thus, under irradiation $f_o(x) \sim \exp\left\{-\frac{\Delta G_{iv}}{T}\right\}$ where $\Delta G_{iv}(x)$ at $S_n \to \infty$ is a strictly kinetic analog of the "free energy of void formation", which plays the role of the nucleation barrier in the limit of infinite supersaturation.

4. The void nucleation rate

As long as the x dependences of $\Delta G_v(x)$ and $\Delta G_{iv}(x)$ are equivalent and have a single well-defined maximum, equation (6)

may be evaluated in a standard manner to give the expression for J^S which is valid for both cases under consideration:

$$J^S = Z W^+(x_c) f_e(x_c) = Z W^+(1) f_e(1) \exp\left\{-\frac{\Delta G(x)}{T}\right\}, \qquad (14)$$

where Z is the Zeldovich factor which depends on the curvature of $\Delta G(x)$ near the maximum x_c:

$$x_c = \frac{4\pi}{3\omega} R_c^3, \quad R_c = \frac{\alpha}{\ell n S}, \qquad (15)$$

$$Z = \left(-\frac{1}{2T}\frac{\partial^2 \Delta G}{\partial x^2}\Big|_{x=x_c}\right)^{1/2} = \frac{1}{2\pi R_c^2}\left(\frac{\omega\alpha}{2}\right)^{1/2}, \qquad (16)$$

$$\frac{\Delta G(x_c)}{T} = \frac{2\pi}{3\omega}\alpha R_c^2, \qquad (17)$$

where R_c is the critical nucleus size. In the one-component case $S \to S_v$, $\alpha \to \alpha_v$ and $R_c \to R_c^v = \alpha_v/\ell n S_v$ while in the two-component case $S \to S_{iv}$, $\alpha \to \alpha_{iv}$, $R_c \to R_c^{iv} = \alpha_{iv}/\ell n S_{iv}$.

Consider the two-component limit in more details. Substituting eqs. (16) and (17) into (14) and taking into account that $f_e(1) = \bar{C}_{iv}/\omega$ one obtains

$$J_{iv}^S = \frac{\mathcal{D}_v \bar{C}_v^2 \beta}{(\omega R_c^{iv})^2}(2\omega\alpha_{iv})^{1/2}\exp\left\{-\frac{2\pi}{3\omega}\alpha_{iv}(R_c^{iv})^2\right\}. \qquad (18)$$

This equation may be used for the evaluation of the void nucleation rate under sufficiently high dose rate (or low temperature) irradiation, when thermal emission of PD from voids may be neglected. Generally, the nucleation barrier is determined by both absorption and emission of PD as can be seen from the expression for the critical nucleus size, which in the macroscopic approximation ($R \gg \alpha$) is given by [4,5]

$$R_c^* = \frac{\Delta^* \alpha_{iv} + \mathcal{D}^* \alpha_i}{\Delta^* \delta_d}, \quad \delta_d = \frac{z_i}{z_v} - 1 = \ell n\left\{\frac{\Omega_i}{\Omega_v}\right\} \qquad (19)$$

where $\mathcal{D}^* = \mathcal{D}_v C_v^e + \mathcal{D}_i C_i^e$ is the thermal self-diffusivity of PD while $\Delta^* = \mathcal{D}_v(\bar{C}_v - C_v^e) \simeq \mathcal{D}_i(\bar{C}_i - C_i^e)$ may be called the "radiation-induced self-diffusivity" of PD. The upper-script "e" in R_c^e means that the void density is negligible, in

which case $S_{iv} = z_i / z_v$, where z_n is the PD capture efficiency of dislocations. Since $z_i > z_v$ we have $S_{iv} > 1$ and $\delta_d > 0$.

At $\Delta^* \alpha_{iv} \gg \mathcal{D}^* \alpha_\gamma$ R_c^* coincides with the defined above R_c^{iv}:

$$R_c^* \simeq \frac{\alpha_{iv}}{\delta_d} = R_c^{iv} \frac{\alpha_{iv}}{\ln\left\{\frac{z_i}{z_v} - 1 + 1\right\}} \simeq \frac{\alpha_{iv}}{\delta_d}, \quad \delta_d \ll 1 \qquad (20)$$

meaning that in this region the nucleation barrier is determined by the absorption of PD alone and voids nucleate at a rate close to given by eq. (18).

In the high temperature region, $\Delta^* \alpha_{iv} \ll \mathcal{D}^* \alpha_\gamma$, thermal emission of PD rather than the void bias limits the nucleation rate, while R_c^* depends on the vacancy supersaturation and the dislocation bias δ_d:

$$R_c^* \xrightarrow[\frac{\Delta^* \alpha_{iv}}{\mathcal{D}^* \alpha_\gamma} \to 0]{} R_c^\gamma = \frac{\mathcal{D}^* \alpha_\gamma}{\Delta^* \delta_d} = \frac{\alpha_\gamma}{\delta_d (S_v - 1)}. \qquad (21)$$

Note that $R_c^\gamma \to \infty$ if $\delta_d \to 0$ meaning that the supersaturation alone is insufficient for the void nucleation to take place under irradiation. The dependence of the nucleation barrier on the kinetic factor δ_d has been investigated by Katz, Wiedersich [6] and Russell 7. Our analysis shows that their result is valid only in the high temperature (or low dose rate) region, where the void bias effect on the nucleation barrier is negligible and $J^s = J_\gamma^s$, where the subscript " γ " emphasizes the dependence of J_γ^s on the surface energy [8].

The temperature dependences of J_{iv}^s and J_γ^s are shown in fig.1 for the reactor irradiation dose rate $K = 10^{-6}$ dpa/s.

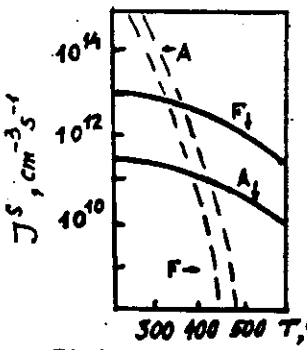

Fig.1. Comparison of $J_{iv}^s(T)$ (solid lines) and J_γ^s (dashed lines) in the neutron irradiated austenitic and ferritic steels. The letter A denotes austenitic steel, where $\Omega_i = 1{,}8\omega$, $\Omega_v = -0{,}1\omega$, while F denotes ferritic steel, where $\Omega_i = 1{,}1\omega$, $\Omega_v = -0{,}5\omega$, [9]. $\gamma = 1\,Jm^{-2}$, $E_v^m = 1{,}1$eV; $E_v^f = 1{,}7$eV, $\beta = 0{,}25$nm; $\omega = \beta^3$.

It is seen that in contrast to $J_\gamma^s(T)$ the temperature depen-

dence of $J^s_{iv}(T)$ is very smooth, the reason being that the nucleation barrier ΔG_{iv} depends only on kinetic factors α_{iv} and δ_d whereas the nucleation barrier entering J^s_v depends on the vacancy supersaturation $S_v = \bar{C}_v \exp(E^f_v/T)$, where E^f_v is the vacancy formation energy.

Another interesting difference between J^s_{iv} and J^s_v is their dependence on the ratio of relaxation volumes of PD, $\Omega_i/|\Omega_v|$, which is higher in fcc metals as compared to bcc ones [9]. Consequently the critical radius R^v_c is higher in bcc than in fcc metals resulting in lower value of $J^s_v \sim \exp\{-\alpha_v (R^v_c)^2\}$. On the other hand, R^{iv}_c entering J^s_{iv}, only weakly depends on $\Omega_i/|\Omega_v|$ [8]:

$$R^{iv}_c \approx 6 \left(\frac{\Omega_i}{\omega}\right)^{2/3} \frac{1-(\Omega_v/\Omega_i)^{2/3}}{\ln(\Omega_i/|\Omega_v|)} \approx 6 \qquad (22)$$

where as the kinetic analog of the surface energy constant, α_{iv}, is lower in bcc than in fcc metals:

$$\alpha_{iv} \approx 6 \left(\frac{\Omega_i}{\omega}\right)^{2/3} (1-(\Omega_v/\Omega_i)^{2/3}). \qquad (23)$$

As a result, the nucleation rate given by J^s_{iv} is higher in bcc than in fcc metals which is in agreement with the experimental data [10]. This trend is illustrated in fig.1 by comparison of nucleation rates in austenitic (fcc) and ferritic (bcc) steels, where the ratio $\Omega_i/|\Omega_v|$ is taken from the ref.[9], while other material constants are chosen to be the same in both cases to emphasize the dependence on the relaxation volumes of PD.

Thus, one can see that the approximation J^s_{iv} neglecting emission of PD describes experimental trends better than a standard theory [6,7] neglecting the size dependence of the void bias. In general case, both these factors should be taken into account in numerical evaluation of J^s which would be close to J^s_{iv} or J^s_v under the low or high temperature irradiation, respectively. Besides a modulus interaction of voids with PD affecting the void bias also should be taken into account. However, gas atoms usually present in irradiated metals, may stabilize void nuclei against the thermal emission of PD, at the same time reducing the void bias to the value determined only by the image interaction. We may conclude that J^s_{iv} is the upper limit for the void nucleation rate under irradiation and its applicability region may be extended by the presence of gas impurities.

5. The stationary number density of voids

As has been shown by Dubinko et al [4,5], the competition between voids limits their maximum number density to the value

$$N_S = Z_i \rho_d / 2\pi R_c^{iv} \qquad (24)$$

where ρ_d is the dislocation density. This allows one to evaluate the duration of the nucleation stage $\Phi_S \sim K N_S / J_{iv}^S$ and follow it qualitatively. For example, in the austenitic steels $N_S \sim 10^{16} cm^{-3}$ which gives after substituting of J_{iv}^S values from fig.1 $\Phi_S = 0{,}01 \ldots 0{,}7 dpa$ at T=200...600 C, respectively. On the other hand, the "incubation" dose for the establishing of the steady state nucleation rate, Φ_Z, is determined by the Zeldovich factor [7]:

$$\Phi_Z \simeq \frac{K}{2Z^2 W^+(x_c)} = \frac{\pi (R_c^{iv})^3 K}{\alpha_{iv} \Delta^*} = 10^{-3} \ldots 10^{-5} dpa, \quad \begin{cases} T = 200 \ldots 600^\circ C, \\ K = 10^{-6} \frac{dpa}{s}, \end{cases} \qquad (25)$$

One can see that $\Phi_Z \ll \Phi_S$ which means that the nucleation is quasi-steady state, i.e. the nucleation rate at $\Phi_Z \ll \Phi \ll \Phi_S$ is given by the expression (18) where $R_c(t)$ should be substituted for R_c^{iv}. $R_c(t)$ is the critical size, corresponding to the instant number density $N(t)$ [4,5]:

$$R_c(t) = \frac{\bar{R}(t) + R_c^{iv} N_S / 2N(t)}{1 + N_S / 2N(t)} . \qquad (26)$$

It is seen that as long as $N(t) \ll N_S$ $R_c(t)$ is close to its minimum value R_c^{iv}, where as at $N(t) \geq N_S$ $R_c(t)$ increases along with the mean void size $\bar{R}(t)$, and hence $J_{iv}^S(R_c(t)) \to 0$. Thus, N_S is the final number density of voids.

6. Summary

1. Stationary nucleation rate of voids under sufficiently intensive irradiation is derived with account of the image interaction of voids with point defects.
2. The maximum nucleation rate is shown to be independent of irradiation conditions and to be determined mainly by the ratio of point defect relaxation volumes $\Omega_i / |\Omega_v|$.
3. The theory predicts higher nucleation rates for bcc metals as compared to fcc ones owing to the lower $\Omega_i / |\Omega_v|$ values in bcc metals.
4. The evaluated nucleation rate is rather high meaning that the homo-

geneous mechanism may dominate the void nucleation at sufficiently high dose rates (or low temperatures). The presence of mobile gas impurities stabilizing voids against the thermal emission of vacancies extends the region of applicability of the present model.

References

1. Ham F.S. Stress assisted precipitation on dislocations // J.Appl. Phys. 1959. Vol. 30. N6. P. 915-926.
2. Wolfer W.G. Advances in void swelling and helium bubble physics// J.Nucl.Mater. 1984. Vol. 122-123. P. 367-378.
3. Bullough R., Wood M.H. Theory of microstructural evolution // Physics of radiation effects in crystals. - Elsevier Science Publishers B.V. 1986. P. 189-224.
4. Dubinko V.I., Ostapchuk P.N., Slezov V.V. Theory of diffusion evolution of void ensemble in crystals under irradiation // Fiz. Met.Metalloved. (SU) 1988. Vol. 65. Issue 1. P. 32-43.
5. Dubinko V.I., Ostapchuk P.N., Slezov V.V. Theory of radiation-induced and thermal coarsening of the void ensemble in metals under irradiation // J.Nucl.Mater. 1989. Vol.161. P. 239-260.
6. Katz J.L., Wiedersich H. Nucleation of voids in materials supersaturated with vacancies and interstitials // J.Chem.Phys. 1971. Vol. 55. N3. P.1414-1425.
7. Russell K.C. Nucleation of voids in irradiated metals // Acta Met. 1971. Vol. 19. P. 753-758.
8. Dubinko V.I. Void nucleation during high dose rate irradiation of metals (in Russian): Preprint KhFTI-88-62. Kharkov: KhFTI AN UkrSSR, 1988. 11p.
9. Sniegovski J.J., Wolfer W.G. On the physical basis for the swelling resistance of Ferritic steels // Ferritic Alloys for use in nuclear energy technologies conf., Snowbird, U.T., USA, 19-23 june 1983.
10. Krishan K. Ordering of voids and gas bubbles in radiation environments // Radiat.Eff. 1982. Vol.66. P.125-155.

Journal of Nuclear Materials 161 (1989) 239–260
North-Holland, Amsterdam

THEORY OF RADIATION-INDUCED AND THERMAL COARSENING OF THE VOID ENSEMBLE IN METALS UNDER IRRADIATION

V.I. DUBINKO, P.N. OSTAPCHUK and V.V. SLEZOV

Institute of Physics and Technology, the Ukrainian Academy of Sciences, Kharkov 310108, USSR

Received 16 December 1987; accepted 30 June 1988

We propose a new physical mechanism of competition between vacancy voids, namely, the radiation coarsening mechanism which results in the growth of large voids at the expense of small ones due to the preferential absorption of radiation-produced interstitials rather than vacancies. The void preference is inversely proportional to their size, hence, small voids absorb extra interstitial atoms and consequently shrink, whereas large voids absorb extra vacancies and grow. Under typical radiation conditions the radiation coarsening rate is a factor of 10^2–10^4 higher than the rate of the well-known Ostwald coarsening induced by the void thermal emission of vacancies. The radiation coarsening is shown to limit the maximum number density of growing voids to the value dependent only on the dislocation density and material constants and independent of the void nucleation rate. A comparison with experimental data shows that it is this void number density that is formed under irradiation at fairly low temperatures where thermal vacancies may be neglected. The theory also explains the irradiation-induced void shrinkage observed in some experiments.

1. Introduction

According to the conventional theory [1–7], the nucleation and growth of vacancy voids under irradiation are explained by the dislocation bias for self-interstitial atoms (SIA), which allows the dislocations to climb by a net influx of SIA and, hence the voids to grow by a net influx of vacancies. The voids also have a bias for SIA, which is however small compared to that of dislocations in the case of large voids. For this reason, the void bias is either neglected or, at most, its effect is subsumed into the dislocation bias. As shown in the present paper, the conventional approach greatly underestimates an important role of the void bias in the evolution of the void ensemble under irradiation.

The conventional theory of void growth gives only an instant growth rate of a void of radius R, while we are interested in the time behaviour of average characteristics of the void ensemble such as the void density $N(t) = \int_0^\infty f(R, t)\,dR$, the average radius $\bar{R}(t) = N^{-1}\int_0^\infty f(R, t)R\,dR$ and the total void volume $V(t) = (4\pi/3)\int_0^\infty f(R, t)R^3\,dR$, which is equal to the material swelling, where $f(R, t)$ is the size distribution of voids and t is the irradiation time. The swelling rate dV/dt can be derived in a standard approximation as the product of the average void volume growth rate $4\pi\bar{R}^2\,d\bar{R}/dt$ and the void density N, provided that the latter does not change with time. Yet, even in this case one has to know N in order to predict $V(t)$.

It is known that the void nucleation theory gives not N but only a steady-state nucleation rate dN/dt [8,9] which is, according to theory, very sensitive to material constants and impurity content. However, experiments do not indicate this sensitivity, since N usually lies within a rather narrow range 10^{21}–10^{22} m^{-3} at temperatures below the peak swelling value and falls down rather sharply at higher temperatures [1–3,10]. Besides, in some experiments N decreases with irradiation time by a factor of 10 or even 10^2

[11–14], which indicates the existence of a mechanism controlling the void number density after t nucleation is over. This mechanism has been proposed by Dubinko et al. [15,16] and will be referred to the radiation-induced coarsening (RIC) mechanism.

The RIC mechanism results in the growth of large voids at the expense of small ones similarly to well-known mechanism of Ostwald ripening or thermally-induced coarsening (TIC) that is due to a mo intense thermal emission of vacancies from small voids than from large ones. Contrary to the TIC, the RI mechanism is based entirely upon the absorption of point defects and is a result of the inverse proportional size dependence of the void bias $\delta_c = \alpha_{iv}/R$, where α_{iv} is the difference between the constant of void interaction with SIA and vacancies. This dependence makes smaller voids absorb net SIA an shrink, while larger voids absorb net vacancies and grow. The rate of this process is governed by the poin defect generation rate which does not influence the TIC rate. Thus, the RIC is the direct response of avoi ensemble to irradiation and has a cooperative nature, i.e., RIC is significant only when the void densit exceeds a critical N_s value. N_s is determined by the dislocation density $\bar{\rho}$ and the dislocation-to-void bia ratio $\bar{\delta}/\alpha_{iv}$ ($\bar{\delta}$ is the average dislocation bias). This will be shown in section 3, while here we focus ou attention on two important opposite limits, namely, $N \ll N_s$ and $N \gg N_s$.

If $N \ll N_s$, then voids nucleate and grow without competing between themselves. It is only in this case that the void growth rate dR/dt is determined by the difference between the dislocation bias and the void bias. This difference may be positive even for very small voids consisting of a few vacancies (see section 3). At higher temperatures, vacancy emission from voids increases and gas is important in the stabilization of small voids helping them to reach the critical size R_C [1,3]. Note that R_C is practically constant as long as $N \ll N_s$, so the RIC mechanism, unlike the void bias, does not influence a steady nucleation rate.

If $N \gg N_s$, the situation is qualitatively different since now the rate of growth or shrinkage of a void of radius R is determined mainly by the difference between its bias α_{iv}/R and the average void bias $\alpha_{iv}/\bar{R}$. The dislocation bias value is of minor importance here because its statistical weight $\bar{\rho}\bar{\delta}$ is small as compared to that of the void bias $4\pi N\bar{R}\bar{\delta}_c = 4\pi N\alpha_{iv} \gg \bar{\rho}\bar{\delta}$. Therefore, $R_C \simeq \bar{R}(t)$, i.e., dislocations do not significantly influence the competition between voids through the RIC mechanism which reduces $N(t)$ down to $N_s = \bar{\rho}\bar{\delta}/2\pi\alpha_{iv}$ as shown rigorously in section 3. Thus the total void volume grows due to the dislocation bias but the stationary density of the voids cannot exceed the N_s value controlled by the RIC mechanism. The void nucleation rate determines only the time necessary for the formation of N_s voids.

The RIC mechanism influences the evolution of voids at fairly low temperatures (or high dose rates). At higher temperatures, the TIC mechanism dominates. In this paper we are constructing a general theory of the postnucleation evolution of the void ensemble in a crystal with dislocations where both RIC and TIC mechanisms are taken into account.

In section 2, a complete set of equations describing the evolution of voids with account of their elastic interaction with point defects is given in the lowest order of the void volume fraction $V \ll 1$. In this approximation, the expression for dR/dt has the same form in all known models [4–7].

In section 3, different RIC and TIC regimes are described and analytical expressions for $N(t)$, $\bar{R}(t)$, $V(t)$ are given. Besides, we show that the void bias can result in the void swelling reduction with dose if the dislocation bias is suppressed.

In section 4 a comparison of theoretical results with experimental data shows that RIC and TIC mechanisms may control the void evolution not only if swelling is saturated but also if it grows steadily at a rate as large as 1%/dpa. In the latter case, the observed stationary void density was close to the calculated N_s value.

In the Appendix we extend the theory to include the effect of the finite void volume fraction. We show that it suppresses the RIC and enhances the TIC mechanism only insignificantly without distorting the qualitative picture of the void evolution presented in this paper.

36

2. General equations

2.1. The evolution equation

To describe the void ensemble randomly distributed in the coordinate space, we introduce the size distribution function $f(R, t)$. At a postnucleation stage, $f(R, t)$ obeys the continuity equation in the size space [18]:

$$\frac{\partial f(R, t)}{\partial t} + \frac{\partial}{\partial R}\left[f(R, t)\frac{dR}{dt}\right] = 0, \tag{1}$$

$$\frac{dR}{dt} = \frac{\omega}{4\pi R^2}\left[J_v(R) - J_i(R)\right], \tag{2}$$

where the subscripts v and i designate vacancies and SIA, respectively; ω is the atomic volume, $J_n(R)$ (n = i, v) is the point defect (PD) flux into a void of radius R.

2.2. The void bias

The PD flux into a void with due account of the inhomogeneity interaction between the void and PD has been derived by Wolfer [20]:

$$J_n(R) = \frac{4\pi}{\omega} D_n R_n^* (\bar{C}_n - C_{cn}), \tag{3}$$

where $\bar{C}_n$ is the mean PD concentration, and C_{cn} is the equilibrium PD concentration at the void surface. R_n^* is the void effective capture radius resulting from the void interaction with PD:

$$R_n^* = R + \alpha_n,$$

$$\alpha_n \equiv \left(\frac{(1+\nu)\mu\omega}{36\pi T}\right)^{1/3} b\left(\frac{\Omega_n}{\omega}\right)^{2/3}, \tag{4}$$

where μ is the shear modulus, ν the Poisson ratio, Ω_n the PD relaxation volume, b the atomic spacing, T the temperature.

Table 1
Physical constants assumed for nickel and steels [15]

Vacancy diffusivity D_v^o ($m^2 s^{-1}$)	10^{-5}
Vacancy migration energy E_v^m (eV)	1.1
Vacancy formation energy E_v^f (eV)	1.75
Surface energy γ (Jm^{-2})	2.0
Burgers vector b (nm)	0.25
Shear modulus μ ($J m^{-3}$)	10^{11}
Poisson's ratio ν	0.3
Atomic volume ω (m^3)	12×10^{-30}
Interstitial relaxation volume $\Omega_i(\omega)$	1.2
Vacancy relaxation volume $\Omega_v(\omega)$	-0.5
Bulk recombination constant β_r (m^{-2})	10^{21}

The void bias for SIA arises as a consequence of a greater relaxation volume of SIA and is given by the difference

$$\delta_c = \frac{R_i^*}{R} - \frac{R_v^*}{R} = \frac{\alpha_{iv}}{R}, \quad \alpha_{iv} \equiv \alpha_i - \alpha_v. \tag{5}$$

Thus the void bias is inversely proportional to the void size, and it is this point rather than the bias value that plays the central role in the RIC mechanism.

2.3. The dislocation bias

According to Ham [21], Margvelashvily and Saralidze [22], the elastic interaction between a dislocation and PD also leads to a new effective capture radius $L_n/2$, where L_n is the distance from the core where the thermal and elastic energies of PD become equal

$$L_n = \frac{\mu b(1+\nu)}{3\pi T(1-\nu)} |\Omega_n|. \tag{6}$$

Consequently, the influx to a dislocation $J_n(b)$ becomes biased for SIA:

$$J_n(b) = \frac{Z_n^\circ}{\omega} D_n(\bar{C}_n - C_{dn}), \tag{7}$$

$$Z_n^\circ = 2\pi / \ln\left(\frac{2R_{dn}^\circ}{L_n\sqrt{e}}\right), \tag{8}$$

where R_{dn}° is the radius of the dislocation supply region [6,7], C_{dn} is the PD equilibrium concentration at the dislocation core.

To derive eqs. (7), (8), one has to assume that dislocations are homogeneously distributed in a crystal. Only this case admits the consideration of a dislocation structure as an ensemble of "isolated" dislocations interacting only with the single selfconsistent diffusion field. The bias of an isolated dislocation is given by

$$\delta_0 = Z_i^\circ - Z_v^\circ = \frac{Z_i^\circ Z_v^\circ}{2\pi} \ln\left(\frac{R_{dv}^\circ L_i}{R_{di}^\circ L_v}\right). \tag{9}$$

The δ_0 value is essentially determined by the $\Omega_i/|\Omega_v|$ ratio and is independent of irradiation conditions as distinct from the mean dislocation bias $\bar{\delta}$, which is observed to increase with the temperature rise and decrease with irradiation dose [23].

In our opinion, the point is that the dislocation structure is generally very inhomogeneous and involves dislocation pile-ups, rafts, dipoles, networks, etc. [24,25].

Naturally, the bias should be different for different substructures resulting in a complex nature of the mean bias $\bar{\delta} = \sum_m \rho_m \delta_m / \bar{\rho}$, where $\rho_m/\bar{\rho}$ is the relative fraction of dislocations with the bias δ_m, $\bar{\rho} = \sum_m \rho_m$ is the mean dislocation density. The existence of the bias spectrum is confirmed by experimental observations of the radiation-induced evolution of the dislocation structure in the absence of voids [1,8,26] which requires, at least, two components with different biases δ_1 and δ_2.

Below we distinguish two structural components, namely, "isolated" and "sessile" ones with densities ρ_0 and ρ_s, respectively. The isolated dislocations have the standard bias δ_0, whereas the bias of the sessile dislocation is such as to compensate the biases of voids and isolated dislocations, thereby equalizing the influxes of SIA and vacancies to the sessile dislocations. Such substructures are stable under irradiation and are the result of the evolution of the dislocation structure. The known example is the dislocation loop

piles [24,25] with the bias δ_l which decreases as the loop size r_l grows: $\delta_l = \delta_0 \lambda / 2\pi r_l$ (λ is the loop spacing), and thus, the piles gradually become stable, i.e., sessile:

$$\delta_l(t) \to \delta_s = \frac{\rho_0 \delta_0 + 4\pi N \alpha_{iv}}{\rho_0 + 4\pi N \bar{R}}. \tag{10}$$

Generally, we believe that any sufficiently dense dislocation substructure may become sessile, since its bias should decrease as the dislocations draw together shadowing each other against PD fluxes. Another possible reason of the sessile dislocation formation resides in impurity atoms and precipitates which may impede the dislocation glide and climb.

The role of sessile dislocations consists in the enhancements of the PD recombination rate which reduces the supersaturation. Besides, it acts as a sink for the isolated dislocations whose density ρ_0 is determined by the equilibrium between the dislocation sources (SIA-loop nucleation, etc.) and sinks (mutual annihilation, escape to the grain boundary or integration with a sessile component). The mean dislocation bias $\bar{\delta} = (\delta_0 \rho_0 + \delta_s \rho_s)/\bar{\rho}$ is close to δ_0 at an initial stage, when the isolated SIA loops are the main components of the dislocation structure, so that $\rho_0 \gg \rho_s$. As the loops grow to form the dislocation network, the inequality becomes reverse $\rho_s \gg \rho_0$, resulting in the mean bias decrease $\bar{\delta}(t) \to \delta_s \ll \delta_0$, even if the mean dislocation density $\bar{\rho} = \rho_0 + \rho_s$ remains constant. At higher temperatures the sessile structures become unstable [25] and do not form, hence $\bar{\delta}(T)$ increases up to the δ_0 value, which is in agreement with the experimental data [23].

The main advantage of this phenomenological model of the dislocation structure is its ability to describe the observed evolution of $\bar{\delta}(t)$ in terms of physically transparent parameters ρ_0 and ρ_s which can be measured from experiment.

2.4. The boundary concentrations of point defects

A crystal under irradiation is a nonequilibrium system, though quasi-equilibrium PD concentrations are sustained near the macrodefect boundaries if the rate of the boundary kinetics is higher than the rate of PD arrival from the matrix [6,7]. In this diffusion-limited approximation, the boundary conditions for voids and dislocations in the absence of external stresses are given by

$$C_{cn} = C_n^e \exp\left(\pm \frac{\alpha}{R}\right); \quad \alpha \equiv \frac{2\gamma\omega}{T}, \tag{11}$$

$$C_{dn} \approx C_n^e = \exp\left(-\frac{E_n^f}{T}\right), \tag{12}$$

where the plus and minus signs correspond to vacancies (n = v) and SIA (n = i), respectively; C_n^e is the equilibrium PD concentration at the flat surface or the straight edge dislocation, E_n^f is the PD formation energy, γ is the surface energy.

2.5. The rate equations

At a constant PD generation rate K, the mean PD concentrations obey the quasistationary rate equations if $d\bar{C}_n/dt \ll K$ [15]:

$$K = \int_0^\infty f(R, t) J_n(R)\, dR + \rho_0 J_n(b) + \rho_s J_s + \beta_r (D_v + D_i) \bar{C}_i \bar{C}_v, \tag{13}$$

where β_r is the recombination constant. The fluxes to the sessile dislocations do not depend on the PD type:

$$\omega J_s = Z_v^s D_v(\bar{C}_v - C_{dv}) = Z_i^s D_i(\bar{C}_i - C_{di}). \tag{14}$$

Eq. (14) may be expressed in terms of the well known sink strengths [4,5]:

$$K = k_n^2 D_n \bar{C}_n + \rho_s J_s + \beta_r(D_v + D_i)\bar{C}_i\bar{C}_v - K_n^e, \tag{15}$$

where k_n^2 is the sum of void and isolated dislocation sink strengths for PD:

$$k_n^2 = 4\pi\int_0^\infty f(R, t)R_n^* \, dR + Z_n^\circ\rho_0, \tag{16}$$

K_n^e is the PD emission rate from voids and isolated dislocations:

$$K_n^e = k_n^2 D_n \bar{C}_n^e, \tag{17}$$

$$\bar{C}_n^e = C_n^e\left(4\pi\int_0^\infty f(R, t)R_n^* \, e^{\pm\alpha/R} \, dR + Z_n^\circ\rho_0\right)/k_n^2, \tag{18}$$

where $\bar{C}_n^e$ is the mean concentration of thermal PD.

Eqs. (1)–(4), (8), (14)–(18) makes a complete set describing the evolution of $f(R, t)$ for the given irradiation conditions K, T, the dislocation parameters ρ_0, ρ_s and the bias factors δ_0, α_{sv}. In the next section we shall show that owing to the RIC mechanism, the size distribution of voids under irradiation takes the universal form obtained with the mathematical formalism of Lifshits and Slezov [18].

3. The postnucleation evolution of the void ensemble

3.1. The void growth rate

Let us present the void growth rate as a sum of two terms after adding and subtracting $\bar{C}_n^e$ to $\bar{C}_n$ in eq. (3) and substituting eq. (3) in eq. (2). We obtain then

$$\frac{dR}{dt} = \dot{R}_T + \dot{R}_K,$$

where $\dot{R}_T$ depends only on the thermal PD concentrations and is given by

$$\dot{R}_T = \frac{D_v R_v^*}{R^2}(\bar{C}_v^e - C_{cv}) - \frac{D_i R_i^*}{R^2}(\bar{C}_i^e - C_{ci}), \tag{19}$$

while $\dot{R}_K$ depends on the PD production rate:

$$\dot{R}_K = \frac{1}{R^2}(\Delta_v^* R_v^* - \Delta_i^* R_i^*), \quad \Delta_n^* \equiv D_n(\bar{C}_n - \bar{C}_n^e). \tag{20}$$

Now we substitute $\bar{C}_n^e$ in eq. (18) into eq. (19) and expand the exponent α/R neglecting the terms $\alpha\alpha_n/R^2$. Then $\dot{R}_T$ takes the form

$$\dot{R}_T = \frac{\alpha}{R}\left[D_v C_v^e\left(\frac{4\pi N}{k_v^2} - \frac{1}{R}\right) + D_i C_i^e\left(\frac{4\pi N}{k_i^2} - \frac{1}{R}\right)\right]. \tag{21}$$

The relation between Δ_v^* and Δ_i^* follows from eqs. (15):

$$\Delta_v^* k_v^2 = \Delta_i^* k_i^2. \tag{22}$$

Substituting it into eq. (20) and performing some algebraic operations we obtain

$$\dot{R}_K \simeq \frac{\Delta^* \alpha_{iv}}{R}\left(1 + \frac{\alpha_i}{R_C^{RIC} - \alpha_i}\right)\left(\frac{1}{R_C^{RIC}} - \frac{1}{R}\right), \tag{23}$$

$$R_C^{RIC} \equiv \frac{\alpha_{iv}}{1 - k_v^2/k_i^2} + \alpha_i, \tag{24}$$

where R_C^{RIC} is the bias-induced void critical radius.

Physically, it is evident that the difference between k_v^2 and k_i^2 is important only for $\dot{R}_K$, whereas in $\dot{R}_T$ is may be safely neglected. Besides, $R_C^{RIC} \gg \alpha_i - b$, therefore we neglect the term α_i/R_C^{RIC} in eq. (23). Then adding $\dot{R}_K$ and $\dot{R}_T$ and using eq. (16) we obtain the following growth rate expression for a macroscopic void ($R \gg \alpha,\ \alpha_n$):

$$\frac{dR}{dt} \simeq \frac{1}{R}(\Delta^* \alpha_{iv} + D^* \alpha)\left(\frac{1}{R_c} - \frac{1}{R}\right), \tag{25}$$

$$\Delta^* \equiv \Delta_v^* \simeq \Delta_i^*,\quad D^* \equiv D_v C_v^e + D_i C_i^e,$$

$$R_C = \left(\bar{R} + R_C^{min}\frac{N_\rho}{N}\right)\Big/\left(1 + \frac{N_\rho}{N}\right), \tag{26}$$

$$R_C^{min} \equiv R_C|_{N=0} = Z^\circ(\Delta^* \alpha_{iv} + D^* \alpha)/\Delta^* \delta_0, \tag{27}$$

$$N_\rho \equiv \Delta^* \rho_0 \delta_0 / 4\pi(\Delta^* \alpha_{iv} + D^* \alpha), \tag{28}$$

where D^* is the thermal self-diffusivity of the PD, while Δ^* may be called the "radiation-induced self-diffusivity" of the PD, whose dependence on the PD type will be neglected below, since the void and dislocation bias effects have already been taken into account when deriving eqs. (25)–(28). The explicit form for Δ^* is given by any of the rate eqs. (15) and (17)

$$\Delta^* \simeq \frac{1}{2}\left[D^* + \frac{D_v D_i (k_c^2 + k_d^2)}{\beta_r (D_v + D_i)}\right](-1 + \sqrt{1 + \chi}), \tag{29}$$

$$\chi \equiv \frac{4 K D_v D_i}{\beta_r (D_v + D_i)\left[D^* + \frac{D_v D_i (k_c^2 + k_d^2)}{\beta_r (D_v + D_i)}\right]^2}, \tag{30}$$

$$k_c^2 \equiv 4\pi \int_0^\infty f(R, t) R\, dR,\quad k_d^2 \equiv Z^\circ \rho_0 + Z^\prime \rho_s, \tag{31}$$

where k_c^2 and k_d^2 are the sink strengths of voids and dislocations, respectively, the elastic interaction with the PD being neglected.

The critical void radius R_C has the minimum value R_C^{min} at $N = 0$. At low temperatures ($\Delta^* \alpha_{iv} \gg D^* \alpha$) R_C^{min} is determined by the α_{iv}/δ_0 ratio which is practically constant if $\Omega_i/|\Omega_v| = 1 - 10$:

$$\frac{\alpha_{iv}}{\delta_0} = \frac{2\pi \alpha_i}{Z_i^\circ Z_v^\circ}\frac{1 - (\Omega_v/\Omega_i)^{2/3}}{\ln(\Omega_i/|\Omega_v|)} \simeq b - \tfrac{1}{2}b. \tag{32}$$

It is seen that the void bias does not suppress the void nucleation if there are isolated dislocations in the crystal.

Eq. (26) shows that R_C is close to R_C^{min} as long as $N \ll N_\rho$, i.e., until there are enough extra vacancies supplied by the isolated dislocations.

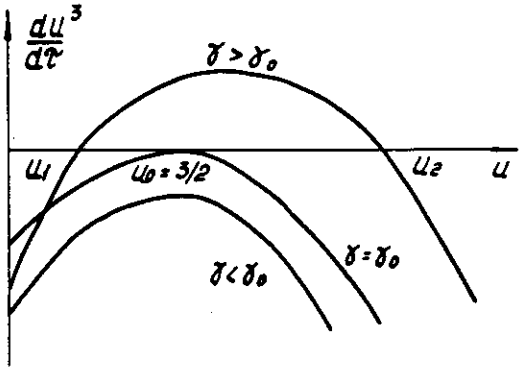

Fig. 1. The void growth rate $du^3/d\tau = \gamma(\pi)(u-1) - u^3$ in terms of the variables $u = R/R_C$, $\tau = 3\ln(R_0/R_C^{min})$ at different γ values. At $dV/dt = 0$ and $\tau^2 \gg 1$, $\gamma(\tau)$ is shown to approach $\gamma_0 = 27/4$ from below for any initial size distribution [18]. This result is still valid if $\rho_0(t)$ is a monotonously decreasing function of time (see section 3). The universal behaviour of $\gamma(\tau)$ at $\tau^2 \gg 1$ leads to the analytical expressions for the size distribution function and its momenta $N(t)$, $\bar{R}(t)$ and $V(t)$ [16,18,27].

In the opposite limit, $N \gg N_\rho$, R_C is close to $\bar{R}$; this means that voids of $R > \bar{R}(t)$ grow at the expense of voids of $R < \bar{R}(t)$, which shrink as a result of the competition for vacancies. The competition rate is determined by the sum $\Delta^* \alpha_{iv} + D^* \alpha$, where the first term corresponds to the RIC, and the second one to the TIC mechanism.

So, the void bias, firstly, reduces the void density N_ρ above which the competition takes place and, secondly, it enhances the competition rate by the $\Delta^* \alpha_{iv}$ value depending on the PD production rate.

The $N/N_\rho \equiv \beta$ ratio may be considered as a controlling parameter, since it determines the character of void evolution. Namely at $\beta \ll 1$ all voids of $R > R_C \approx R_C^{min} =$ constant grow in agreement with the conventional theory. In the opposite limit, $\beta \to \infty$, taking place when all dislocations are sessile ($N_\rho \sim \rho_0 = 0$), the conventional theory predicts that irradiation does not influence the void ensemble, whereas, in accordance with our theory, the effect of the RIC mechanism in this case is the largest. Let us consider it in greater detail and compare with the TIC mechanism.

3.2. The "pure" coarsening regime, $\rho_0 = 0$

In this case, the void ensemble as a whole absorbs SIA and vacancies in equal amounts thus conserving its volume with time:

$$dV/dt = 4\pi \int_0^\infty f(R, t) R^2 \frac{dR}{dt} dR = 0,$$

i.e., $V = V_0 =$ constant. However, due to the competition, $N(t)$ diminishes, while $\bar{R}(t) = R_c(t)$ grows. Gradually, the initial size distribution $f_0(R)$ becomes "forgotten" i.e., $f(R, t)$ takes the universal form [16] that does not depend on $f_0(R)$ (see fig. 1). Consequently, the momenta $\bar{R}(t)$ and $N(t)$ depend only on what sinks dominate the PD balance at the time. Consider two limits.

3.2.1. Recombination limit

It is valid if most PD recombine in the bulk or at dislocations of a stationary density $\bar{\rho} = \rho_s$, the condition being

$$k_c^2 \ll K/\Delta_s^*, \tag{33}$$

where

$$\Delta_s^* \equiv \frac{Z^s \rho_s D_v D_i}{2\beta_r (D_v + D_i)} \left(-1 + \sqrt{1 + \frac{4K\beta_r (D_v + D_i)}{D_v D_i (Z^s \rho_s)^2}} \right). \tag{34}$$

In this case, $\Delta^* \approx \Delta_s^* = \text{constant}$, while [16]

$$\bar{R}(t) = \left[\tfrac{4}{9}(\alpha_{iv}\Delta_s^* + D^*\alpha)t\right]^{1/3}; \quad \frac{\bar{R}^3}{(\bar{R})^3} \equiv C_3 = 1.11, \tag{35}$$

$$N(t) = \frac{27V_0}{16\pi C_3(\alpha_{iv}\Delta_s^* + \alpha D^*)t}. \tag{36}$$

At $K = 0$ ($\Delta^* = 0$) or $\alpha_{iv} = 0$, eqs. (35) and (36) coincide with the known expressions of the TIC theory [18]. Under irradiation ($K > 0$, $\Delta^* > 0$), it is the void bias ($\alpha_{iv} > 0$) which results in the RIC, the rate of the latter $\alpha_{iv}\Delta^*$ being a function of the PD production rate.

3.2.2. Void domain limit: $k_c^2 \gg K/\Delta_s^*$

In this limit the supersaturation is mainly determined by the sink strength of the voids:

$$\Delta^*(t) \approx K/4\pi N(t)\bar{R}(t), \tag{37}$$

and, hence, changes with time. This causes a more rapid variation of $\bar{R}$ and N with time in the RIC region $\Delta^*\alpha_{iv} \gg D^*\alpha$:

$$\bar{R}(t) = \frac{4C_3}{81}\frac{\alpha_{iv}Kt}{V_0}; \quad N(t) = \frac{3V_0}{4\pi C_3\bar{R}(t)^3} \sim t^{-3}. \tag{38}$$

However, the void domination is transient since its sink strength decreases with time $k_c^2(t) \sim t^{-2}$, and subsequently, at $t > (\Delta_s^*/K^3)^{1/2}V_0^{3/2}/\alpha_{iv}$ the void evolution enters in the recombination limit, eqs. (33)–(36).

3.2.3. Region of applicability

The irradiation time t_c required to attain the universal regime, i.e., to "forget" the initial size distribution, can be estimated from the criterion of smallness of the parameter of the asymptotic solution of the set eqs. (1), (25)–(31) [16,18]:

$$\tau^{-2} = \left(3\ln\left(\bar{R}(t_c)/\bar{R}_0\right)\right)^{-2} = 10^{-1}. \tag{39}$$

According to eqs. (35) and (38), the dose of the RIC regime onset is given by (if $\alpha = 0$)

$$Kt_c = \phi_K = \begin{cases} \dfrac{9\times 13}{2}\dfrac{K\bar{R}_0^3}{\Delta_s^*\alpha_{iv}} & \text{at} \quad k_c^2 \ll \dfrac{K}{\Delta_s^*}, \\ \dfrac{81\times 13}{2}\dfrac{V_0\bar{R}_0}{\alpha_{iv}C_3} & \text{at} \quad k_c^2 \gg \dfrac{K}{\Delta_s^*}, \end{cases} \tag{40}$$

whereas the TIC regime begins (if $\alpha_{iv} = 0$) at a dose of $Kt_c = \phi_T$, where

$$\phi_T = \frac{9\times 13}{2}\frac{K\bar{R}_0^3}{D^*\alpha}. \tag{41}$$

The RIC and TIC regions on the K, T plane are shown schematically in fig. 2, where it can be seen that the peak swelling coordinates of nickel (and consequently, of most steels) lie deeply in the RIC region. The peak ϕ_K and ϕ_T values are listed in table 2 for the initial parameters $V_0 = 10^{-2}$, $\bar{R}_0 = 1$ nm. The ratio $\phi_K/\phi_T \approx \alpha D^*/\alpha_{iv}\Delta^* \sim 10^{-3}$ equals the TIC-to-RIC rate ratio, which shows that the RIC mechanism entirely dominates under typical irradiation conditions.

It is clear that the "pure" coarsening regime may take place not only if ρ_0 rigorously equals zero, but also if ρ_0 falls off rather rapidly with time: $\rho_0(t) \sim t^{-m}$, where m must be greater than 1 in the

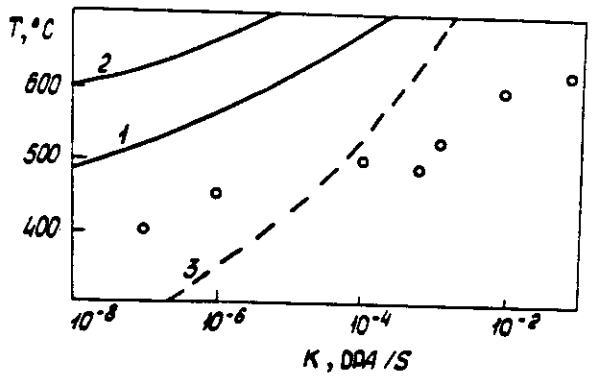

Fig. 2. Graph showing RIC and TIC regions in the K, T plane. The TIC region is above curve 1 if $k_c^2 = 10^{14}$ m^{-2}. At $\rho_0 = 0$, $k_c^2(t) \to 0$ and curve 1 turns into curve 2. Curve 3 separates the regime of void domination (above) from the recombination regime (below) at $k_c^2 = 10^{14}$ m^{-2}. Points (○) denote the experimentally observed swelling peak parameters T, K for nickel [2].

recombination limit and 3 in the void domination limit. In these cases, according to eqs. (36) and (38), $\beta(t) = N(t)/N_\rho(t) \to \infty$ and these equations are still valid, the only correction being the substitution of the final void volume

$$V_\infty = V_0 + \int_0^\infty \frac{dV}{dt} dt = \text{constant}$$

for the initial one V_0.

We shall show in section 4 that the "pure" coarsening regime is observed in some experiments but here we would like to emphasize its methodological importance. According to the conventional view, irradiation itself does not influence the void ensemble in the absence of alternative PD sinks. Taking account of the void bias qualitatively changes this viewpoint, showing that irradiation makes voids compete between themselves thus leading to a decrease in their density $N(t)$ at a rate some orders of magnitude greater than the TIC rate. A driving force of the TIC process is the reduction of the free energy of the system through the reduction of the surface energy of voids per unit volume. By contrast, under irradiation the evolution of a void ensemble is driven by the void bias, the mean value of which $\alpha_{iv}/\bar{R}(t)$ decreases in the RIC process in accordance with the general Le Châtelier principle. This kinetic criterion replaces the energetic one and determines the direction of time changes in the open dissipative system, which a crystal under irradiation is.

3.3. Void coarsening in a real crystal

Obviously, the void formation does not take place if $\rho_0 = 0$, since in this case $V_0 = \text{constant} = 0$. On the other hand, the presence of isolated dislocations under irradiation is equivalent to the production of extra vacancies, due to which small voids tend to grow faster than large ones because of the factor R^{-1} in the expression for void growth eq. (25). A balance between this stabilizing factor and the destabilizing effect of

Table 2
Typical dose levels required to reach the universal coarsening regime as calculated by eqs. (40) and (41) at different temperatures, K corresponding to the peak swelling of nickel. ϕ_T is the TIC onset dose for $\alpha_{iv} = 0$. ϕ_K is the RIC onset dose for $\alpha = 0$

K (dpa/s)	10^{-7}	10^{-6}	10^{-3}	10^{-2}
T (°C)	400	450	525	600
ϕ_T (dpa)	430	144	1770	512
ϕ_K (dpa)	0.8	0.8	0.4	0.6
ϕ_T/ϕ_K	540	180	4×10^3	850

the RIC mechanism determine the maximum density of voids which can grow at given irradiation conditions. We may state a theorem.

Theorem 1. A stationary void density cannot exceed $2N_\rho$.

Proof. We rewrite eq. (26) in the form

$$N = \frac{N_\rho}{\bar{u}-1}\left(1 - \frac{R_C^{\min}}{R_C(t)}\right), \quad \bar{u} \equiv \frac{\bar{R}(t)}{R_C(t)}, \tag{42}$$

where, by definition, $R_C(t) > R_C^{\min}$, the inequality increasing with time. We are interested in the behaviour of the mean dimensionless void radius $\bar{u}(t)$. A void growth rate $du^3/d\tau$ as a function of u and τ is depicted in fig. 1. It is seen that if the $du^3/d\tau$ curve does not intersect the abscissa, then $R_C(t)$ grows faster than any void radius making voids shrink at $R_C > R$. As a result, $N(t)$ decreases. To stop this shrinkage, a stable point u_2 must exist, which attracts both small ($u < u_2$) and large ($u > u_2$) voids. Consequently, the mean void radius eventually reaches this point $\bar{u}(t) \to u_2$, where voids grow at the same rate as their critical radius: $\bar{R}(t)/R_C(t) = \bar{u} = u_2 = \text{const}$. According to eq. (42), a stationary density of growing voids at $R_C(t) \gg R_C^{\min}$ is given by $N_s = N_\rho(u_2 - 1)^{-1}$, where $u_2 > 3/2$ as follows from fig. 1. This means that $N_s \leqslant 2N_\rho$ which was to be proved.

Thus, the maximum density of growing voids N_s does not depend on the void nucleation rate which determines only the time it takes to reach N_s from below. After that N remains constant if $N_\rho = \text{constant}$. However, N_ρ depends on the density of isolated dislocations which can vary with time due to the evolution of the dislocation structure. If $N_\rho(t)$ increases substantially, then the critical void radius becomes small making possible the nucleation of $N_\rho - N$ new voids. On the other hand, if $N_\rho(t)$ decreases, then an extra number of voids $N - N_\rho$ has to shrink. The time necessary for it can be estimated on the assumption of $N \gg N_\rho$ at the beginning of the process, which means that $N(t)$ decreases by the law of "pure" coarsening given by eqs. (36) and (38). The necessary time t_ρ is then a root of the equation $N(t_\rho) = 2N_\rho$, i.e.,

$$t_\rho \sim 3V_0/\Delta_s^*\rho_0\delta_0 \quad \text{at} \quad k_c^2 \ll K/\Delta_s^*, \tag{43}$$

$$t_\rho \sim \frac{3\gamma_0 V_0^{4/3}}{K}\left(\alpha_{iv}^2\rho_0\delta_0\right)^{-1/3} \quad \text{at} \quad k_c^2 \gg K/\Delta_s^*, \tag{44}$$

where V_0 is the initial void volume which does not vary significantly for the time t_ρ.

The limit, eq. (44), is characteristic of reactor irradiation. For the nickel constants $\Omega_i = 1.2\omega$, $\Omega_v = -0.5\omega$, and $V_0 \leq 1\%$, $\rho_0 \geq 10^{13}\ \text{m}^{-2}$, the necessary dose is $Kt_\rho \leqslant 3$ dpa. The estimate, eq. (43), corresponds to imitation experiments. For example, at $K = 2 \times 10^{-3}$ dpa/s and peak temperature $T = 525\,^\circ\text{C}$ in nickel, $Kt_\rho \leqslant 5$ dpa. Thus, the shrinkage of extra voids takes a very little dose compared to doses of substantial dislocation structure changes at the late stage of irradiation [10].

According to eq. (28), in the RIC region $\alpha D^*/\alpha_{iv}\Delta^* \ll 1$, N_ρ tends to the universal limit determined only by the density of isolated dislocations and material constants:

$$N_\rho \to \frac{\rho_0\delta_0}{4\pi\alpha_{iv}}, \quad \text{if} \quad \frac{D^*\alpha}{\Delta^*\alpha_{iv}} \to 0. \tag{45}$$

A typical ρ_0 value at a steady stage of swelling is about $10^{13}\ \text{m}^{-2}$ (see section 4) which gives, in view of eq. (32), a reasonable estimate for $N_\rho \sim 10^{22}\ \text{m}^{-3}$.

Swelling sometimes shows a tendency for saturation with dose, which, according to our theory, should cause a reduction in $N(t) - N_\rho(t)$. This can easily be seen from eq. (28), where the numerator $\Delta^*\rho_0\delta_0$ is the swelling rate, and the denominator is the rate of void coarsening. If $\rho_0(t) = \rho_0(t_0)(t_0/t)^m$ monotonously decreases with time ($m > 0$), then voids enter the coarsening regime with decreasing sources, which was described by Slezov and Shikin [27] with account of the TIC mechanism only. The consideration of the

RIC mechanism within the same mathematical scheme (see fig. 1) leads to the following expression for the void density:

$$N(t) = \frac{\Delta^* \delta_0 \rho_0(t)}{\Delta^* \alpha_{iv} + D^* \alpha} \frac{1}{4\pi(\bar{u}-1)}, \tag{46}$$

where $\bar{u}$ lies within the limits $1 < \bar{u} < 3/2$ unlike the $\rho_0 =$ constant case, where $\bar{u} \geqslant 3/2$. The exact $\bar{u}$ value depends on the power "m" and on the type of sinks dominating in the PD balance. Let us consider two opposite limits.

3.3.1. Recombination limit: $k_c^2 \ll K/\Delta_s^*$

$$\bar{u} = 1 + \frac{C_{3m}}{\gamma_0}(1-m)\bar{u}^3, \quad \gamma_0 = 27/4, \tag{47}$$

where $1 \leqslant C_{3m} \leqslant 1.11$, if $0 \leqslant m \leqslant 1$.

$$\bar{R}(t) = \bar{u}\left\{\tfrac{4}{9}(\Delta_s^* \alpha_{iv} + D^* \alpha)t\right\}^{1/3}, \tag{48}$$

$$V(t) = \delta_0 \Delta_s^* \int_0^t \rho_0(t')\,\mathrm{d}t', \tag{49}$$

Eq. (47) is not valid in the case of $m > 1$, which corresponds to the pure coarsening regime (see section 3.2.3), where $\bar{u} = 1$. In the opposite case, $m = 0$ ($\rho_0 =$ constant), $\bar{u} = 3/2$. $N = N_s$ and swelling increases at a constant rate $\mathrm{d}V/\mathrm{d}Kt = \delta_0 \rho_0 \Delta_s^* K^{-1}$. This rate is independent of irradiation conditions K and T at intermediate temperatures, where $\Delta_s^* \sim K\rho_s^{-1}$, so $\mathrm{d}V/dKt \approx \delta_0 \rho_0/\rho_s$. At the same time, both N and $\bar{R}$ strongly depend on temperature if $D^*\alpha \gg \Delta^* \alpha_{iv}$ due to the TIC mechanism. As we shall see in section 4, such trends are observed experimentally though they have not been explained by theory so far.

3.3.2. Void domination limit: $k_c^2 \gg K/\Delta_s^*$

In the RIC region ($\Delta^* \alpha_{iv} \gg D^* \alpha$), $\bar{u}$ is given by the following equation at $0 \leqslant m \leqslant 3$:

$$\bar{u} = 1 + \frac{(3-m)C_{3m}}{3\gamma_0(m+1)}\bar{u}^3, \quad 1 \leqslant C_{3m} \leqslant 1.11. \tag{50}$$

In this case the relationship between $\bar{R}(t)$ and $V(t)$ has the same form as in the pure coarsening regime, eq. (38), except for the numerical factor:

$$\bar{R}(t) = \frac{4C_{3m}\bar{u}^3}{3\gamma_0(m+1)} \frac{\alpha_{iv} Kt}{V(t)}. \tag{51}$$

Since eqs. (48) and (51) do not depend on the theory external parameters ρ_0, ρ_s, they can unambiguously be verified by experiment (see section 4). The explicit expressions for $\bar{R}(t)$ and $V(t)$ are

$$\bar{R}(t) = \left\{\frac{\alpha_{iv} Kt}{\delta_0 \rho_0(t)}\right\}^{1/4} \psi(m); \quad \psi(m) \equiv \bar{u}^{3/2}\left[\frac{4(3-m)C_{3m}}{3(m+1)^2\gamma_0^2}\right]^{1/4}. \tag{52}$$

$$V(t) = \tfrac{2}{3}\left[\alpha_{iv}^2 \delta_0 \rho_0(t)\right]^{1/4}(Kt)^{3/4}\phi(m); \quad \phi(m) \equiv \frac{C_{3m}\psi^3(m)}{2(\bar{u}-1)}. \tag{53}$$

At $m > 3$, the pure coarsening regime takes place, where $\bar{u} = 1$. At $m = 0$, the void number density is constant, i.e., $N = N_s$, $\bar{u} = 3/2$, $\psi(0) = \phi(0) = 1$, but the swelling rate decreases with dose: $\mathrm{d}V/\mathrm{d}Kt \sim (Kt)^{-1/4}$.

The type of the regime depends on initial conditions and the m value. At $m > 1/3$, $k_c^2(t) \to 0$; so the void domination regime is inevitably replaced by the recombination regime. On the other hand, at $m < 1/3$, $k_c^2(t)$ increases, so the void domination regime is the final one. A change of regimes takes place when $k_c^2(t) = K/\Delta_s^*$. If $m = 1/3$, $k_c^2 =$ constant, and hence there can be only one regime which is determined by the initial relation between k_c^2 and K/Δ_s^*.

In a particular case of constant ρ_0 ($m = 0$), the void domination regime is the final one with $\Delta^*(t)$ decreasing as $t^{-1/4}$. Thus, voids inevitably enter the TIC region when $\alpha_{iv}\Delta^*(t) \ll D^*\alpha =$ constant, and we obtain the result of Ryazanov and Maksimov [28]:

$$\bar{R}(t) = \left(\tfrac{1}{2}D^*\alpha t\right)^{1/3}; \quad N(t) = \left(\frac{K\delta_0\rho_0}{2\pi D^*\alpha \bar{R}(t)}\right)^{1/2}. \tag{54}$$

The dose required to reach this limit $(Kt)_T$ strongly depends on the temperature,

$$(Kt)_T = \left(\frac{\alpha_{iv}^2}{\delta_0\rho_0}\right)^3\left(\frac{K}{D^*\alpha}\right)^4, \tag{55}$$

and is attainable only at sufficiently high temperatures.

Above we have shown that N can reach the N_s value early enough if the void nucleation rate is sufficiently high, and a subsequent void evolution is described by our theory irrespective of a specific nucleation mechanism. The range of the theory applicability may be determined from a direct and unambiguous comparison with experimental data.

Before analysing the experimental data, we shall discuss another important consequence of the void bias to SIA.

3.3.3. Radiation-induced void shrinkage

So far we considered a very simple model of the dislocation structure where the bias of isolated dislocations was due only to elastic interaction with PD, whereas dislocations interacting between themselves were supposed to be immobile, i.e., sessile. In this case, according to eq. (27), $R_C^{min} =$ constant leads to the late-stage approximation $\bar{R}(t)/R_C^{min} \gg 1$. However, in reality, the dislocation bias may depend on various factors such as dislocation core structure, impurities, etc. For example, impurity atoms may screen the elastic field of dislocations making them neutral sinks for PD. Contrary to sessile dislocations, the neutral ones can absorb extra vacancies if voids are biased towards SIA. Naturally, the void volume $V(t)$ decreases in this case. To consider this situation, we write the swelling rate expression following from eq. (25) in the first approximation of $\rho_0/k_c^2 \ll 1$:

$$\frac{dV}{dt} \approx \Delta^*\rho_0\delta_0\left(1 - \frac{Z^\circ(\Delta^*\alpha_{iv} + D^*\alpha)}{\Delta^*\delta_0\bar{R}(t)}\right). \tag{56}$$

If $\rho_0 = 0$, then we obtain the pure coarsening regime, where $dV/dt = 0$. Now consider the case $\delta_0 = 0$, where we have

$$\frac{dV}{dt} = -\frac{Z^\circ\rho_0}{\bar{R}(t)}(\Delta^*\alpha_{iv} + D^*\alpha) < 0. \tag{57}$$

At $K \neq 0$ ($\Delta^* = 0$), eq. (57) describes the void shrinkage during annealing induced by the void surface tension. If voids and dislocations are neutral ($\alpha_{iv} = 0$, $\delta_0 = 0$), then irradiation does not effect their evolution. The void bias at $\delta_0 = 0$ results in a radiation-induced void shrinkage at a rate $\Delta^*\alpha_{iv}/D^*\alpha$ times greater than the thermal one.

Though $V(t)$ decreases, larger voids can grow by the RIC mechanism for some time, and thus $\bar{R}(t)$ may increase, at least at the beginning of the process, and strongly depends on the initial size distribution of

voids. We have considered the limit $\delta_0 = 0$, though according to eq. (56), $dV/dt < 0$ if the dislocation bias is smaller than the threshold value δ_{th}:

$$\delta_0 < \delta_{th} \equiv \frac{Z^{\circ}(\Delta^* \alpha_{iv} + D^* \alpha)}{\Delta^* \bar{R}(t)} \tag{58}$$

4. Comparison with experimental data

We begin with the experiments where irradiation results in the $N(t)$ decrease, which is the most obvious consequence of the RIC mechanism. The only alternative process here is the coalescence of neighbouring voids, which is however insignificant at $V \ll 1$, since the distances between voids are far greater than their sizes.

Such an experiment was performed by Arkell and Williams [29] who irradiated samples of ferritic steel FV 607 with 1 meV electrons ($K = 5 \times 10^{-3}$ dpa/s) at $T = 300$–$500\,^{\circ}$C to the doses of 30–40 dpa. Swelling was observed at temperatures up to 500 °C with the peak values lying in the range of 400–450 °C. A 2-hour annealing at 550 °C of samples irradiated at 450 °C resulted in no appreciable changes of the void parameters: $V_0 = 4\%$, $R_0 = 7$ nm, $N_0 = 3 \times 10^{22}$ m^{-3}. It was concluded that at 550 °C a thermal shrinkage of voids was negligible and could not prevent the void growth under irradiation at this temperature. Besides, the 2-hour irradiation at 550 °C ($Kt = 30$ dpa) performed after the 450 °C irradiation resulted in: (i) a shrinkage of 75% of voids, (ii) a growth of remaining voids; (iii) a decrease of swelling by 50%.

Hains and Williams (see ref. [29]) suggested that the shrinkage effect at 550 °C irradiation may be due to the presence of additional IVD traps acting only at 550 °C and reducing the supersaturation Δ^* thereby enlarging R_C as compared to the 450 °C case. But even a complete suppression of $\Delta^* \to 0$ cannot make voids shrink faster than in annealing, where $\Delta^* = 0$ and voids are still unchanged [29].

With account of the void bias the explanation is straight-forward, since in that case the decrease in δ_0 is sufficient to increase both R_t and the shrinkage rate. In particular, if $\delta_0 = 0$, then $R_C = \bar{R} + Z^{\circ}\rho_0/4\pi N$, and only larger voids ($R > R_t$) continue growing, whereas the remaining voids ($R < R_C$) shrink at a rate $\Delta^* \alpha_{iv}/D^* \alpha \sim 10^2$ times greater than the thermal rate at the dose rate reported in ref. [29]. The dose required for a complete void shrinkage at $\delta_0 = 0$ is about 3 dpa, which is an order of magnitude lower than in the experiment. This shows that at 550 °C the dislocations are not completely neutral but rather have a bias in the range from 0 to $\delta_{th} - 0.02$ (see eq. (58)). The δ_0 reduction at 550 °C may be attributed to the appearance after $Kt > 9$ dpa [29] of small precipitates that change the dislocation elastic fields. However, for the illustration of the void bias effect a particular reason of the δ_0 decrease is of no importance, since only the RIC mechanism is able to explain the growth of large voids at the expense of small ones as observed in ref. [29].

For a quantitative analysis let us consider the experiments by Hudson et al. [11,12] who also reported a decrease in N during irradiation followed by a saturation of swelling $V(t) \to V_\infty \approx 10\%$. The latter indicates the realization of the pure coarsening regime, where the dose dependence of void parameters is not influenced by the dislocation structure.

In the nickel samples irradiated with C^{2+} ions to a dose of 350 dpa at $K = 2 \times 10^{-3}$ dpa/s, $T = 525\,^{\circ}$C [11], voids were distributed homogeneously in the crystal grains, while dislocations formed a dense network at $Kt > Kt_0 = 40$ dpa. Their total sink strength was lower than the strength of bulk recombination: $k_c^2 + \tilde{\rho} \ll (K\beta_i/D_v)^{1/2}$. In this case, eq. (48) takes a simple form

$$\bar{R}(t) = \bar{u}\left(\tfrac{4}{9}\alpha_{iv} t\right)^{1/3} \left(\frac{D_v K}{\beta_i}\right)^{1/6} \left(1 + \frac{D^* \alpha}{\Delta^* \alpha_{iv}}\right)^{1/3}, \tag{59}$$

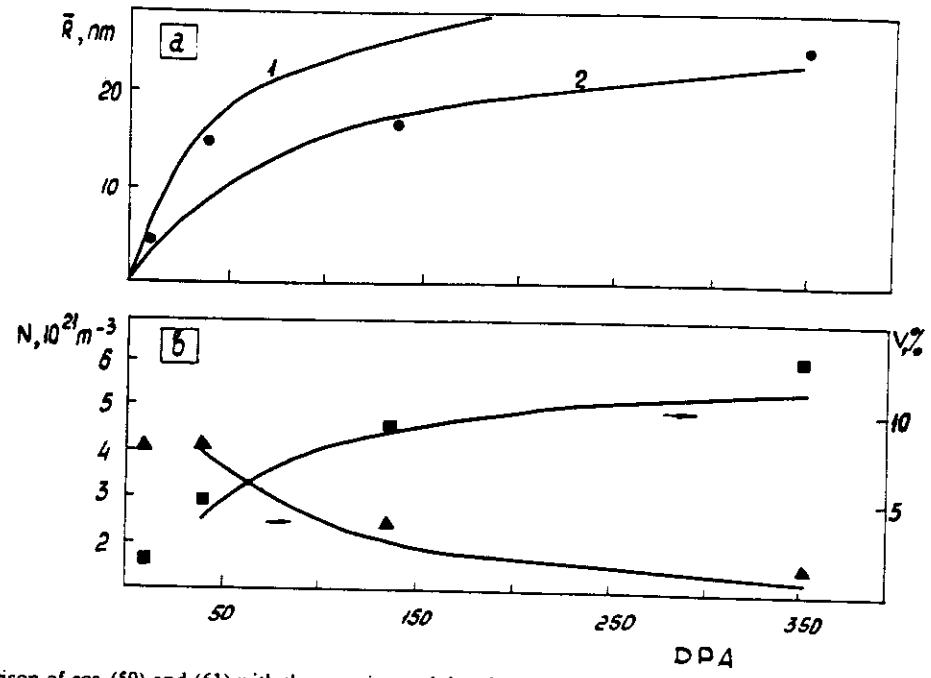

Fig. 3. Comparison of eqs. (59) and (61) with the experimental data [11] on nickel irradiation at $K = 2 \times 10^{-3}$ dpa/s, $T = 525\,^{\circ}$C. (a) Curve 1 corresponds to eq. (59) at $\bar{u} = 3/2$, curve 2 at $\bar{u} = 1$; (●) are the experimental $\bar{R}(t)$ values. (b) The dose dependence of N according to eq. (61) at $\bar{u} = 1$ with $V(t)$ taken from the experiment. (▲) are the experimental $N(t)$ values, (■) are the $V(t)$ values.

where the TIC correction is negligible: $D^*\alpha/\Delta^*\alpha_{iv} = 5 \times 10^{-3}$. The only uncertainty in eq. (59) is connected with the factor $\bar{u}$ varying within a narrow range from 3/2 (all voids grow $V(t) \sim t$) to 1 ($dV/dt = 0$). Experimental points lie very close to the $\bar{u} = 1$ curve (see fig. 3a), which is consistent with an observed saturation of swelling (see fig. 3b). The swelling rate is independent of the void bias

$$\frac{dV}{dt} = \delta_0 \rho_0 \left(\frac{D_v K}{\beta_r} \right)^{1/2} \xrightarrow[t > t_0]{} 0. \tag{60}$$

The tendency of dV/dt to go to zero means that $\rho_0(t) \to 0$ and consequently $N(t)$ has to decrease due to the RIC mechanism:

$$N(t) = \frac{27}{16\pi} \frac{V_\infty}{\alpha_{iv} t} \left(\frac{\beta_r}{K D_v} \right)^{1/2}. \tag{61}$$

This is also confirmed by experimental values (fig. 3b).

A swelling of steel samples irradiated under the same conditions $K = 2 \times 10^{-3}$ dpa/s, $T = 525\,^{\circ}$C [12] also showed a saturation tendency, namely, at $Kt = 400$ dpa swelling was only twice as large as at $K = 40$ dpa. At the same time, $N(t)$ decreased by two orders of magnitude, i.e., far more rapidly than in nickel. Besides, voids were distributed patchily, i.e., dense clusters were surrounded with denuded zones. A high void density within the clusters indicates the realization of the void domination limit, where the RIC rate is the greatest. According to eq. (51), at two different times t_1 and t_2, $N(t)$ and $V(t)$ are related as $N(t_2)/N(t_1) = (t_1/t_2)^3 (V(t_2)/V(t_1))^4$. A substitution of experimental values, $t_2/t_1 = 10$, $V(t_2)/V(t_1) = 2$, gives $N(t_2) = 1.6 \times 10^{-2} N(t_1)$ in agreement with experiments for both the solution-annealed and cold-worked steels: in the first case $N(t)$ decreased from 10^{21} m^{-3} to 10^{19} m^{-3}, in the second case from 7×10^{22} m^{-3} to 7×10^{20} m^{-3} [12].

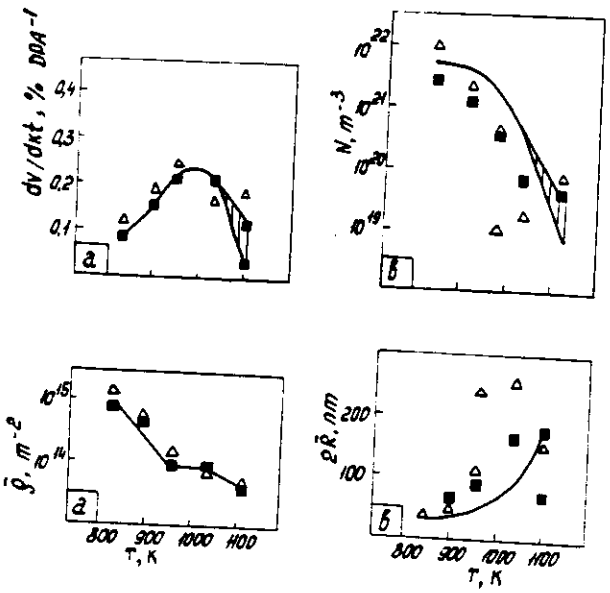

Fig. 4. Steady swelling rate and microstructure versus temperature in austenitic alloy P7 irradiated by Ni ions ($K = 6 \times 10^{-3}$ dpa/s, $Kt = 70$ dpa) with simultaneous implantation of He and D. (a) Experimental dV/dKt and $\bar{\rho}$ values [30]. (■) double ion irradiation. He/dpa = 20; (△) triple ion irradiation. He/dpa = 20. D/dpa = 50. (b) Solid curves correspond to $N_s(T)$ and $\bar{d}(T)$ values calculated from eqs. (62) and (48) by substituting dV/dKt and $\bar{\rho}$ values from experiment (fig. 4a). (■, △) are the experimental $N(T)$ and $\bar{d}(T)$ values [30].

As a rule, the $N(t)$ decrease is observed at a late stage of irradiation [13]. This may be explained by an "ageing" of the dislocation structure since more dislocations form sessile substructures leaving less fresh isolated dislocations. Consequently, the swelling tends to saturation as was the case in the above experiments [11,12]. However, the present theory is also valid for evaluating a stationary void density if the latter is close to the upper limit N_s. To demonstrate this, let us express N_s only in terms of the measurable parameters $\bar{\rho}$ and dV/dKt, excluding the unknown ρ_0:

$$N_s = \frac{K}{2\pi} \frac{dV/dKt}{\Delta^* \alpha_{iv} + D^* \alpha}. \tag{62}$$

It is seen that in the recombination limit, $\Delta^* = \Delta_s^* = \text{const}$, the swelling rate dV/dKt must be constant if $N = N_s = \text{const}$. Such a steady-state swelling is often observed [10,30]. Fig. 4a shows the temperature dependences of a steady swelling rate and a mean dislocation density as measured by Farrell and Packan [30] who irradiated an austenitic alloy P7 by Ni ions with a simultaneous implantation of He and D stimulating the void nucleation. In fig. 4b a comparison of experimental N and $\bar{d} = 2\bar{R}$ values with those following from eqs. (62) and (48) at $Kt = 70$ dpa is shown. The temperature dependence of N_s can be divided into two parts, where the low temperature one ($T < 950\,^\circ$K) is determined by the RIC mechanism ($\Delta^* \alpha_{iv} > D^* \alpha$) and, consequently, is very smooth (see eq. (45)), while at higher temperatures $N_s(T)$ falls down rather sharply due to the TIC mechanism operating there. An agreement of the theoretical $N_s(T)$ and $\bar{d}(T)$ values with $N(T)$, $\bar{d}(T)$ values given by the experiment shows that the stationary void density is determined by the coarsening mechanisms up to 1100 K, i.e., over the whole range of vacancy void formation.

Since He is produced in materials under reactor irradiation, it is reasonable to expect there high nucleation rates, so that N could reach N_s. This is confirmed by the experimental data of Garner [10] which indicate a wide temperature interval 400–600 °C of reactor irradiation of austenitic alloys that swell at a constant rate $dV/dKt = 1\%$/dpa, the mean dislocation density $\bar{\rho}$ being about 6×10^{14} m^{-2}. Substituting these experimental values in eq. (62) we obtain $N_s \approx \bar{\rho}(dV/dKt)/2\pi\alpha_{iv} = 10^{22}$ m^{-3} for the RIC region (400–500 °C), while in the TIC region (500–600 °C) $N(T)$ monotonously decreases with temperature down to 10^{20} m^{-3}, which is in agreement with the experimental data. Note that here $\Delta^* = K/\bar{\rho}$ and $\rho_0 = (dV/dKT)\bar{\rho}/\delta_0 = 10^{13}$ m$^{-2} \ll \bar{\rho} \approx \rho_s$.

5. Discussion

We have demonstrated that the size dependence of the void bias results in a radiation-induced competition between voids that limits their density to the value determined by the controlling parameters ρ_0, δ_0 and α_{iv}. The comparison with experimental data shows that this void density is observed at fairly low temperatures. This result is consistent with the present-day view on the void formation from the fine overpressurized gas bubbles [1]. If the bubble density $N_b \geq N_s$, then the density N_s of vacancy voids would grow at the postnucleation stage irrespective of the nucleation rate. However, the duration of a transient period required to reach N_s depends on the gas concentration and other irradiation conditions. This is confirmed by experimental data. The proposed RIC mechanism explains the observed decrease in N with dose under conditions excluding the influence of TIC mechanism and direct coalescence of voids. All this shows that the evolution of voids is influenced by the void bias to the same extent as by the dislocation bias, and hence they both have to be taken into consideration.

For a quantitative estimation we have used the α_{iv} value derived in the isotropic continuum approximation that seems to be a good one, since it coincides with the values derived by Golubov and Kajpetskaya [31] by means of numerical simulation. Higher-order corrections due to the void volume fraction have been omitted here, which makes the theory independent of the model for the dR/dt derivation. The consideration of the first-order corrections is shown (see Appendix) to suppress the RIC mechanism and to enhance the TIC mechanism insignificantly without distorting the qualitative picture of the void evolution presented in this paper.

A quantitative agreement of eqs. (48), (51) and (62) with experiment demonstrates their applicability to a description of the void ensemble evolution in a real radiation environment. However, the dislocation structure enters into the present theory as an external parameter that is not derived within its framework. To make the theory complete, one should derive the controlling parameters δ_0 ρ_0, ρ_s, α_{iv} selfconsistently with due regard for the dislocation structure evolution and the impurity effect. In particular, further efforts are necessary to study the mechanisms of δ_0 reduction which causes the void shrinkage under irradiation, and hence, the suppression of swelling.

An important consequence of the present theory is the impossibility of a stationary state of a void ensemble under irradiation of a purely diffusion origin. Indeed, if $\rho_0\delta_0 = \text{constant} \neq 0$, then $N = \text{constant}$ but $\bar{R}(t)$ grows due to the dislocation bias. On the other hand, if $\rho_0 = 0$, then $V = \text{constant}$, but $N(t)$ decreases, while $\bar{R}(t)$ increases due to the RIC mechanism. However, this is contrary to the observations of stable void lattices under irradiation, where voids neither grow nor shrink [32]. This discrepancy has been explained by Dubinko et al. [33] who proposed a new mechanism of void interaction that impedes the disordering effect of the coarsening mechanism without letting the voids grow. The mechanism is based upon the void absorption of SIA loops formed via condensation of SIA. At a stage when all SIA condensing in loops return to the voids, the void growth is saturated. Besides, larger voids absorb more SIA loops as compared to smaller ones. This suppresses the void coarsening and makes possible the formation of a stationary state. The main distinguishing feature of this mechanism is its rigid relation to the crystal structure, namely, it exists only in crystals where SIA loops can glide. This is just the case in most bcc metals where the void lattice is observed. By contrast, in most fcc metals, SIA loops encircle an extrinsic stacking fault and are not able to glide. In the latter case, the dislocation interaction between voids does not arise and their evolution may be described within the framework of the present theory.

6. Summary

1. The RIC mechanism is based upon the size dependence of the void bias towards SIA.
2. The coarsening mechanisms limit the maximum density of growing voids to the N_s value independent of the void nucleation rate.

3. In the limit $\alpha_{iv} \to 0$ the present theory turns into conventional one, which states that N is not limited and cannot decrease under irradiation if voids do not coalesce.
4. An experimentally observed N approaches N_s at fairly low temperatures including the peak swelling temperature.
5. According to the present theory, the $\rho_0(t)$ decrease results in the decrease of $N(t)$ and $V(t)$ saturation tendency. A decrease of $\delta_0(t)$ results in a decrease of both $N(t)$ and $V(t)$, i.e., in the suppression of swelling. Both these effects are observed experimentally.
6. A quantitative agreement of the theory with experimental data demonstrates its validity for most fcc metals where annihilation of voids and SIA loops can be neglected.

Appendix

A.1. The supply region concept

The PD concentration in a crystal under irradiation and elastic strain is described by the diffusion equation [7]

$$\frac{\partial C_n}{\partial t} = -\mathrm{div} j + K - \beta_r (D_v + D_i) C_v C_i, \tag{A.1}$$

$$j_n = -\frac{D_n}{\omega} \nabla C_n - \frac{D_n C_n}{\omega T} \nabla E_n, \tag{A.2}$$

where j_n is the PD flux, E_n is the energy of interaction between PD and the strain field.

To derive the void growth rate rigorously, one should solve eq. (A.1) with appropriate boundary conditions at all PD sinks, which is obviously a hopeless task. Three approaches have been developed to simplify the problem. One of them is concerned with spatially periodic sink arrays (Ham's eigenfunction method [19]), and the other two (Brailsford et al. [4] and Kosevich et al. [6]) deal with completely random sink distributions.

Brailsford et al. [4] described the real material with discrete sinks as an effective lossy medium containing a homogeneous distribution of these same sinks, with strengths determined self-consistently. Following this philosophy, the void should be surrounded by a sink-free region before being placed in the effective medium. If voids are the only sinks under consideration, then a radius of the sink-free region would simply equal the mean distance between the voids $(3/4\pi N)^{1/3}$. However, in the presence of dislocations the solution is not straightforward. Therefore, for simplicity, such a sink-free region has been omitted entirely [4,5].

Following Kosevich et al. [6], Slezov and Bereznyak [7] have defined the "region of influence" (referred to here as a supply region) of the macrodefect which is the analogue of the sink-free region. For this purpose, they assumed the PD concentration to be a sum of two components $C = C_0 + C_1$ (for the present, we omit the subscripts denoting the PD type). The physical meaning of this division is to distinguish explicitly between the concentration of thermal PD, C_0, which is due to the thermal emission from macrodefects, and the concentration of radiation-produced PD, C_1, that are absorbed from the supply region of the macrodefect. Accordingly, the PD fluxes take the form $j = j_0 + j_1$. The supply region is then defined self-consistently by a requirement of the zero influx j_1 across the boundary of the region: $(j_1 e_r)|_{r=R_s^\circ} = 0$, $e_r = r/r$, where r is the radius vector directed outwards the sink centre, and R_s° is the radius of the supply region which is assumed to be spherical for a cavity (s = c) and cylindrical for a dislocation (s = d).

Note that $(j_0 e_r)|_{r=R_s^\circ} \neq 0$ due to nonuniformity of the boundary conditions C_s at different macrodefects. Hence, there is no supply region for the thermal PD. However, R_s° may be used instead of the unknown radius of the sink-free region in our calculations of C_0.

Here we develop this approach further to account for the elastic void–PD interaction which makes R_s° depend on the PD type and results in the void bias.

By definition, the flux of radiation-produced PD into an s-type sink, $J_1(r_s)$, is equal to the PD generation rate K times the supply region volume which is related to the concentration C_1 at $r \geq R_s^\circ$. We are interested in the $J_1(r_s)$ value averaged over all possible positions of other macrodefects. As a result of the averaging, C_1 changes only inside the supply region; outside we have $C_1|_{r>R_s^\circ} = C^*$, which is common for all macrodefects present. The concentration C^* is sustained by the balance of all the sources and sinks and is determined by the condition that the total volume of the supply regions should make up the crystal bulk. If only spherical cavities and straight dislocations are present, then the condition takes the explicit form

$$\frac{4\pi}{3}\int_0^\infty f(R, t)\left[R_c^\circ(R)\right]^3 \mathrm{d}R + \pi\bar{\rho}(R_d^\circ)^2 = 1, \tag{A.3}$$

provided that the volume fraction of macrodefects is small

$$Q \equiv \frac{4\pi}{3}\int_0^\infty f(R, t)R^3 \mathrm{d}R + \pi\bar{\rho}b^2 \ll 1, \tag{A.4}$$

where b is the atomic spacing characterizing the dislocation core size.

The C_1 variation inside the supply region in the absence of the bulk recombination is given by the equation

$$\omega \operatorname{div} j_1 - K = 0, \tag{A.5}$$

with the conditions at the sink surface ($r = r_s$) and the supply region boundary $r = R_s^\circ$:

$$C_1|_{r=r_s} = 0, \quad (j_1 e_r)|_{r=R_s^\circ} = 0.$$

Neglecting for the present the elastic interaction of PD with macrodefects (in eq. (A.2) $E = 0$), we obtain from eq. (A.5) the expressions for PD fluxes into a void $J_1(R)$ and per unit length of the dislocation $J_1(b)$, and also the relations between R_s° (s = c, d) and C^*:

$$J_1(R) = \frac{4\pi}{3\omega}K\left[(R_c^\circ)^3 - R^3\right], \tag{A.6}$$

$$(R_c^\circ)^3 = \frac{3DRC^*}{K}\left[1 - \frac{3}{2}\frac{R}{R_c^\circ} + \frac{1}{2}\left(\frac{R}{R_c^\circ}\right)^3\right]^{-1}, \tag{A.7}$$

$$J_1(b) = \frac{\pi}{\omega}K\left[(R_d^\circ)^2 - b^2\right], \tag{A.8}$$

$$(R_d^\circ)^2 = 2DC^*/K\left[\ln\left(\frac{R_d^\circ}{b}\right) - \tfrac{1}{2}\right] \tag{A.9}$$

In the first order of $R/R_c^\circ \ll 1$ and $b/R_d^\circ \ll 1$ we obtain

$$J_1(R) \approx \frac{4\pi}{\omega}DC^*\left(1 + \frac{3}{2}\frac{R}{R_c^\circ}\right), \tag{A.10}$$

$$J_1(b) \approx 2\pi DC^*/\omega \ln(R_d^\circ/b), \tag{A.11}$$

$$R_d^\circ \approx \left[\pi\bar{\rho} + 2\pi N\bar{R}\ln(R_d^\circ/b)\right]^{-1/2}, \quad k^2 = k_c^2 + k_d^2 = \frac{Z^\circ}{\pi}(R_d^\circ)^{-2}, \tag{A.12}$$

$$R_c^\circ \approx (R_d^\circ)^{2/3}\left[\tfrac{1}{2}R_d^\circ \ln(R_d^\circ/b)\right]^{1/3}. \tag{A.13}$$

In contrast to j_1, the total PD fluxes do not vanish at the supply region boundaries because of thermal PD exchange between macrodefects. To take into account this exchange, one should solve the equation for C_0

not only inside the supply region but everywhere. After the averaging procedure the equation takes the form [7]

$$D\Delta C_0 - \frac{D}{l^2}\left[C_0 - (\bar{C} - C^*)\right]\theta(r - R_s^\circ) = 0,$$

$$C_0(r_s) = C_s,\ C_0|_{r\to\infty} = \bar{C} - C^*;\quad \theta(x) = \begin{cases} 1 & \text{for } x > 0, \\ 0 & \text{for } x < 0, \end{cases} \tag{A.14}$$

where $\bar{C}$ is the mean total concentration of PD, and l^{-2} is the sink strength of all macrodefects for thermal PD:

$$l^{-2} = \frac{\bar{\rho} J_0(r_d)}{D(\bar{C} - C^* - C_d)} + \int_0^\infty \frac{f(R, t) J_0(R)\, dR}{D(\bar{C} - C^* - C_c)} = k^2. \tag{A.15}$$

Eq. (A.14)* leads to

$$J_0(R) = \frac{4\pi}{\omega} DR(\bar{C} - C^* - C_c)\left(1 - \frac{R}{l + R_c^\circ}\right)^{-1}. \tag{A.16}$$

$$J_0(b) = \frac{2\pi}{\omega} D \frac{\bar{C} - C^* - C_d}{\ln\left(\frac{R_d^\circ}{b}\right) - K_0\left(\frac{R_d^\circ}{l}\right)/R_d^\circ K_0'\left(\frac{R_d^\circ}{l}\right)}. \tag{A.17}$$

where $K_0(x)$ is the Bessel function of the imaginary argument, $K_0' = (d/dx)K_0(x) < 0$. At $R_d^\circ/l \sim 1$, which is usually the case, $K_0(x)/K_0'(x) \approx -2/3$.

The quasi-stationary rate equations complete the set of equations:

$$K(1 - Q) - \int_0^\infty f(R, t)\left[J_1(R) + J_0(R)\right] dR - \bar{\rho}\left[J_1(b) + J_0(b)\right] = 0, \tag{A.18}$$

giving, together with eq. (A.3), the mean concentration of thermal PD far from the macrodefects:

$$C_0|_{r\to\infty} \equiv \bar{C}^e \approx \frac{4\pi \int_0^\infty f(R, t) R C_c(R)\, dR + 2\pi\bar{\rho} C_d / \ln(R_d^\circ/b)}{4\pi \int_0^\infty f(R_1 t) R\, dR + 2\pi\bar{\rho}/\ln(R_d^\circ/b)}. \tag{A.19}$$

Thus, $C^* = \bar{C} - \bar{C}^e \approx K/D(2\pi\bar{\rho}/\ln(R_d^\circ/b) + 4\pi N\bar{R})$ is the radiationinduced PD supersaturation which becomes zero at $K = 0$.

Note that the above expressions coincide with the expressions following from the simplified lossy continuum approach [4,5] only to the zero approximation of $Q \ll 1$. Higher-order corrections following from refs. [4,5] underestimate the influxes of radiation-produced PD (R/l instead of $3R/2R_c^\circ$ in eq. (A.10) and overestimate the influxes of thermal PD (R/l instead of $R/(l + R_c^\circ)$ in eq. (A.16)). The explanation is that the lossy continuum is an additional sink for the radiation PD and an additional source for the thermal PD which are both extended in [4,5] into the supply region free from other macrodefects.

Evolution of voids and dislocations under irradiation is governed by the difference between SIA and vacancy influxes. Above we did not consider this difference, neglecting the elastic interaction of macrodefects with PD for the sake of simplicity. As a result, the supply regions did not depend on the PD type ($R_{sv}^\circ = R_{si}^\circ$, where the subscripts v and i designate vacancies and SIA, respectively); and only the difference of thermal PD influxes was nonzero: $J_v(r_s) - J_i(r_s) \sim D_v(\bar{C}_v^e - C_{sv}) - D_i(\bar{C}_i^e - C_{si})$. To describe the radiation effects, let us consider PD as centres of dilatation interacting with macrodefects; this makes R_s° depend on the PD type and leads to macrodefect biases.

A.2. The void bias

The interaction between a spherical void and a nearby PD is induced by the image distortion field of the PD (the size effect) and by the distortion field of the void due to its surface tension (the modulus effect), the latter diminishing for a sufficiently large void $R > 1$ nm [20] and neglected below. The energy E_n^{im} (n = i, v) of image interaction between the spherical void and a centre of dilatation, at a radial distance r, has the series form [5,20]:

$$E_n^{im} = -\frac{(1+\nu)^2\mu\omega}{36\pi(1-\nu)}\left(\frac{\Omega_n}{\omega}\right)^2\left(\frac{b}{R}\right)^3\sum_{m=2}^{\infty}\frac{m(m-1)(4m^2-1)}{m^2+m(1-2\nu)+1-\nu}\left(\frac{R}{r}\right)^{2m+2}. \tag{A.20}$$

Ω_n is the PD relaxation volume. The void bias for SIA has been shown by Wolfer [20] to arise as a consequence of a greater relaxation volume of SIA in the approximation of $R/R_c^\circ \to 0$. More rigorously, eq. (A.5) should be solved with account of eq. (A.20). This gives a new relation between R_{cn}° and $D_nC_n^*$:

$$D_nC_n^* = \tfrac{1}{3}K(R_{cn}^\circ)^3\int_R^{R_{cn}^\circ}\left(1-\frac{r^3}{R_{cn}^{\circ 3}}\right)\exp\left(\frac{E_n^{im}}{T}\right)\frac{dr}{r^2}, \tag{A.21}$$

which, after the substitution into eq. (A.6), leads to

$$J_{1n}(R) = \frac{4\pi}{\omega}D_nC_n^*R_n^* - \frac{4\pi}{3\omega}KR^3, \tag{A.22}$$

$$R_n^* \equiv \left(\int_R^{R_{cn}^\circ}\exp\left(\frac{E_n^{im}}{T}\right)\left(\frac{1}{r^2}-\frac{r}{R_{cn}^{\circ 3}}\right)dr\right)^{-1}. \tag{A.23}$$

Note that if $E_n^{im} \to 0$ and $R/R_{cn}^\circ \to 0$, then $R_n^* \to R$. Thus, R_n^* is the void effective capture radius resulting from the void interaction with PD and from the influence of other sinks. If only R/R_{cn}° tends to zero, then we obtain the result of Wolfer [20], i.e. eq. (4).

The elastic interaction between dislocations and PD results in the dependence of eq. (A.9) on the PD type ($\frac{1}{2}L_n$ substitutes for b):

$$D_nC_n^* = \tfrac{1}{2}(R_{dn}^\circ)^2K\ln\left(\frac{2R_{dn}^\circ}{L_n\sqrt{e}}\right). \tag{A.24}$$

Eqs. (A.21), (A.24) and (A.3) make a set for determining R_{cn}°, R_{dn}° and C_n^* with due account of the elastic interaction.

An exact size dependence of the void bias $\delta_c = (R_i^* - R_v^*)/R$ is nonmonotonous due to the increase of the difference $R_i^* - R_v^*$ with the void size. As a result, the RIC rate is lower than that in the zero order in $V \ll 1$. For example, the time dependence of the average void radius in the pure RIC regime ($\rho_0 = 0$) is given to the first order in V_0 by (compare with eqs. (35) and (38))

$$\bar{R}(t) = \left(\tfrac{4}{9}\Delta_s^*\alpha_{iv}t\right)^{1/3}\left(1-\frac{V_0}{6-V_0}\right)^{1/3}, \quad k_c^2 \ll \frac{K}{\Delta_s^*}, \tag{A.25}$$

$$\bar{R}(t) \simeq \frac{4C_3}{81}\frac{\alpha_{iv}Kt}{V_0}\left(1-\frac{V_0}{6-V_0}\right), \quad k_c^2 \gg \frac{K}{\Delta_s^*}. \tag{A.26}$$

On the other hand, the volume fraction corrections enhance the TIC rate. This can be found from eq. (A.16), since the interaction between voids and PD is not important for TIC. In the pure TIC regime, we have to the first order in V_0

$$\bar{R}(t) = \left(\tfrac{4}{9}D^*\alpha t\right)^{1/3}\left(1+\sqrt{3V_0}\right)^{1/3}. \tag{A.27}$$

As can be seen from eqs. (A.25) to (A.27), the volume fraction effect is small even in the $V_0 \to 1$ limit and does not change the results obtained in the zero approximation of $V_0 \to 0$.

References

[1] W.G. Wolfer, J. Nucl. Mater. 122 & 123 (1984) 367.
[2] V.F. Zelenskij et al., Nekotorye Problemy Fiziki Radiatsionnykh Povrezhdenij Materialov (Some Problems of Radiation Damage of Materials) (Naukova Dumka, Kiev, 1979).
[3] M.R. Hayns and M.H. Wood, J. Nucl. Mater. 87 (1979) 97.
[4] A.D. Brailsford, R. Bullough and M.R. Hayns, J. Nucl. Mater. 60 (1976) 246.
[5] R. Bullough and M.H. Wood, in: Physics of Radiation Effects in Crystals (Elsevier, Amsterdam, 1986) p. 189.
[6] A.M. Kosevich, Z.K. Saralidze and V.V. Slezov, Zh. Ehksp. Teor. Fiz. 52 (1967) 1073.
[7] V.V. Slezov and P.A. Bereznyak, in: Physics of Radiation Effects in Crystals (Elsevier, Amsterdam, 1986) p. 575.
[8] K.C. Russell, Acta Metall. 26 (1978) 1615.
[9] I.L. Katz and H. Wiedersich, J. Chem. Phys. 55 (1971) 1414.
10] F.A. Garner, J. Nucl. Mater. 122 & 123 (1984) 459.
11] J.A. Hudson, D.J. Mazey and R.S. Nelson, J. Nucl. Mater. 41 (1971) 241.
12] D.J. Mazey, J.A. Hudson and R.S. Nelson, J. Nucl. Mater. 41 (1971) 257.
13] W.G. Johnson, J.H. Rosolovski, A.M. Turkalo and T. Lauritzen, J. Nucl. Mater. 47 (1973) 155.
14] S.G. Agarwell, G. Ayrault, D.I. Potter, A. Taylor and F.V. Nolfi, Jr., J. Nucl. Mater. 85 & 86 (1979) 653.
15] V.I. Dubinko, P.N. Ostapchuk and V.V. Slezov, Vopr. At. Nauki Tekhn. Ser.: Fiz. Radiatsionnykl Povrezhd. i Rad. Materialoved 1 (39) (1987) p. 35.
16] V.I. Dubinko, P.N. Ostapchuk and V.V. Slezov, Vliyanie oblucheniya na diffuzionnuyu ehvolyutsiyu ansamblya por v krist, Preprint KhFTI 86-16 (Kharkov Institute of Physics and Technology) (KhFTI AN SSSR, Kharkov, 1986).
17] W. Ostwald, Z. Phys. Chem. 34 (1900) 495.
18] I.M. Lifshits and V.V. Slezov, Zh. Ehksp. Teor. Fiz. 35 (1958) 479.
19] F.S. Ham, J. Phys. Chem. Solids 6 (1958) 335.
20] W.G. Wolfer, in: Proceedings Int. Conf. on Fundamental Aspects of Radiation Damage in Metals, Gatlingburg, Tennessee, USA, 1975, p. 812.
21] F.S. Ham, J. Appl. Phys. 30 (1959) 915.
22] I.G. Margvelashvili and Z.K. Saralidze, Fiz. Tverd. Tela 15 (1973) 2665.
23] N.A. Demin, Yu.V. Konobeev and O.V. Tolstikova, Fiz. Met. Metalloved. 58 (1984) 98.
24] V.I. Dubinko, A.A. Turkin and V.V. Yanovskij, Fiz. Met. Metalloved. 59 (1985) 291.
25] V.I. Dubinko, A.A. Turkin and V.V. Yanovskij, Fiz. Met. Metalloved. 59 (1985) 686.
26] A.N. Orlov and Yu.V. Trushin, Ehnergii tochechnykh defektov v metallakh, M.: Ehnergoatomizdat (1983).
27] V.V. Slezov and V.B. Shikin, Fiz. Met. Metalloved. 4 (1964) 7.
28] A.I. Ryazanov and L.A. Maksimov, Kinetika koalestsentsii por v kristalle s dislokatsiami v usloviyakh ob'emnoj generatsii tochechnykh defektov, Preprint IAE-2493 (IAE, Moscow, 1975).
29] D.R. Arkell and T.M. Williams, J. Nucl. Mater. 74 (1978) 144.
30] K. Farrell and M.H. Packan, J. Nucl. Mater. 85 & 86 (1979) 683.
31] S.I. Golubov, E.N. Kamnetskaya, Fiz. Met. Metalloved. 54 (1982) 1061.
32] K. Krishan, Radiat. Eff. 66 (1982) 121.
33] V.I. Dubinko, A.V. Tur, A.A. Turkin and V.V. Yanovskij, Vopr. At. Nauki Teh. Ser.: Fiz. Rad. Povrezhd. i Rad. Materialoved. 1 (39) (1987) 40. See also J. Nucl. Mater. 161 (1989) 57.

Phys. Met. Metall. Vol. 68 No. 1, pp. 17–25, 1989
Printed in Great Britain

0031–918X/89 $10.00+.00

UDC 621.785.78.001

DIFFUSION INTERACTION OF NEW-PHASE PRECIPITATES AT RANDOM DISTANCES*

V. I. DUBINKO, A. A. TURKIN, A. V. TUR and V. V. YANOVSKIY

Khar'kov Physicotechnical Institute, Academy of Sciences Ukr.S.S.R.

(*Received* 29 *December* 1987)

A precise solution is found to the problem of the diffusion interaction of two spherical precipitates in a supersaturated solid solution of impurity atoms. Simple analytical formulae are obtained for the growth rates and motion of precipitates in the two extreme cases where they are close to and a long way from one another. Besides mutual screening at close distances, there is also found to be a pumping effect which transfers impurity atoms from a smaller to a larger precipitate, as a result of which the larger precipitate absorbs a smaller one without coming into direct contact with it. The criterion of size instability of two neighbouring similar precipitates is obtained. The influence of pair correlations on the evolution of an assembly of precipitates is discussed.

In many ways the physical properties of real crystals are governed by their defect structure. Defects can be divided into two categories: point and macrodefects. The former represent the least disturbance of crystal order: vacancies, interstitial atoms, impurity atoms and very simple complexes thereof. Macrodefects — voids, dislocations, precipitates of a new phase and so on — consist of a large number of point defects and they can be exchanged by the diffusion mechanism of transfer. That involves interaction between macrodefects, due both to elastic distortions of the crystal lattice and non-uniform distribution of point defects near macrodefects. The first mechanism, elastodiffusion interaction, has been investigated in detail in [1] and is not considered here. This study is concerned with purely diffusion interaction between two spherical macrodefects at arbitrary distances from one another. This type of interaction is very important as regards the evolution of an assembly of macrodefects.

In particular, as shown in [2, 3], diffusion together with dislocation interaction is what decides the conditions involved in the transfer of vacancies and gas voids from random to spatially ordered distribution. Because of the diffusion interaction, correlations arise between the distribution of macrodefects in relation to one another and their rates of growth or dissolution, which may affect the hardening kinetics of the new phase in the process of diffusion decomposition of solid solutions, and so on. Interest in those processes has increased in recent times, as can be seen from a number of publications (e.g. [4, 5]) in which the influence of the local environment on the evolution of individual precipitates has been observed experimentally. The problem of the diffusion interaction of two voids has previously been solved in the widely spaced approximation [6]. However, as we shall see, correlation effects are most marked in the opposite extreme case where the distance between void surfaces is not greater than their size. (By definition, below we shall be talking about voids, because the only difference between them and precipitates concerns the elastic distortions of the matrix, which we are

* *Fiz. metal. metalloved.*, 68, No. 1, 21–28, 1989.

PQMM 68:1-B

not taking into account). That brings in a new physical effect — the pumping of vacancies from one sized void to another, which may end with the absorption of a smaller by a larger void without coming into contact. The final part of this paper is a discussion of the influence of pair correlations on the evolution of an assembly of macrodefects.

THE PROBLEM

Let us consider two vacancy voids of radius R_1 and R_2 at a distance l from one another in an isotropic material supersaturated with vacancies. Growth of the voids by absorption of vacancies is a slower process than that of establishing a quasistationary distribution of vacancies [7], so we shall make use of the stationary equation of diffusion

$$\Delta U = 0, \tag{1}$$

where $U = c(\mathbf{r}) - c_\infty$ is the deviation of vacancy concentration $c(\mathbf{r})$ from constant c_∞ at large distances from voids. A concentration of vacancies in local equilibrium is established in the immediate vicinity of the void surfaces, and it depends on the value of σ the surface tension of voids. This, of course, is valid for the diffusion-limited case where the characteristic time of internal diffusion of vacancies is much greater than that of being distributed in the void surface. Assuming also that the voids recover their spherical shape by surface diffusion in the course of growth, we can give the boundary conditions as

$$U \mid_{S_i} = c_i - c_\infty, \quad c_i = c_0 \exp\left(\frac{2\sigma\omega}{TR_i}\right), \quad U \xrightarrow[|\mathbf{r}| \to \infty]{} 0. \tag{2}$$

Here $i = 1, 2$; c_0 is the thermal concentration of vacancies near the flat surface of material; ω — the atomic volume, T — the temperature. Equation (1) and boundary conditions (2) enable us to calculate the vacancy flows to voids, which are what decide their growth rate

$$\dot{R}_i = -\frac{\omega}{4\pi R_i^2} \int_{S_i} (\mathbf{j}_{S_i} \mathbf{n}_i)\, dS_i, \tag{3}$$

where $\mathbf{j} = -\frac{D}{\omega}\nabla U$; D is the diffusion coefficient, $\mathbf{n}_i$ — the external perpendicular to the surface of the i-th void. Integration is carried over the void surface.

The rate of displacement of the centre of gravity of a void relative to the fixed matrix is described by the vector sum of vacancy flows on different surface elements of the void:

$$\mathbf{v}_i = -\frac{3\omega}{4\pi R_i^2} \int_{S_i} \mathbf{n}_i (\mathbf{n}_i \mathbf{j} \mid_{S_i})\, dS_i. \tag{4}$$

Thus, the major problem consists in solving Equation (1) with boundary conditions (2).

PRECISE SOLUTION

The diffusion problem (1), (2) is analogous to that of finding the potential of an electric field outside spheres with given boundary potentials U_1 and U_2, the solution of which in bispherical coordinates is in the form [8]

$$U(\xi, \eta) = \{U_1 \sum_{k=0}^{\infty} \frac{\operatorname{sh}\left[\left(k-\frac{1}{2}\right)(\eta-\eta_2)\right]}{\operatorname{sh}\left[\left(k+\frac{1}{2}\right)(\eta_1-\eta_2)\right]} \exp\left[-\left(k+\frac{1}{2}\right)\eta_1\right] P_k(\cos\xi) +$$

$$+ U_2 \sum_{k=0}^{\infty} \frac{\operatorname{sh}\left[\left(k+\frac{1}{2}\right)(\eta_1-\eta)\right]}{\operatorname{sh}\left[\left(k+\frac{1}{2}\right)(\eta_1-\eta_2)\right]} \exp\left[-\left(k+\frac{1}{2}\right)|\eta_2|\right] \times$$

$$\times P_k(\cos\xi)\}\sqrt{2(\operatorname{ch}\eta - \cos\xi)}, \tag{5}$$

where coordinates ξ and η are used in the ranges $0 \le \xi \le \pi$, $\eta_2 \le \eta \le \eta_1$; $P_k(\cos\xi)$ — where ξ, η and φ are related with the Cartesian coordinates as follows (Fig. 1):

$$x = \frac{a \operatorname{sh}\eta}{\operatorname{ch}\eta - \cos\xi}, \quad y = \frac{a \sin\xi\cos\varphi}{\operatorname{ch}\eta - \cos\xi}, \quad z = \frac{a \sin\xi \cdot \sin\varphi}{\operatorname{ch}\eta - \cos\xi}. \tag{6}$$

Values a, η_1, η_2 are connected with the radii of and distance between voids by (see Fig. 1)

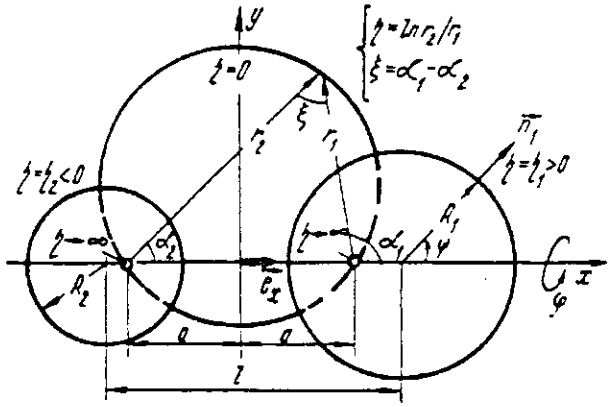

Fig. 1. Two voids in a biospherical system of coordinates.
Void surfaces are coordinate surfaces $\eta = \text{const}$.

$$\operatorname{sh}(\eta_1 - \eta_2) \equiv \operatorname{sh}\mu = \frac{1}{2R_1R_2}\{[l^2 - (R_1 + R_2)^2][l^2 - (R_1 - R_2)^2]\}^{1/2}, \tag{7}$$

$$\operatorname{sh}\eta_1 = \frac{R_2}{l}\operatorname{sh}\mu, \quad \operatorname{sh}|\eta_2| = \frac{R_1}{l}\operatorname{sh}\mu, \quad a = \frac{R_1R_2}{l}\operatorname{sh}\mu, \quad R_i = \frac{a}{\operatorname{sh}|\eta_i|}.$$

Relations (5) and (7) give the complete definition of the distribution of vacancies round voids, from which we can obtain precise formulae for the rates of growth and motion of voids for any parameters R_1, R_2, l. For instance, for the first void these formulae are:

$$\dot{R}_1 = -\frac{D}{R_1}\left\{U_1 - 2\,\mathrm{sh}\,\eta_1 \sum_{k=0}^{\infty} \frac{U_2 - U_1 \exp[-(2k+1)\,\eta_1]}{\exp[(2k+1)\,(\eta_1-\eta_2)]-1}\right\}. \tag{8}$$

$$\mathbf{v}_1 = -\mathbf{e}_x \frac{6D}{l}\frac{R_2}{R_1}\,\mathrm{sh}\,\mu \sum_{k=0}^{\infty} \frac{\mathrm{ch}\,\eta_1 - (2k+1)\,\mathrm{sh}\,\eta_1}{\exp[(2k+1)\,(\eta_1-\eta_2)]-1} \times$$

$$\times\,(U_2 - U_1 \exp[-(2k+1)\,\eta_1]). \tag{9}$$

where $\mathbf{e}_x$ is a unit vector lying along the x axis from the second to the first void. The first term in brace brackets of relation (8) corresponds to the growth of an isolated void, the second describes the influence of a second void on the growth rate of the first. Equations (8), (9) can be given in the compact form:

$$\dot{R}_1 = -\frac{D}{R_1}(U_1 - F(0)), \quad \mathbf{v}_1 = -\mathbf{e}_x \frac{3D}{l}\frac{R_2}{R_1}\,\mathrm{sh}\,\mu \left.\frac{\partial F(\beta)}{\partial \beta}\right|_{\beta=0}, \tag{10}$$

where the function $F(\beta)$ is defined by the equality

$$F(\beta) = 2\,\mathrm{sh}\,(\eta_1+\beta) \sum_{k=0}^{\infty} \frac{U_2 - U_1 \exp[-(2k+1)\,\eta_1]}{\exp[(2k+1)\,(\eta_1-\eta_2)]-1} \exp[-(2k+1)\,\beta] \tag{11}$$

or, in symmetrical form over U_1, U_2

$$F(\beta) = \mathrm{sh}\,(\eta_1+\beta) \sum_{k=0}^{\infty} \left(\frac{U_2}{\mathrm{sh}\,[m\,(\eta_1-\eta_2)+\beta]} - \frac{U_1}{\mathrm{sh}\,[m\,(\eta_1-\eta_2)+\eta_1+\beta]}\right). \tag{12}$$

We shall use the above formulae to investigate various extreme cases which are of physical interest.

VOIDS AT LARGE DISTANCES FROM ONE ANOTHER ($l \gg R_1, R_2$)

Using (7) it is easy to see that in this extreme case $\eta_1,\ |\eta_2| \gg 1$, which means that the series in (8), (9) converge rapidly. Leaving only the first terms of those series we get

$$\dot{R}_1 = \left(1 + \frac{R_1 R_2}{l^2}\right)\left(\dot{R}_1^{(0)} - \frac{R_2^2}{R_1 l}\dot{R}_2^{(0)}\right); \tag{13}$$

$$\mathbf{v}_1 = \mathbf{e}_x \cdot 3\left(\frac{R_2}{l^2}\right)^2\left(1 + \frac{R_2^2}{l}\right)\left(\dot{R}_2^{(0)} - \frac{\dot{R}_1^2}{R_2 l}\dot{R}_1^{(0)}\right), \tag{14}$$

where $\dot{R}_{1,2}^{(0)} = \frac{D}{R_{1,2}}(c_\infty - c_{1,2})$ are the growth rates of isolated voids in an infinite medium.

Formula (13) indicates the difference between the growth rate of the void and $\dot{R}_1^{(0)}$ even where a concentration c_∞ (i.e. $\dot{R}_2^{(0)}=0$) is maintained on the surface of the second void. In that case $\dot{R}_1 > \dot{R}_1^{(0)}$ and physically this is explained by the fact that the concentration gradient and, therefore, the flow between voids, is greater than the concentration gradient of an isolated void in the corresponding region.

The formulae obtained for the growth rate (13) and motion of voids (14) are in agreement with the

results of [6]. The case in question plays an important part. The fact is that condition $2R<l$ is always satisfied for single voids (if it is not, the voids merge). That means that $R/l<1/2$ and the approximation described is well satisfied for almost all distances, although the second approximation is more adequate for shorter distances. The necessity of changing to that approximation is important for describing the interaction of different sized voids because then $\frac{R_{1,2}}{l}<1$ may not be satisfied.

VOIDS AT SHORT DISTANCES ($R_1, R_2 \gg l-R_1-R_2 \equiv \lambda$)

In this case, as follows from (7), η_1, $|\eta_2| \ll 1$, so the series in (8), (9) converge slowly, making their use rather difficult. These can, however, be transformed to asymptotic series (over the parameter $\mu=\eta_1-\eta_2$) which are convenient for investigating the extreme case in question. Leaving the principle terms of the series in (A.5), (A.7), for the rates of void growth and motion we get

$$\dot{R}_1 = \dot{R}_1^{(0)}\left[1 - \frac{R_2}{R_1+R_2}\left(\gamma + \psi\left(1+\frac{R_2}{R_1+R_2}\right)\right) + \frac{R_2}{R_1+R_2}\times\right.$$
$$\left.\times\frac{c_2-c_1}{c_\infty-c_1}\left(\frac{1}{2}\ln\frac{2R_1R_2}{\lambda l}+\gamma\right)\right]; \tag{15}$$

$$\mathbf{v}_1 = -\mathbf{e}_x\frac{3D}{l}\frac{R_2}{R_1}\left[U_2\gamma + U_1\psi\left(1+\frac{R_2}{R_1+R_2}\right)\right] -$$
$$-\frac{R_2}{R_1+R_2}\left(U_2\zeta(2) - U_1\zeta\left(2, 1+\frac{R_2}{R_1+R_2}\right)\right) + \frac{1}{2}(U_2-U_1)\ln\frac{2R_1R_2}{\lambda l}\Big]. \tag{16}$$

Here $\gamma=0{\cdot}5772$ is the Euler–Masceroni constant; $\psi(\nu)$ — the ~~diagram~~ digamma function; $\zeta(s)$ — the Riemann zeta-function, $\zeta(s, \nu)$ the generalized Riemann zeta-function of [10].

The first term in (15) describes the growth of an isolated void, and the second — the slowing down of growth rate due to ~~vacancy flows with~~ screening of vacancy flows from "infinity" by a neighbouring void, while the third accounts for the direct pumping of vacancies from smaller to larger voids. Calculation of the second term of (15) shows that the change in the growth rate of voids as a result of screening is not more than 30% which does not qualitatively alter the character of evolution. On the other hand, unlike the screening effect, the pumping of vacancies from one void to another makes no contribution to the changes in total volume of voids although it does give rise to a new important effect — the dissolution of a smaller near a larger void, which thus absorbs the smaller without coming into direct contact. In the case of widely spaced voids this does not occur and an analytical description was originally given in [9], which was concerned with the diffusion interaction of closely spaced voids.

We shall show below that an accurate construction of the collision integral of voids in dimension space does involve taking account of that transfer.

The transfer effect is also reflected by the behaviour of two single voids because it gives rise to instability in dimension space. Actually, assuming that $R_1=R+\Delta R_1$ and $R_2=R+\Delta R_2$ (15) we get the following equation for the size discrepancy of the voids $r=\Delta R_2-\Delta R_1$,

$$\dot{r} = \frac{\dot{R}^{(0)}}{R}\left[\alpha + \frac{\pi^2}{8} - 2 + \frac{c_R}{c_\infty - c_R}\frac{2\sigma\omega}{TR}\left(\gamma + 1 - \frac{\alpha}{2} + \frac{1}{2}\ln\frac{2R^2}{\lambda l}\right)\right] r, \tag{17}$$

where $\alpha=\gamma+\psi(3/2)\approx 0{\cdot}614$, $c_R=c_0\exp\left(\frac{2\sigma\omega}{TR}\right)$. The criterion of instability is given in the form

$$c_R \frac{2\sigma\omega}{TR}\left(\gamma + 1 - \frac{\alpha}{2} + \frac{1}{2}\ln\frac{2R^2}{\lambda l}\right) - (c_\infty - c_R)\left(2 - \alpha - \frac{\pi^2}{8}\right) > 0, \tag{18}$$

and where it is satisfied the void size discrepancy increases with time. For instance, for the case of slight supersaturation ($c_\infty - c_0 \ll c_0$), this criterion is satisfied for voids of a size which is consistent with inequality $R<R_*$, where

$$R_* \approx \left(8{,}3 + 3\ln\frac{R}{\lambda}\right) R_k, \quad R_k = \frac{2\sigma\omega c_0}{T(c_\infty - c_0)}. \tag{19}$$

With (15) and (16) it can be shown that the distance between the surfaces of close, almost identical voids λ varies with time according to

$$\frac{d\lambda}{dt} \approx -0{,}6\dot{R}^{(0)} + 2D\frac{(R_2 - R_1)(c_1 - c_2)}{R_1 R_2}\ln\frac{R}{\lambda}, \tag{20}$$

in which the second term is always positive and tends to ∞ where $\lambda \to 0$. So the surfaces of dissolving voids ($R^{(0)}<0$) draw apart ($d\lambda/dt>0$) and those of the growing voids are established at an equilibrium distance governed by the condition $d\lambda/dt=0$. The size instability of voids then continues to grow.

Equation (17) describes the linear stage of instability. Where the size incompatibility grows the condition $R_1, R_2 \gg \lambda$ no longer holds so, to describe the subsequent evolution of voids we must consider the following extreme case.

A SMALL VOID CLOSE TO A LARGER ONE ($R_2 \gg \lambda \gg R_1$)

The interaction of voids in this case is described by three equations:

$$\dot{R}_1 = \frac{D(c_2 - c_1)}{R_1}; \tag{21}$$

$$\dot{R}_2 = \dot{R}^{(0)} - \left(\frac{R_1}{R_2}\right)^2 \dot{R}_1; \tag{22}$$

$$\dot{l} = 3\dot{R}_2^{(0)} - 3\left[\left(\frac{R_1}{2\lambda}\right)^2 - \left(\frac{R_1}{R_2}\right)^2\right]\dot{R}_1. \tag{23}$$

It is easy to see that the rate of change in the radius of voids does not in this approximation depend on the distance between them. Besides that, the trajectories of systems (21), (22) on the phase plane (Fig. 2) show that the size incompatibility continues to grow, with the smaller voids being dissolved. Then it follows from (21)–(23) that $d\lambda/dt>0$, which means that effective "collisions" of voids occur without any direct contact.

CONCLUSIONS

The above analysis of two-particle diffusion interaction of macrodefects explains certain features of the latter stages of Ostwald hardening of an assembly of precipitates in which the larger ones grow at the expense of the smaller. In the first consequential theory of that process, constructed by Lifshitz and Slezov [7] the growth rate of each precipitate was only thought to be dependent on its size and the mean level of supersaturation over point defects. In this "mean field" approximation, correlation between the size and position (local environment that is) of precipitates has not been taken into account. In the

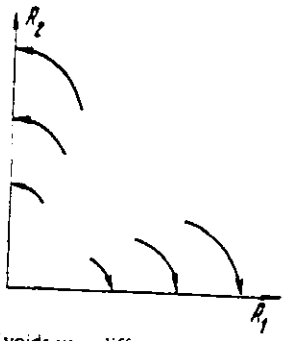

Fig. 2. Behaviour of voids very different in size on phase plane (R_1, R_2). The larger void is growing.

case of a finite volume fraction such correlations must obviously result in deviation of the real growth rate of precipitates from the value which is the average over the positions of its neighbours and has actually been used in the theory of [7].

The pumping transfer of material between nearest precipitates described above plays an important part here, since it decides the fate of each specific precipitate. The effect has been studied experimentally in [5], in which there are examples where initially identical precipitates either grew or were dissolved, depending on the local environment, which means the disposition of nearest neighbours. On the basis of those observations the authors of [5] query the use of the theory of Lifshitz and Slezov, according to which there should not be such a dependence. That conclusion is incorrect for two reasons. First of all, the theory of Lifshitz and Slezov only predicts the behaviour of the mean characteristics of an assembly, rather than individual precipitates. Secondly, the influence of the fluctuation behaviour of neighbouring particles on the particle size distribution function was taken into account by Lifshitz and Slezov in the "kinetic" approximation, introducing the integral of "collisions" between precipitates [11], by which the authors understood either direct merging or diffusion interaction of neighbouring precipitates. An important characteristic of "collision" is the length t_{co}, which means the time taken for two neighbouring voids to become one. As shown above t_{co} is governed by the process of transfer of material from smaller to larger precipitate, because the pumping is what prevents their direct contact. An accurate conclusion as regards the "collision" integral therefore requires the use of the above formulae for two-particle precipitate interaction.

APPENDIX

We transform the series

$$S = \sum_{k=0}^{\infty} \frac{\exp[-(2k+1)\nu]}{\exp[(2k+1)\mu]-1} \tag{A.1}$$

to a form convenient for the investigation of μ values ($\mu \ll 1$).

For this we must examine the function

$$f(x) = e^{-x\nu}(e^{x\mu}-1)^{-1}. \tag{A.2}$$

After direct and reverse Mellin [10] transformation of function $f(x)$ we get

$$f(x)=\frac{1}{2\pi i}\int_{\sigma-i\infty}^{\sigma+i\infty}\mu^{-s}\Gamma(s)\,\zeta(s,v)\,x^{-s}ds,\ \sigma>1, \tag{A.3}$$

where $v=1+\nu/\mu$, $\zeta(s,v)$ is the generalized Riemann zeta-function [10].

Thus the S sum we are seeking can be given in the form of an integral

$$S=\sum_{k=0}^{\infty}f(2k+1)=\frac{1}{2\pi i}\int_{\sigma-i\infty}^{\sigma+i\infty}\mu^{-s}\left(1-2^{-s}\right)\Gamma(s)\,\zeta(s,v)\,\zeta(s)\,ds,\ \sigma>1, \tag{A.4}$$

where $\zeta(s)$ is the Riemann zeta-function.

The integration contour in (A.4) is to the right of all the singularities of the integrand. At point $s=1$ the integrand has a second-order pole, and points $s=-(2k+1)$, $k=0, 1, 2, \ldots$ are first-order poles. Shifting the integration contour to the left and circumventing the poles, we get the formula for the sum of S as an asymptotic series to the powers of μ

$$S=\frac{1}{2\mu}\left(\ln\frac{2}{\mu}-\psi(v)\right)+\mu\sum_{k=0}^{\infty}\frac{B_{2k+2}B_{2k+2}^{(v)}\left(2^{2k+1}-1\right)}{(2k+2)!\,(2k+2)}\mu^{2k}, \tag{A.5}$$

where $\psi(v)=\frac{d}{dv}\ln\Gamma(v)$ is the digamma-function (psi-function); $B_m=B_m(1)$ —the Bernulli number, $B_m(v)$ — Bernulli polynomial [10]

$$S'=\sum_{k=0}^{\infty}\frac{(2k+1)\exp[-(2k+1)v]}{\exp[(2k+1)\mu]-1} \tag{A.6}$$

is transformed in the same way.

Finally we get the formula

$$S'=\frac{1}{2\pi i}\int_{\sigma-i\infty}^{\sigma+i\infty}\mu^{-s}\left(1-2^{1-s}\right)\Gamma(s)\,\zeta(s,v)\,(s-1)\,ds=$$

$$=\frac{1}{2\mu^2}\zeta(2,v)-\frac{1}{12}\left(v-\frac{1}{2}\right)-\sum_{k=1}^{\infty}\frac{B_{2k+2}B_{2k+1}^{(v)}}{(2k+2)!}\left(2^{2k+1}-1\right)\mu^{2k}. \tag{A.7}$$

REFERENCES

1. Ya. Ye. Geguzin and M. A. Krivoglaz, *Dvizhenive makroscopicheskikh vkhucheniy v tverdykh tel* (*Motion of Macroscopic Inclusions in Solids*), Moscow, Metallurgiya (1971).
2. V. I. Dubinko, V. V. Slezov, A. V. Tur and V. V. Yanovskiy, The theory of the gas bubble lattice, *Rad. effects*, **100**, 85 (1986).
3. V. I. Dubinko, A. V. Tur, A. A. Turkin and V. V. Yanovskiy, (Ordering mechanism of vacancy voids in a material under irradiation), *J. Nucl. Mater.*, **161**, 57 (1989).
4. C. W. J. Beenaker, Numerical simulation of diffusion-controlled droplet growth: dynamic correlation effects, *Phys. Rev.*, **A33**, 4482 (1986).
5. P. W. Voorhees and R. J. Schaefer, In situ observation of particle motion and diffusion interactions during coarsening, *Acta. Met.*, **35**, 327 (1987).
6. L. A. Maksimov and A. I. Ryazanov, (The diffusion interaction of voids), *Fiz. metal. metallored.*, **41**, 284 (1976).
7. I. M. Lifshitz and V. V. Slezov, (The kinetics of diffusion decomposition of supersaturated solid solutions), *Zh. eksp. teor. fiz.*, **35**, 479 (1958).

8. G. Bucholz, Calculation of electrical and magnetic fields.
9. V. I. Dubinko, A. V. Tur, A. A. Turkin and V. V. Yanovskiy, (Diffusion interaction of voids at random distances), preprint KhFTI 85–8, Moscow, TsNIIatominform (1985).
10. G. Bateman and A. Eyrdyne. *Higher Transcendental Functions*.
11. I. M. Lifshitz and V. V. Slezov, The kinetics of precipitation from supersaturated solid solution. *J. Phys. Chem. Sol.*, 19, 35 (1961).

Journal of Nuclear Materials 161 (1989) 57–71
North-Holland, Amsterdam

A MECHANISM OF FORMATION AND PROPERTIES OF THE VOID LATTICE IN METALS UNDER IRRADIATION

V.I. DUBINKO, A.V. TUR, A.A. TURKIN and V.V. YANOVSKIJ

Institute of Physics and Technology, the Ukrainian Academy of Sciences, Kharkov 310108, USSR

Received 10 December 1987; accepted 10 August 1988

We propose a new mechanism of interaction between voids, which is based on the elastically induced absorption of self-interstitial dislocation loops (SIA-loops) from the matrix. The main peculiarity of this dislocation interaction is its rigid relation to the crystal structure, namely, it arises only in the crystals, where SIA-loops can glide, and exists only between voids lying along the same loop-gliding directions. Void ordering is shown to originate from competition between the dislocation interaction and radiation-induced diffusion coarsening of voids, which leads to shrinkage of unfavourably positioned voids, if the void density exceeds the critical value. Voids in the superlattice thus formed have immediate neighbours along the loop-gliding directions, copying the host lattice due to the coincidence of the loop-gliding directions with close-packed directions of the matrix. The proposed model explains why the superlattice forms more readily in bcc than fcc metals and gives analytical expressions for the void lattice parameter and stationary size, being in good agreement with experimental data over the whole temperature range of superlattice formation.

1. Introduction

The formation of void and bubble lattices copying a crystal lattice arouses a great interest since it is a characteristic example of self-organization in an open dissipative system which a crystal under irradiation is. Since the first observations of vacancy void (Evans, 1971 [1]) and gas bubble (Sass and Eyre, 1973 [2]) lattices, a large body of experimental data has been obtained, according to which there are two common features in the ordering of voids and bubbles [3]: (i) a random distribution of voids or bubbles always precedes their ordering; (ii) the ordered cavity lattice has the same symmetry and alignment as the host lattice has. Other properties of the void lattice are summarized in section 2.

A great number of theoretical models have been proposed to explain ordering (their survey can be found in refs. [3–5]). However, none of the models proposed explains satisfactorily all substantial properties of the void lattice such as symmetry, saturation and preferential formation in bcc metals.

One can group the previous theoretical models into two broad categories according to the type of the void–void interaction considered, i.e., elastic or diffusion one. Models based upon the elastic and isotropic diffusion interactions cannot explain the symmetry of the void lattice and the saturation of its parameters with dose [3]. On the other hand, models based upon anisotropic diffusion of self-interstitial atoms (SIA) [6,7], apart from their intrinsic difficulties [30] contradict the conventional theory of void swelling. For example, the model of Woo and Frank [6] based on Foreman's proposal [27] on one-dimensionally propagating crowdion is supposed to explain ordering if the mean free path of a crowdion, L_c, is approximately equal to the mean distance between voids, l *. However, L_c decreases exponentially with temperature T in contrast to $l(T)$ which increases; as a consequence, they can meet only in a very narrow temperature range, whereas void lattice formation is observed over a rather wide temperature interval [3] (see also section 8.3). Besides, the crowdion model is inconsistent with the conventional concept of a dislocation preference towards SIA migrating isotropically.

* If L_c is essentially less than l, then the voids do not interact, while in the case of $L_c \gg l$ the nucleation of voids in interstitial positions should not take place, so a random distribution of voids would not have been observed, which is contrary to experiments.

To explain gas bubble ordering, Dubinko et al. [8] have proposed a new mechanism of interaction between bubbles, which is transferred by SIA-loops punched out by overpressurized bubbles. This interaction is repulsive and arises only between neighbouring bubbles lying along the same loop-punching directions. The main peculiarity of the dislocation interaction is its rigid relation with the crystallographic structure even of those crystals which are elastically and diffusionally isotropic. This is due to coincidence of loop-punching directions with Z close-packed directions of the host matrix, where Z is the coordination number. In a simple cubic lattice we have $Z = 6$, while in bcc $Z = 8$, and in fcc $Z = 12$. As a result of the dislocation repulsion and an isotropic diffusion attraction (due to absorption of SIA), a random distribution of bubbles becomes unstable and transforms into a lattice where the bubbles have immediate neighbours along the same directions as atoms in the host matrix have. This model predicts that bubbles can order only at low temperatures and high dose levels necessary for the dislocation interaction to arise, which is in agreement with experimental observations.

Contrary to bubbles, vacancy voids grow at rather high temperature via absorption of extra vacancies. At a random stage, the growth of large voids at the expense of smaller ones is observed [3], and void ordering is associated with a saturation of swelling with dose. A stationary void density is 10^2 times smaller and the void size is nearly 10 times greater than those for bubbles, and both usually show a strong temperature dependence. In spite of these differences, we shall show below that void ordering can also be explained by the dislocation mechanism of interaction between the voids arising in this case due to the absorption of SIA-loops formed diffusionally in the matrix. In our model a crystal structure manifests itself only in the choice of loop-gliding directions which determine a symmetry of the dislocation interaction between voids or bubbles. As for the rest, a crystal is considered as a diffusionally and elastically isotropic solid solution of point defects produced by irradiation.

In section 3 we consider the diffusion mechanism of growth and interaction of voids and show that the formation of a stationary state (random or ordered) cannot be explained by isotropic diffusion mechanisms only.

In section 4 we demonstrate that as a result of SIA-loop absorption, the voids lying along the close-packed directions attract each other in much the same manner as bubbles repulse one another due to SIA-loop punching. The dislocation attraction between voids together with the diffusion repulsion results in the formation of locally ordered configurations of voids which then grow at the expense of random voids that shrink. By this mechanism the void lattice emerges, wherein the voids have immediate neighbours along the same directions as atoms in the host matrix. Thus the symmetry of void and bubble lattices receives a common explanation since it is determined by the mode of the SIA-loop gliding.

An analysis of stability and saturation criteria presented in sections 5 and 6 leads to simple analytical expressions of the stationary void lattice constant a_s and the mean radius $\bar{R}_s$, which are compared with experimental data in section 7. The comparison shows a good agreement between calculated and experimental values of a_s and $\bar{R}_s$, which is achieved without any adjustable parameters. One of the most important advantages of the present model is the explanation it offers for the preferential void lattice formation in bcc metals, which is due to the fact that the conversion of SIA-Frank sessile loops (formed via condensation of SIA) into glissile loops takes place earlier in bcc than in fcc metals. In the latter case, the conversion loop size is far greater than the mean void size. As a consequence, in the majority of fcc metals the dislocation interaction between voids does not arise, and the void evolution is governed by the isotropic diffusion of point defects, which does not lead to ordering.

2. Experimental data

Below we list a summary of experimentally observed properties of the void lattice which must be explained by theory.

(1) At first, a random distribution of voids is formed, which then orders in local regions, subsequently spreading to adjacent areas [3,4].

(2) The void lattice has the same symmetry and alignment as the host matrix in bcc and fcc metals, while in hcp Mg the void alignment is found parallel to the basal plane [3,4].

(3) A saturation of the void lattice parameters (and consequently, of the material swelling) as a function of dose is observed unambiguously at least in niobium [12,13].

(4) The perfection of the void lattice increases with dose, i.e., the void lattice is stable in the size and coordinate space [2,19].

(5) The mean void radius $\bar{R}_s$ and the superlattice constant a_s both increase with temperature, while the $a_s/\bar{R}_s$ ratio decreases varying from 15 to 4 in most metals [3].

(6) The void lattice forms more easily in bcc metals, ch as Mo, Nb, Ta, W, than in fcc metals, among hich there are only two exceptions Al and Ni. Besides, irtial ordering has been observed in hcp Mg [3].

(7) An increase of temperature in the process of radiation may result in the destruction of the void ttice, the latter, however, recovers after a subsequent ecrease of temperature to the initial value [13].

(8) Postirradiation annealing leads to the shrinkage f voids, which, however, remain locally ordered at least the beginning of the annealing [13].

Thus the void lattice is an open dissipative structure, hich is stable under special irradiation conditions.

. A diffusion mechanism of growth and interaction of oids

The physical basis of nucleation and growth of SIA-oops and vacancy voids is the same, viz., the dislocation preference towards SIA along with a relative neurality of voids as sinks for point defects. Strictly speaking, the voids are also biased for SIA, but the value of heir bias is inversely proportional to the void size, so hat sufficiently large voids are almost neutral [14]. Iowever, the size dependence of the void bias results in radiation-induced competition between voids [15], i.e., he growth of large voids at the expense of small ones, which is observed experimentally at a random stage of oid evolution [3].

The diffusion growth of a void of radius R with ccount of its bias can be expressed as [15]:

$$\frac{dR}{dt} = \frac{1}{R^2}(\Delta^*\alpha_{iv} + D^*\alpha) \times \left\{\left(1 + \frac{N_\rho}{N}\right)\frac{R}{\bar{R}} - 1 - \frac{N_\rho}{N}\frac{R_c^\circ}{\bar{R}}\right\}, \quad (1)$$

$$N_\rho = \frac{\Delta^*\rho_0\delta_0}{4\pi(\Delta^*\alpha_{iv} + D^*\alpha)}, \quad R_c^\circ = \frac{Z_i^\circ\rho_0}{4\pi N_\rho}, \quad (2)$$

$$D^* = D_v c_v^\circ + D_i c_i^\circ, \quad \Delta^* = D_v(\bar{c}_v - \bar{c}_v^\circ), \quad (3)$$

where $\alpha = 2\gamma\omega/T$, γ is the void surface energy, ω is the atomic volume, T is the temperature, D_n is the point defect diffusivity in the lattice (index $n = v$ designates vacancies, while $n = i$ – SIA), c_v° is the equilibrium concentration of vacancies in a perfect crystal ($c_v^\circ \gg c_i^\circ$ in metals, and hence c_i° is neglected below), $\bar{c}_v^\circ$ and $\bar{c}_v$ are the mean vacancy concentrations in a crystal containing voids and dislocations without and under irradiation, respectively. Thus, the Δ^* value is a characteristic of a crystal supersaturation with vacancies caused by irradiation. A level of Δ^* is determined by the quasi-stationary balance equations

$$K - k_n^2 D_n(\bar{c}_n - c_n^\circ) - \beta_r(D_v + D_i)\bar{c}_v\bar{c}_i = 0, \quad (4)$$

$$k_n^2 = 4\pi\int_0^\infty Rf(R, t)\,dR + Z_n^\circ\rho_0 \quad (n = i, v), \quad (5)$$

where k_n^2 is the total sink strength of voids and dislocations, K the point defect production rate, β_r the recombination constant, $f(R, t)$ the void size distribution function, $N = \int_0^\infty f\,dR$ the void number density, $\bar{R}$ the mean void radius, ρ_0 is the density of "isolated" dislocations, whose bias factor δ_0 is determined only by the difference in elastic interaction with vacancies and SIA [15]:

$$\delta_0 = Z_i^\circ - Z_v^\circ, \quad Z_n = \frac{2\pi}{\ln(2/k_n L_n)}. \quad (6)$$

$$L_n = \frac{\mu b(1+\nu)|\Omega_n|}{36\pi(1-\nu)T}. \quad (7)$$

α_{iv} is the constant of the void bias factor $\delta_c = \alpha_{iv}/R$. In the isotropic approximation we can write [15]

$$\alpha_{iv} = \left[\frac{(1+\nu)\mu\omega}{36\pi T}\right]^{1/3}\left[\left(\frac{\Omega_i}{\omega}\right)^{2/3} - \left(\frac{\Omega_v}{\omega}\right)^{2/3}\right]b, \quad (8)$$

where μ is the shear modulus, ν the Poisson ratio, b the interatomic spacing, Ω_n the point defect relaxation volume.

Apart from voids and "isolated" dislocations, there can be other sinks of point defects in a crystal, such as immobile network dislocations, which absorb vacancies and SIA in equal numbers and do not climb [15]. For the sake of simplicity, we do not take them into consideration. Besides, eqs. (1)–(5) are derived in the zero approximation of $k_n R \to 0$, and in the first approximation of $\alpha_{iv}/R \ll 1$, $\alpha/R \ll 1$, which is valid in the case of large enough voids and a low volume fraction of macrodefects:

$$Q = \tfrac{4}{3}\pi\int_0^\infty R^3 f(R, t)\,dR + \pi\rho_0 b^2 \ll 1.$$

It can be easily seen from eq. (1) that the critical void radius R_c (voids with $R > R_c$ grow, while with $R < R_c$ they shrink) is determined by the dislocation-to-void density ratio, i.e., by the N_ρ/N value:

$$R_c = \left(\bar{R} + R_c^\circ\frac{N_\rho}{N}\right)\left(1 + \frac{N_\rho}{N}\right)^{-1}. \quad (9)$$

If $N_\rho/N \gg 1$, then R_c is close to the minimum R_c° value which controls the void nucleation rate. In this case all voids grow at the expense of "isolated" dislocations absorbing extra SIA, which results in the material swelling [14–16]. In the opposite limit $N_\rho/N \to 0$, all radiation-produced vacancies and SIA are divided between the voids, the total volume of which is consequently constant:

$$V = \tfrac{4}{3}\pi\int_0^\infty R^3 f(R, t)\,dR = V_0 = \text{const}.$$

However, the void size distribution changes with time, since R_c equals the mean void radius $\bar{R}$, i.e., large voids ($R > \bar{R}$) grow at the expense of small ones ($R < \bar{R}$). This process of void coarsening is based upon two different physical mechanisms. The first one is the mechanism of "thermal coarsening" (known as Ostwald ripening mechanism) driven by a more intense thermal emission of vacancies from smaller voids due to a larger curvature of their surface [17]. The second mechanism of "radiation-induced coarsening" proposed by Dubinko et al. [15] originates from the size dependence of the void bias factor $\delta_c = \alpha_{iv}/R$, according to which smaller voids absorb an excess of radiation-produced SIA and shrink, while larger voids absorb an excess of vacancies and grow. In eq. (1) the term $D^*\alpha$ relates to the thermal coarsening, and $\Delta^*\alpha_{iv}$ to the radiation-induced coarsening.

Diffusion fluxes of point defects to voids result also in the diffusion interaction between voids in the coordinate space [9]. Vacancy fluxes cause the diffusion repulsion of voids, whereas SIA fluxes cause the diffusion attraction. In general, according to ref. [9], the variation of distance between two voids, $2l$, with time due to the diffusion interaction is given by

$$\frac{d2l}{dt} = \frac{3}{2}\left(\frac{R}{l}\right)^2\left(\frac{dR}{dt}\right)_D, \quad (10)$$

where $(dR/dt)_D$ is the void growth rate due to the absorption of point defects.

In a stationary state we have $(dR/dt)_D = 0$, i.e., the diffusion interaction vanishes, and the elastic interaction between voids in isotropic materials is attractive at any distance [8]. Obviously, an attractive interaction alone cannot even stabilize the void lattice. Besides, a purely diffusion stationary state of the void ensemble under irradiation is unstable due to the mechanisms of coarsening which are able to make 90% of voids shrink in less than 5 dpa (displacements per atom) [15]. Such a reduction in the void number density has been observed experimentally by Loomis and Gerber [13] in Nb after a rise of temperature during irradiation (see section 8.5 in the text). The competition between voids ceases as voids become ordered, but it can be stopped only by a steady source of extra vacancies, i.e., when $\rho_0\delta_0 = \text{constant}$ and the total void volume increases with time. This is contrary to the observations of swelling saturation following the void lattice formation [12,13]. We may conclude that the formation of a stationary void lattice (or even a random stationary state) cannot be explained within the framework of isotropic diffusion mechanisms.

4. A dislocation mechanism of void interaction

It follows from the above that the mechanism of void ordering must impede the disordering effect of the coarsening mechanism without letting the voids grow. Moreover, it has to be linked with the crystallographic structure of the host lattice. We shall show that a mechanism satisfying these requirements is based upon the absorption of SIA-loops formed in the matrix via a condensation of SIA. Contrary to voids, the loops are able to move fast (glide) in the matrix if there is a force acting in the direction parallel to the loop Burgers vector, which exceeds the Peierls force $b\sigma_p$ [8]. A void

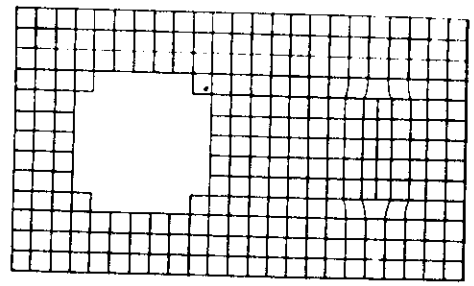

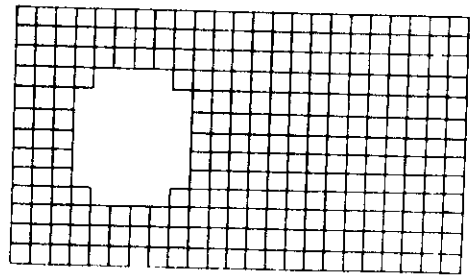

Fig. 1. Illustration of SIA-loop absorption effects. A decrease in vacancy number in the void is equal to the number of SIA in the loop. The maximum shift of the void "centre of gravity" Δx_{max} is calculated before the relaxation to an equilibrium shape.

produces the attractive force F_l per unit length of a SIA loop of radius r_l lying at a distance x from the void centre, where

$$F_l = \frac{3r_l R^2 b\gamma}{x^4}; \quad \frac{r_l}{x}, \frac{R}{x} \ll 1; \tag{11}$$

is derived in the isotropic approximation of linear elasticity theory [11], assuming that the loop plane is perpendicular to the void direction and that $x \gg R$. Loops of radius $r_l \lesssim R$, for which $F_l > b\sigma_p$, glide towards the void and annihilate with it, thus reducing the void volume by $\pi r_l^2 b$ and shifting its "centre of gravity" in the direction of the loop gliding by $\Delta x_{max} = \frac{1}{4} r_l^2 b / R^2$. The surface diffusion restores a spherical shape of the void around a new "centre of gravity" and with a new radius reduced by the value $\Delta R = \pi r_l^2 b / 4\pi R^2 = \frac{1}{3}\Delta x_{max}$. The process occurs in the same fashion as in the case of loop punching [8] but in the inverse sequence, i.e., the loop "pushes" the void in the direction of gliding (see fig. 1).

The maximum distance of annihilation between a loop and a void, l_p, is given by the equilibrium condition $F_l(l_p) = b\sigma_p$:

$$l_p = \left(\frac{3\gamma}{\sigma_p}\right)^{1/4} R^{3/4}. \tag{12}$$

Each crystal is characterized by its set of glide directions, along which voids can punch out or absorb loops. As a rule, these are Z close-packed directions of the lattice [8,10]. Thus, a void can absorb SIA-loops from loop-supply-cylinders (LSCs) * of length l_p and radius R extended in the close-packed directions, if the loops are able to glide. If loops are sessile or the σ_p value is too high ($\sigma_p > \sigma_p^{max}$, which will be estimated below), then the loop-void annihilation can be neglected.

4.1. Interaction of voids in the coordinate space

Consider two voids aligned along a glide direction at a distance of $2l < 2l_p$. Each void absorbs SIA-loops from $Z-1$ "free" LSCs of lengths l_p and from one LSC of length l which is extended in the direction of another void. Since $l < l_p$, the number of loops arriving from the occupied direction is less than that from the opposite "free" direction, i.e., voids attract each other. The velocity of the dislocation-induced void motion $(\mathrm{d}l/\mathrm{d}t)_l$ equal the rate of nucleation of favorably oriented loops per unit volume $\dot{n}_l$ times the difference of LSC volumes along the "free" and "occupied" directions, and times the mean shift due to the absorption of one loop $\langle \Delta x \rangle$:

$$\left(\frac{\mathrm{d}l}{\mathrm{d}t}\right)_l = \dot{n}_l (l - l_p)\pi R^2 \langle \Delta x \rangle. \tag{13}$$

Assuming that loops cross the LSC section homogeneously, the $\langle \Delta x \rangle$ value is given by

$$\langle \Delta x \rangle = \tfrac{1}{2}\Delta x_{max} = \tfrac{1}{2}\Delta R \tag{14}$$

The rate of the dislocation-induced void shrinkage equals ΔR times the total number of loops arriving from all directions per unit time:

$$\left(\frac{\mathrm{d}R}{\mathrm{d}t}\right)_l = -\Delta R \dot{n}_l \left[(Z-1)l_p + l\right]\pi R^2. \tag{15}$$

According to the eqs. (13)–(15), the relation between $(\mathrm{d}l/\mathrm{d}t)_l$ and $(\mathrm{d}R/\mathrm{d}t)_l$ is given by

$$\left(\frac{\mathrm{d}l}{\mathrm{d}t}\right)_l = \frac{3}{2}\left(\frac{\mathrm{d}R}{\mathrm{d}t}\right)_l \frac{1 - l/l_p}{Z - 1 + l/l_p}. \tag{16}$$

Taking into account the dislocation attraction [eq. (16)] and the diffusion repulsion [eq. (10)] between voids, the net velocity of the void motion is given by

$$\frac{\mathrm{d}l}{\mathrm{d}t} = \frac{3}{4}\left(\frac{R}{l}\right)^2 \left(\frac{\mathrm{d}R}{\mathrm{d}t}\right)_D - \frac{3}{2}\left|\left(\frac{\mathrm{d}R}{\mathrm{d}t}\right)_l\right| \frac{1 - l/l_p}{Z - 1 + l/l_p}, \tag{17}$$

where $\dot{R}_D > 0$, $\dot{R}_l < 0$. The distance dependence of $\mathrm{d}l/\mathrm{d}t$ (fig. 2) shows that voids aligned along a close-packed direction can form a stable couple (at $l = l_1$) due to the cooperation between dislocation attraction and diffusion repulsion of voids. Voids aligned along other directions diffusionally repulse each other and do not form a couple. It is far more difficult to derive an equation of motion of a void that has more than one immediate neighbour because of the multidimensionality of the problem and other factors complicating the solution of a many-body problem. Consequently, eq. (17) is valid only qualitatively when considering the motion of voids in a void ensemble, similarly to the use of a pairwise atomic potential in the description of the crystallization process.

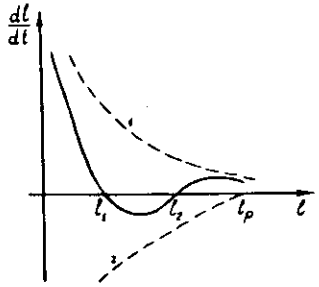

Fig. 2. Dependence of the rate of void motion $\mathrm{d}l/\mathrm{d}t$ on the spacing of voids lying along a loop-gliding direction (full line). Line 1 corresponds to the diffusion repulsion, line 2 to the dislocation attraction.

Thus, the dislocation mechanism of the void–void interaction is closely related to the crystallographic structure of a material, owing to which within an initially random ensemble the voids, that have a sufficient number of immediate neighbours along close-packed directions, form locally ordered regions coexisting with locally random regions, where voids have few immediate neighbours along close-packed directions.

4.2. Interaction of voids in the size space

The most important consequence of the loop absorption is that it makes a void growth depend not only on the void size (as in the case with point defect absorption) but also on the location of void's immediate neighbours (which is not the case in the isotropic point defect absorption). To show this, we write eq. (1) in the approximation of large voids ($R \gg R_c^\circ$) as:

$$\left(\frac{\mathrm{d}R}{\mathrm{d}t}\right)_D \approx \frac{q}{4\pi N R^2}\left\{\left(1 + \frac{N}{N_\mu}\right)\frac{R}{\bar{R}} - \frac{N}{N_\mu}\right\},$$

$$q \equiv 4\pi \int_0^\infty R^2 \left(\frac{\mathrm{d}R}{\mathrm{d}t}\right)_D f(R, t)\,\mathrm{d}R$$

$$= \Delta^* \rho_0 \delta_0 \left(1 - \frac{R^\circ}{\bar{R}}\right) \approx \Delta^* \rho_0 \delta_0. \tag{18}$$

where $q = (\mathrm{d}V/\mathrm{d}t)_D$ is the swelling rate due to the absorption of extra vacancies by voids. The same number of extra SIA aggregates to form SIA-loops per unit volume, if straight dislocations are neglected. Since all loops from LSCs with the Burgers vectors parallel to the LSC directions get into the voids, the loop-induced decrease of a void volume equals q times the LSC volume times the $2/Z$ factor which is the ratio of the number of loops with an appropriate orientation to the total number of loops.

When voids are small, their LSCs do not overlap ($l \gg l_p \sim \bar{R}^{3/4}$), and the only effect of the loop absorption is a decrease of net void growth rates, which are at this stage practically independent of void positions in the matrix. When $l < l_p$, the locally ordered voids (see the previous section) have an advantage in growth over the locally random ones because their LSCs are shorter, i.e., the net vacancy influxes are larger than those of random ones (see fig. 3).

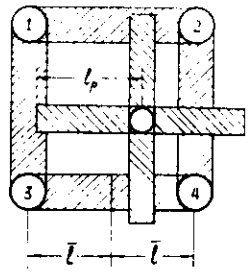

Fig. 3. Two-dimensional illustration of the division of voids into "ordered" and "random" for $l_p > l$. Voids 1, 2, 3, 4 represent an elementary cell of "ordered" voids, whose LSCs (dashed) have a length l. In the middle of the cell a "random" void is depicted, for which the LSC length is $l_p > l$.

Another consequence of the LSC overlap is that loops nucleated outside them cannot form new crystal planes by coalescence, because in the process of growth they get inevitably into one of the LSCs and are absorbed by voids. This increases the void shrinkage rate $(\mathrm{d}R/\mathrm{d}t)_l$ by a factor of η, which will be estimated below. After summation, the net rates of growth (or shrinkage) of "ordered" $(\mathrm{d}R/\mathrm{d}t)_o$ and "random" $(\mathrm{d}R/\mathrm{d}t)_r$ voids are given by

$$\left(\frac{\mathrm{d}R}{\mathrm{d}t}\right)_o = \frac{q}{4\pi N R^2}\left\{\left(1 + \frac{N}{N_\mu}\right)\frac{R}{\bar{R}} - \frac{N}{N_\mu} - 2\pi R^2 \eta N l\right\}, \tag{19}$$

$$\left(\frac{\mathrm{d}R}{\mathrm{d}t}\right)_r = \frac{q}{4\pi N R^2}\left\{\left(1 + \frac{N}{N_\mu}\right)\frac{R}{\bar{R}} - \frac{N}{N_\mu} - 2\pi R^2 \eta N l_p\right\}, \tag{20}$$

where N is the total void density and $\bar{R}$ is the radius averaged over both "ordered" and "random" voids. According to the eqs. (19) and (20) the SIA loop absorption, first, increases the void critical radius R_c and, second, results in the shrinkage of the voids of the radii exceeding a maximum value R_{max}. Obviously, R_{max} is larger for "ordered" voids than for "random" ones, while it is the opposite case with the R_c value. Since after the LSC overlap all SIA condensing in loops return into voids, the total void volume saturates, though the volume fraction of "ordered" voids may grow at the expense of "random" ones. This process is analogous to the diffusion void coarsening, but the criterion of void

* We use the abbreviation similar to that of Woo and Frank [6] for the crowdion-supply-cylinders (CSCs).

owth or shrinkage is now dependent on the void sition. It is possible to estimate the η value from the ddition of conservation of the total void volume ich takes a simple form after the shrinkage of ran- m voids is over $(dV/dt)_\eta = q(1 - 2\pi\bar{R}^2 i\eta)$ whence

$$N_\eta(\bar{R}) = \frac{1}{2\pi N i \bar{R}^2} = \frac{1}{2\pi N i (\bar{R})^2}. \tag{21}$$

s. (19) and (20), after substituting eq. (21) in it and roducing the following notation $u = R/\bar{R}$, $\beta \equiv N/N_\rho$, 1 be written as

$$\left(\frac{R}{i\bar{R}}\right)_\alpha = \frac{q}{4\pi N \bar{R}^2 u^2}(u-1)(\beta - u), \tag{22}$$

$$\left(\frac{R}{i\bar{R}}\right)_r = \frac{q}{4\pi N \bar{R}^2 u^2}(u-u_1)(u_2-u), \tag{23}$$

ere

$$_2 = \frac{i}{i_p}\frac{1+\beta}{2}\left(1 \mp \sqrt{1 - \frac{i_p}{i}\frac{4\beta}{(1+\beta)^2}}\right).$$

The plot of $(dR/dt)_{\alpha,r}$ is shown in fig. 4 for differ- β values.

At $\beta < 1$, a stable size of "ordered" voids, R°_{max}, ncides with $\bar{R}$ ($u_2^\circ = 1$). A stable size of "random" ds, R'_{max}, is smaller than $\bar{R}$ ($u_2' < 1$), but still exists $i_p < i(1+\beta)^2/4\beta$. It means that the dislocation chanism favouring small voids saves them from a nplete shrinkage, and "random" voids coexist with dered" ones in a stationary state. The complete inkage of "random" voids is possible only if $i_p > i(1$ $3)^2/4\beta$, in which case the location effect of the ocation mechanism prevails over the size effect.

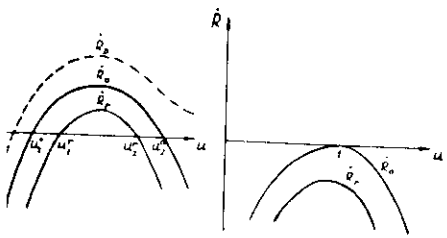

4. Plot of the growth rates of "ordered" (upper curves) "random" (lower curves) voids at different β values, rding to eqs. (22) and (23). (a, left) $\beta > 1$, nonstationary : $u_1^\circ = 1$, $u_2^\circ = \beta$; $u_1' < 1$, $u_2' < \beta$. $\beta < 1$, stationary state: $< \beta$, $u_2^\circ = 1$; $u_1' < \beta$; $u_2' < 1$. (b, right) $\beta = 1$, "ordered" s are in a stable stationary state, $u_1^\circ = u_2^\circ = 1$; all "ran- " voids shrink, $(dR/dt)_r < 0$. The dashed curve corre- onds to the purely diffusion void growth rate $(dR/dt)_D$.

However, this condition is hard to reach if $\beta \ll 1$, because with $i_p > i$ the void growth is saturated and further increase of i_p is inhibited. Another consequence of the i_p saturation at $i_p \gtrsim i$ is that $R'_{max} \mid_{\beta \ll 1} \approx \bar{R}i/i_p \lesssim \bar{R}$. It means that stable sizes of "ordered" and "random" voids differ only insignificantly.

On the other hand, at $\beta > 1$ both "random" and "ordered" voids are unstable, because the critical radius here is equal to ($u_1^\circ = 1$) or even larger than $\bar{R}$ ($u_1' > 1$). It means that the voids with $R > R_c \geq \bar{R}$ grow at the expense of small voids ($R < R_c$) due to diffusion coarsening.

Finally, at $\beta = 1$ "ordered" voids are in a stable stationary state $u_1^\circ = u_2^\circ = 1$, whereas all "random" voids shrink, $(dR/dt)_r < 0$, as soon as $i_p > i$. Thus, the two conditions $\beta = 1$ and $i_p = i$ determine the point on the ($\bar{R}$, N) plane where the phase transition from the random to ordered state takes place. Let us follow this process from the very beginning.

5. Void lattice formation

At an early stage of nucleation and growth, voids are randomly distributed until $i_p > \bar{R}^{3/4} < i$. As the voids grow on, their LSCs overlap, leading to a saturation of swelling and division of voids into locally ordered and random ones. A subsequent evolution of the void ensemble depends on the void density.

If $N < N_\rho$, then the diffusion coarsening mechanism is too weak to remove "random" voids (see above) and a "mixed" stationary state is established which is random from the experimental point of view, since $R'_{max} \leq R^\circ_{max}$.

In the opposite case of $N > N_\rho$, large voids, both "ordered" and "random", grow at the expense of small ones due to diffusion coarsening. As a result, $N(t)$ drops and reaches N_ρ, and then all "random" voids shrink, while "ordered" voids come to a stable state (see fig. 4). The void lattice thus formed copies the host lattice due to coincidence of loop-gliding directions with closepacked directions of the matrix.

We may conclude that, besides the ability of SIA-loops to glide, a sufficiently high void density $N \geq N_\rho$ is required for void lattice formation.

6. Void lattice parameters

As shown above, the overlap of LSCs taking place at $i_p \geq i$, means that SIA-loops cannot escape voids, and, hence, are not able to coalesce to form new straight

dislocations and crystal planes. Consequently, the condition $i_p = i$ means a saturation of swelling and gives us a relationship between stationary i and $\bar{R}_s$ values, or, in the case of the void lattice, a relationship between the lattice parameter a_s (the void spacing along ⟨100⟩ directions) and the mean void size $\bar{R}_s$:

$$a_s = mi_p = m\left(\frac{3\gamma}{\sigma_p}\right)^{1/4}\bar{R}_s^{1/4}, \tag{24}$$

where

$$m = \begin{cases} 4/\sqrt{3} & \text{for bcc lattice,} \\ 2\sqrt{2} & \text{for fcc lattice.} \end{cases}$$

Another relationship between a_s and $\bar{R}_s$ follows from the condition of the void ordering, i.e., $N = N_\rho$:

$$a_s = (\kappa/N_\rho)^{1/3}, \ \kappa = \begin{cases} 2 \text{ for bcc lattice} \\ 4 \text{ for fcc lattice.} \end{cases} \tag{25}$$

Generally, $\bar{R}$ enters into the expression for N_ρ [eq. (2)] via the supersaturation Δ^*, which is, according to the balance equations [eq. (4)], given by

$$\Delta^* \approx \begin{cases} K/4\pi N_\rho \bar{R}, & 4\pi N_\rho \bar{R} \gg K/\Delta_r^*, \\ \left(\dfrac{KD_v}{\beta_r}\right)^{1/2} \equiv \Delta_r^*, & 4\pi N_\rho \bar{R} \ll K/\Delta_r^*, \end{cases} \tag{26}$$

where the upper approximation is valid when voids are the main sinks for point defects, whereas the lower one should be used when the bulk recombination of point defects dominates. In the latter case a_s does not actually depend on $\bar{R}_s$.

Note that in the void lattice case we have calculated both a_s and $\bar{R}_s$ owing to the ordering criterion $\beta = 1$ ($N = N_\rho$), whereas in the random case we have the inequality $\beta < 1$ and, hence, know only the region of stationary $N < N_\rho$ and $\bar{R} > \bar{R}_s$ values.

In the region of "radiation coarsening" ($\Delta^*\alpha_{iv} \gg D^*\alpha$) $N_\rho = \rho_0\delta_0/4\pi\alpha_{iv}$, therefore a_s and $\bar{R}_s$ do not depend directly on the irradiation conditions K and T:

$$a_s = \left(\frac{4\pi\kappa\alpha_{iv}}{\rho_0\delta_0}\right)^{1/3}, \ \bar{R}_s = \left(\frac{4\pi\kappa\alpha_{iv}}{m^3\rho_0\delta_0}\right)^{4/9}\left(\frac{\sigma_p}{3\gamma}\right)^{1/3}, \tag{27}$$

$$\frac{a_s}{\bar{R}_s} = \left(\frac{\rho_0\delta_0}{4\pi\kappa\alpha_{iv}}\right)^{1/9}\left(\frac{3\gamma}{\sigma_p}\right)^{1/3} m^{4/3}. \tag{28}$$

In the region of "thermal coarsening" ($\Delta^*\alpha_{iv} \ll D^*\alpha$) voids are usually the main sinks, hence a_s and $\bar{R}_s$ are given by

$$a_s = \frac{(2\pi\kappa)^{1/7}}{m^{2/7}}\left(\frac{\sigma_p}{3\gamma}\right)^{1/14}\left(\frac{D^*\alpha}{K\rho_0\delta_0}\right)^{3/14},$$

$$\bar{R}_s = \frac{(2\pi\kappa)^{4/7}}{m^{12/7}}\left(\frac{\sigma_p}{3\gamma}\right)^{3/7}\left(\frac{D^*\alpha}{K\rho_0\delta_0}\right)^{2/7}, \tag{29}$$

$$\frac{a_s}{\bar{R}_s} = \frac{m^{10/7}}{(2\pi\kappa)^{1/7}}\left(\frac{3\gamma}{\sigma_p}\right)^{5/14}\left(\frac{K\rho_0\delta_0}{D^*\alpha}\right)^{1/14}. \tag{30}$$

In the isotropic approximation, the α_{iv}/δ_0 ratio entering in eqs. (27) and (28) is practically constant [15]:

$$\alpha_{iv}/\delta_0 = b\left(1 - \left(\frac{\Omega_v}{\Omega_i}\right)^{2/3}\right)\Big/\ln\left(\frac{\Omega_i}{|\Omega_v|}\right) - b,$$

$$\text{if } \left|\frac{\Omega_i}{\Omega_v}\right| = 1 - 10.$$

A simple model of Frenkel and Kontorova gives the following estimate for the Peierls stress [18] $\sigma_p \sim 4 \times 10^{-5}\,\mu$. Thus, the only parameter in eqs. (27)–(30) which has to be determined is a stationary dislocation density ρ_0. According to experiment, ρ_0 varies from 10^{12} m^{-2} to 10^{14} m^{-2}, the ratio $a_s/\bar{R} \sim \rho_0^{1/9}$, $\rho_0^{1/14}$ remaining practically unchanged.

Above, we have taken into account only SIA-loops, in which case $\rho_0 = 2\pi\bar{r}_i n_i$, where $2\bar{r}_i$ is the mean loop size, n_i is the loop stationary density, which is sustained by the balance between the loop nucleation and absorption rates. However, before the overlap of LSCs takes place, the loops can grow and coalesce to form a dislocation network which is still present at the void ordering stage. Naturally, with the dislocations absorbing extra SIA, the net void volume grows. In this case, ρ_0 is the total dislocation density, and eqs. (27)–(30) describe initial parameters of the void lattice. However, without a further supply of growing loops, the dislocation network density should fall significantly and can be safely neglected in eqs. (27)–(30). This is also confirmed by experiments [13,19].

7. Region of void lattice formation

It follows from the above that a sufficiently high void nucleation rate is necessary for the ordering, so that N could reach the critical value N_ρ. Realization of this criterion is likely at low and medium temperatures, when R_c° is not too large. Since impurities strongly influence the void nucleation, they can stimulate (or

impede) void lattice formation. However, according to our model, the void lattice parameters should be independent of the impurity concentration, provided that the latter does not influence ρ_0, δ_0 or σ_p values.

According to eq. (29), the void spacing increases with temperature and reaches the mean spacing between the dislocations of the network, l_d, since the temperature dependence of the latter is weaker. At $\bar{l} \geq l_d$, the dislocations screen the loop-induced interaction between voids, reducing its range to l_d. Consequently, the void lattice does not form, though a saturation of swelling still can take place as a result of the loop absorption process.

Thus, our model predicts void lattice formation from a random state at sufficiently low temperatures ($N_p(T) > l_d^{-3}$) in those materials, where a high void density is nucleated ($N \geq N_p$) and SIA-loops can glide ($l_p < l_p^{max}$). The symmetry of the void lattice is determined by orientation of loop-gliding directions, and its parameters – by the dislocation density ρ_0, irradiation conditions K, T and by the material constant according to eqs. (24) and (25).

8. Comparison with experimental data

8.1. Mode of ordering

According to our theory, the void ordering starts when the mean range of the dislocation interaction $l_p \sim \bar{R}^{3/4}$ exceeds a half of the mean distance between randomly distributed voids. At the random stage, the growth of large voids at the expense of small ones can take place, if $N > N_p$. At $l_p > \bar{l}$, locally ordered voids appear which then grow at the expense of random ones, while the total void swelling saturates, as most of the SIA-loops are absorbed by voids. Exactly the same mode of ordering is observed experimentally [3,4].

8.2. Symmetry

Voids in the lattice formed through the dislocation mechanism have immediate neighbours along loop-gliding directions. The observed copying of the host matrix by the void lattice is due to coincidence of the loop-gliding directions with close-packed directions of the matrix. This coincidence has been observed experimentally [10] and explained theoretically [18] by the fact that along the close-packed directions the Burgers vector has a minimal length. An interesting exception to this rule is found in CaF_2-type compounds, where a simple cubic lattice forms irrespective of its fcc structure [5]. However, the voids in CaF_2 are formed in a simple cubic sublattice of fluorine atoms, leaving the fcc sublattice of Ca undamaged. Therefore, it is only natural to suggest that the void lattice in CaF_2 has a simple cubic symmetry, since the SIA-loops are related to the fluorine sublattice and glide along 6 close-packed ⟨100⟩ directions. Thus, this "exception" provides an additional evidence for the dislocation model of ordering.

Another exception is the ordering in hcp Mg, where void alignment is found parallel to the basal plane [3]. This may be in agreement with the dislocation model provided that the SIA-loops in Mg condense primarily on the basal plane and glide in the perpendicular direction, thereby giving rise to one-dimensional dislocation interaction between voids. However further investigations are needed here.

Table 1
The Nb + 0.4% oxygen microstructure versus irradiation conditions according to ref. [13]. N_p, $\bar{R}_s$ and V_s are the stationary values calculated at $\Omega_i/|\Omega_v| = 1.05$ (the first number)–2 (the second number). Subscript "ex" denotes experimental data

	Temperature and exposure dose		
	50 dpa at 777 °C	50 dpa at 957 °C	50 dpa at 777 °C + 50 dpa at 957 °C + 50 dpa at 777 °C
$\rho_0 = 2\pi n_i \bar{r}_i$ (m^{-2})	9×10^{13}	3×10^{13}	4×10^{13}
$l_d = (\pi\rho d)^{-1/2}$ (nm)	90	90	126
$\bar{l} = (\frac{4}{3}\pi N_{ex})^{-1/3}$ (nm)	15	49	20
$\bar{R}_{ex}$ (nm)	3	18	5
$\bar{R}_s = (\frac{\sigma_p}{3\gamma})^{1/3}(6N_p)^{-4/9}$ (nm	6–4	25–13	9–6
N_{ex} (m^{-3})	7×10^{22}	2×10^{21}	3×10^{22}
N_p (m^{-3})	$(3-4)\times10^{22}$	$(1-4)\times10^{21}$	$(1-3)\times10^{22}$
$V_{ex} = \frac{4}{3}\pi N \bar{R}_{ex}^3$	0.008	0.049	0.016
$V_s = \frac{2\sigma_p}{9\gamma}(6N_p)^{-1/3}$	0.02–0.016	0.05–0.03	0.025–0.02

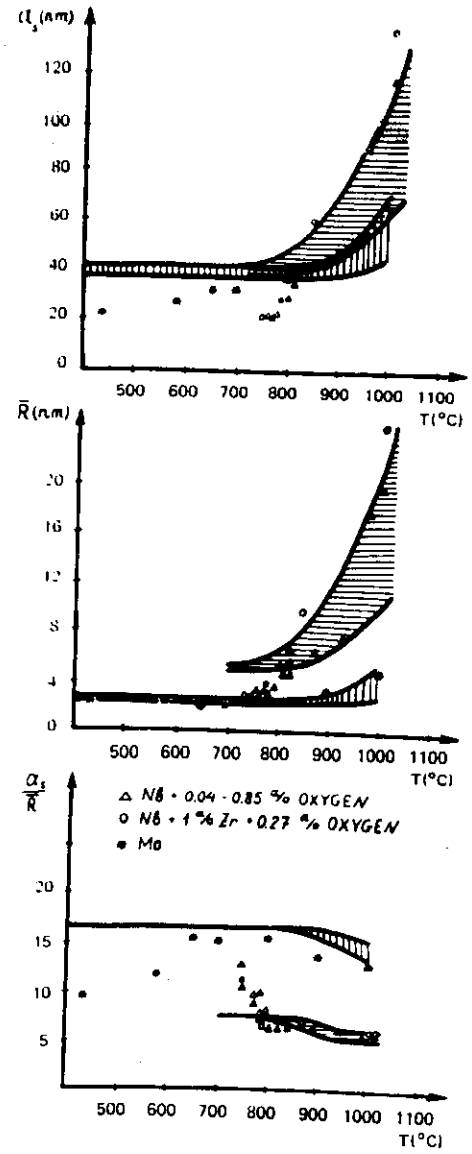

Fig. 5. Regions of a_s and $\bar{R}_s$ values for Mo (shaded with vertical lines) and Nb (horizontal lines) calculated according to eqs. (24) and (25) at the following parameters: $\rho_0 = 10^{14}$ m^{-2}; $b = 0.25$ nm; $\gamma = 2$ J m^{-2}; $\sigma_p = 10^6$ J m^{-3} (Mo), 10^7 J m^{-3} (Nb); $E_v^f + E_v^m = 4.3$ eV (Mo), 3.2 eV (Nb); $K = 10^{-6}$ dpa/s (Mo), 5×10^{-3} dpa/s (Nb); $\Omega_i/|\Omega_v| = 1.05$ (upper bounds) to 2 (lower bounds). (•) experimental a_s and $\bar{R}_s$ values in Mo according to refs. [19,20]; (△, ○) a_s and $\bar{R}_s$ in Nb according to refs. [13,26].

8.3. Dose rate and temperature effect

Comparison of experimental and theoretical a_s and $\bar{R}_s$ values is shown in table 1 and fig. 5. It can be seen from figs. 5 and 6 that their temperature dependences are alike: they are nearly constant in the radiation coarsening region ($\Delta^* a_{iv} > D^* a$) and increase with temperature in the thermal coarsening region ($\Delta^* a_{iv} < D^* a$). At the same time, the $a_s/\bar{R}_s$ ratio slightly decreases, being in agreement with the general rule, viz., void lattice formation at temperatures below the peak swelling value [3].

Variations in K and T with voids remaining in the radiation coarsening region should not, according to the theory, effect a_s and $\bar{R}_s$. This conclusion has been proved experimentally [3]. For example, in Mo irradiated at 650 °C by neutrons at $K = 10^{-6}$ dpa/s and also irradiated at 870 °C by 2 MeV nitrogen ions at $K = 7\times10^{-3}$ dpa/s [17], a_s was 34 nm and 22 nm, and $\bar{R}_s$ was 1.9 nm and 2 nm, respectively.

Temperature dependence of a_s and $\bar{R}_s$ in Nb is stronger than in Mo (fig. 5) because of a lower self-diffusion energy $E_v^f = E_v^m = 3.2$ eV in Nb than in Mo, where $E_v^f + E_v^m = 4.3$ eV. As a result, the void lattice in Nb is formed primarily in the region of thermal coarsening (see fig. 6). Loomis and Gerber [13] have found the following relationship between a_s and $d_s = 2\bar{R}_s$ in Nb: $a_s = 5.91\ (\bar{d}_s)^{0.73}$, which is very close to our $a_s = (10.7\gamma/\sigma_p)^{0.25}(\bar{d}_s)^{0.75}$. Comparison of the coefficients of the powers of $\bar{d}_s$ gives a reasonable value of $\sigma_p = 2\times10^7$ J $m^{-3} = 5\times10^{-4}\mu$.

According to table 1, the void spacing $\bar{l}$ in Nb increases with temperature and at 957 °C reaches 49 nm, which is comparable with the spacing between network dislocations $l_d \approx 90$ nm, the latter screening the interaction of voids. As a result, the perfection of the

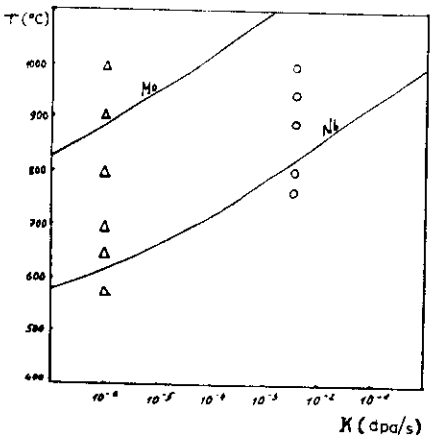

Fig. 6. Graphic representation of regions of radiation coarsening $\Delta^* \alpha_{iv} > D^* \alpha$ (above the curve) and thermal coarsening $\Delta^* \alpha_{iv} < D^* \alpha$ (below the curve) on the K, T plane. (△) and (○) are the irradiation conditions, under which the void lattice has been observed in Mo and Nb, respectively.

void lattice at 957 °C is much worse than at 777 °C, when $l = 15$ nm $\ll l_d \approx 90$ nm, and the dislocation network does not interfere with the void interaction.

8.4. Effect of impurities

Loomis and Gerber [13] have found that a threshold oxygen concentration is required to induce ordering in Nb. Once this concentration is achieved, the superlattice parameters are independent of the oxygen concentration. In "pure" Nb (< 0.04 at% below the threshold oxygen concentration) voids remain random at all temperatures, even after their growth comes to a standstill (N, $\bar{R}$, V = constant). At 777 °C, the observed loop density $\rho_0 \approx 2\pi \bar{r}_i n_i \approx 10^{14}$ m^{-2} is reported to be the same in both "pure" and O-doped Nb, which corresponds to $N_p \approx \rho_0 \delta_0 / 4\pi \alpha_{iv} \approx 3 \times 10^{22}$ to 6×10^{22} m^{-3} at $\Omega_i / |\Omega_v| = 1$ to 10, respectively. In "pure" Nb the observed void density $N = 2 \cdot 10^{22}$ m^{-3} is less than N_p, and hence, is insufficient for the ordering ($\beta < 1$), whereas in O-doped Nb $N \approx 7 \times 10^{22}$ m$^{-3} \geq N_p$ which induces the void ordering. Though the quantitative difference in N is small, the void behaviour completely changes in accordance with predictions of the theory.

A high concentration of nitrogen has also been reported to be a prerequisite for void ordering in stainless steel irradiated by electrons [28]. This is the only case of ordering in metals induced by electrons, which shows that it is not the nature of the radiation that influences the ability of voids to order but, rather, the radiation environment associated with each kind of the projectile. Since it is thin foils that are irradiated with electrons, a strong influence of close sample surfaces usually decreases the void density. That is why even in the mentioned experiment by Fisher and Williams [28] the ordering was observed only in thicker parts of the wedgeshaped foil.

On the other hand, no such threshold effects due to impurities have been observed in neutron- or ion-irradiated Mo and its alloys, where the void lattice readily forms even without impurities, since the void concentration is sufficiently high.

8.5. Radiation stability

According to the present theory, the void lattice, once formed, is stable if N_p does not vary with time. If N_p decreases, then an extra number of voids $N - N_p$ has to shrink in order to restore a balance between diffusion and dislocation mechanisms (see section 4.2). On the other hand, if N_p increases, then the critical void radius becomes small (see fig. 4), making possible the nucleation of $N_p - N$ new voids at the expense of the voids with $R > \bar{R}$ which at $\beta < 1$ have to shrink.

The simplest way to change N_p is to shift the irradiation temperature into the region $D^* \alpha > \Delta^* \alpha_{iv}$, where N_p strongly depends on T. Such an experiment has been carried out by Loomis and Gerber in Nb [13]. After initial irradiation up to a dose of 50 dpa at 777 °C, a stable void lattice formed wherein $l = 15$ nm $\ll l_d = 90$ nm. After additional irradiation up to 50 dpa at 957 °C, 90% of the voids shrink leaving the remaining voids in a new stationary but almost disordered state, where $l = 49$ nm was of the same order as $l_d \approx 90$ nm. After subsequent irradiation at a lower temperature of 777 °C up to 50 dpa (the total dose being 150 dpa), a new population of small voids nucleated, while large old voids shrank to their size, and the void lattice formed again, wherein $l = 20$ nm $\ll l_d = 126$ nm. A slight increase in l compared to the first irradiation at 777 °C is due to an observed decrease in ρ_0 from 10^{14} m^{-2} down to 4×10^{13} m^{-2}. As we can see, these very detailed experimental observations by Loomis and Gerber agree with the predictions of the present theory with a surprising accuracy.

The void lattice can also lose its stability due to the variation of the internal parameters δ_0 or α_{iv}, which influence N_p, T and K remaining unchanged. The point

is that δ_0 and α_{iv} are generally complex functions of radiation environment, e.g., impurity content, phase and dislocation structure, etc. For example, the void preference parameter α_{iv} can be increased by impurity precipitation on void surfaces which make an additional barrier to vacancy absorption. A similar mechanism has been proposed qualitatively by Evans [22] as an explanation of his observation of void shrinkage that destroyed the void lattice during reactor irradiation of MO at constant T and K. According to eq. (2), the increase of α_{iv} leads to a decrease of N_p, and hence, to the shrinkage of $N - N_p$ smaller voids. Besides, according to eq. (18), if $\alpha_{iv} > \bar{R} \delta_0 / Z_i$, then the swelling rate must become negative ($q < 0$), since the average void preference $\alpha_{iv} / \bar{R}$ exceeds the dislocation preference δ_0 / Z_i. Exactly this behaviour has been reported by Evans [22], which is contrary to the version by Frank and Woo [6], who ascribed the void lattice disordering observed by Evans to void coalescence.

8.6. Annealing

According to the present theory, irradiation is a prerequisite for void ordering, since it is the only way to produce SIA-loops. However, if irradiation is performed at a temperature below stage III ($T < 200$ °C for Mo), when vacancies are immobile, then the void ordering could take place during a subsequent annealing at a high temperature due to the absorption of SIA-loops, formed via condensation of SIA.

This conclusion is confirmed by a remarkable experiment by Evans et al. [23], who managed to produce a partial void ordering by annealing Mo samples for 1 h at 900 °C after neutron irradiation at 60 °C. This result is very important since isolated SIA are not present during the annealing and, hence, the ordering cannot be explained by the models [6,7] based upon anisotropic SIA diffusion. On the other hand, a large number of small SIA-loops has been observed directly in this experiment.

Imperfection of the void alignment in ref. [23] is explained by a limitation in the number of SIA-loops formed after irradiation. Consequently, the void lattice cannot exist long after all SIA-loops are absorbed. Evolution of a void ensemble during annealing is determined by two factors, firstly, by the thermal void coarsening and, secondly, by the dislocation network that acts as a sink for vacancies. In a random state, the size distribution of voids is broad, which favours the coarsening. In the lattice, the distribution is sharper and almost all voids shrink, thereby maintaining a local ordering since shrinking voids diffusionally repulse each other. In both cases, swelling decreases, since according to eq. (18), at $K = 0$ we have

$$dV/dt = q = -\rho_0 Z^* D^* \alpha / \bar{R} < 0$$

This conclusion is confirmed by Loomis and Gerber [13] who observed the void shrinkage during annealing in Nb at 975 °C for 10^4 s independently of the void ordering. The swelling $V(t)$ decreased from 0.005 to 0.002 (random voids) and from 0.008 to 0.002 (void lattice). A calculation of $E_v^m + E_v^f$ for Nb using the $V(t)$ decrease gives the 3.2 eV value, which is in agreement with reference data [10,21] and explains a strong temperature dependence of the void lattice in Nb (see fig. 5). Thus, the experimental data confirm our conception of the void lattice as an open dissipative structure stable only under irradiation when both diffusion and dislocation mechanisms of mass transfer between voids cooperate.

8.7. Role of host lattice

It follows from the above that the void lattice can form only in those crystals where sufficiently small SIA-loops ($r_i \leq \bar{R}$) can glide. The experimental data available (see, for example, ref. [10]) show that this property is characteristic of most bcc metals, where very small SIA-loops with $b = (1/2)a\langle 110 \rangle$ unfault to form perfect loops with $b = (1/2)a\langle 111 \rangle$ (a = lattice constant). On the other hand, in fcc metals SIA aggregate to form the sessile Frank loops with $b = (1/3)a\langle 111 \rangle$ which encircle an extrinsic stacking fault and are not able to glide. Usually, the loops remain faulted until they touch the surface, or intersect to form a network. One of the factors responsible for this difference between bcc and fcc metals is a stacking fault energy γ_F which is about 200–300 erg/cm^2 for bcc and 20–50 erg/cm^2 for fcc metals [18]. It is known [24], that a high γ_F value stimulates the unfaulting process and this explains not only the greater readiness of bcc metals to form the void lattice, but also the known exceptions to this rule, namely, ordering in fcc Ni, Al and their alloys having anomalously high values of $\gamma_F \sim 200$ erg/cm.

An agreement of this criterion with experimental data is one of the most important arguments in favour of the present model, since other models give no criterion at all *. Besides, it offers a practical recommenda-

* The argument that lower void densities in fcc metals prevent the void ordering [6,7] does not seem to be consistent with the void lattice observed in Al [29], where the void density is very low ($\sim 4 \times 10^{20}$ m^{-3}).

tion for producing void lattices in other fcc metals by adding alloying components that increase γ_F, or stimulate the unfaulting process in some other way.

9. Discussion

In this paper we have tried to demonstrate that the dislocation mechanism of void interaction together with the diffusion coarsening mechanism determine the region of formation of the void lattice, its main properties and characteristic parameters, which are in good agreement with experimental data. We used no adjustable parameter, and the only external parameter of the theory, the SIA-loop density $\rho_0 = 2\pi n_1 \bar{r}_1$, was taken from the experiment [13] in Nb and was used for a_s and $\bar{R}_s$ calculations in both Nb and Mo.

From a geometrical point of view, our model is close to that of Woo and Frank [6] based on one-dimensional propagation of SIA-crowdions along close-packed directions of the matrix. However, the existence of such long-travelling crowdions raises doubts [3], whereas the formation and gliding of SIA-loops is a well-established process. Besides, the void ordering in Mo during the postirradiation annealing [23] cannot be explained by diffusion of isolated SIA, which are not present under such conditions (see section 8.6). Moreover, a shrinkage of "random" voids has been taken for granted by Woo and Frank who have not considered the diffusion coarsening mechanism. Without the latter one has to consider the limit $\beta \to 0$, in which "random" voids do not shrink completely but come to a stable size (which is somewhat smaller than that of "ordered" voids), because small voids gain more isotropically diffusing vacancies than large ones. It is useful to compare the void ordering with a classical crystallization process, the latter being the result of the competition (and cooperation) between energy and entropy. In our case, the SIA-loop absorption suppresses the void competition and favours the ordered state, where SIA influxes to voids are minimal. However, if the anticompetition effect is too strong, the locally ordered voids coexist with locally random ones. Thus, a stable random void distribution is analogous to metal glass formed by cooling from high temperature, being too fast for the formation of a long-range order.

We should also point out an important connection between ordering and swelling saturation. According to our model, both phenomena have a common nature, namely, the SIA-loop absorption, though the swelling saturation can take place without ordering if $\dot{l}_p \geq \dot{l}$ but $N < N_\rho$. Generally, using eqs. (21) and (20) a swelling rate dV/dt for $\dot{l}_p \leq \dot{l}$, $\bar{R} \gg R_c^\circ$ can be written as

$$\frac{dV}{dt} = q\left(1 - \dot{l}_p/\dot{l}\right) = \rho_0 \delta_0 \Delta^* \left(1 - (V/V_s)^{1/4}\right), \qquad (31)$$

$$V_s = \frac{2\sigma_p}{9\gamma}(6N)^{-1/3}, \quad N = \begin{cases} N_\rho \text{ for void lattice,} \\ < N_\rho \text{ for random voids.} \end{cases} \qquad (32)$$

At $V = V_s$ the voids are in a stable state (V_s = constant, N = constant, $\bar{R}$ = constant) which is not possible in the diffusion limit $\sigma_p \to \infty$ even at $\rho_0 \delta_0 = 0$ (see section 3).

The inequality $V_s < 1$ gives us a quantitative criterion for the "gliding ability" of SIA-loops necessary for lattice formation: $\sigma_p < \sigma_p^{max} = 9/2\gamma(6N_\rho)^{1/3} \sim 10^8$ J $m^{-3} \sim 10^{-2}\mu$.

Eq. (31) can be used to estimate the dose necessary to approach V_s, since $V = V_s$ only at $t \to \infty$. For example, the dose $Kt_{0.9}$, at which $V = 0.9V_s$ in Nb lies within the range between 0.1 and 15 dpa, if $\Omega_i/|\Omega_v|$ changes from 10 to 1.05. According to experiment ref. [13], $V(t) \approx$ constant at $Kt \geq 20$ dpa. Note that in the diffusion limit ($\sigma_p/\sigma_p^{max} \gg 1$), $V \sim (Kt)^{3/4}$ even in the "slowest" regime of void domination ($N\bar{R} \gg \rho_0$) and at $Kt_{0.9}$ is 7 times greater than V_s. Thus, it is difficult to explain the saturation only by the domination of voids as point-defect sinks, as has been attempted in ref. [19].

Since the loop-gliding is a basic property of crystals, it seems reasonable to undertake further studies in order to elucidate the relation between this property and swelling resistance of materials. A general trend, i.e., higher swelling resistance of bcc than fcc metals, is in agreement with our theory.

With regard to bubble ordering, we should stress here that the main difference between loop-punching by bubbles and loop-absorption by voids is that the former is a prerequisite for the bubble formation at low temperatures independently of the host lattice type. Consequently, the bubble lattice also forms in fcc Cu and Au, where the void lattice has not been observed [25].

10. Summary and outstanding problems

1. A new mechanism of interaction between voids is proposed, which is based on SIA-dislocation loop absorption induced by the loop elastic attraction to voids.

2. The main characteristic property of the dislocation interaction is its rigid relation to the crystal structure, namely, it arises only in those crystals, where SIA-loops formed by irradiation can glide, and results in: (i) attraction between the voids lying along the same

loop-gliding directions, and (ii) the dependence of the void growth (or shrinkage) on the position in the matrix.

3. As voids grow, the range of their dislocation interaction l_p reaches the void spacing $\dot{l}$, which results in the formation of a stable stationary state, when the diffusion growth of voids is compensated by their dislocation shrinkage.

4. A sufficiently high void number density $N \geq N_\rho$ is required for void lattice formation through the shrinkage of unfavourably positioned voids.

5. Voids in a lattice formed through this mechanism have immediate neighbours along loop-gliding directions. The observed copying of the host matrix by the void lattice is due to coincidence of the loop-gliding directions with close-packed directions of the matrix.

6. The conditions of void lattice saturation ($\dot{l}_p = \dot{l}$) and stability ($N = N_\rho$) lead to simple analytical expressions of both the lattice constant a_s and the mean void radius $\bar{R}_s$ through the known or measurable irradiation and material parameters. The calculated dose rate and temperature dependences of a_s and $\bar{R}_s$ are in good quantitative agreement with experimental data.

7. At the present time the dislocation model of void ordering is the only one which explains (a) the preferable formation of the void lattice in bcc metals, (b) the void ordering during postirradiation annealing in molybdenum [23]. In both cases the necessary dislocation interaction between voids arises due to the formation of sufficiently small ($r_1 \leq R$) perfect SIA-loops observed experimentally.

8. In most fcc metals the SIA-loops formed under irradiation are sessile; this formally corresponds to the diffusion limit of the present theory $\sigma_p \to \infty$, in which voids remain random. A conventional theory of radiation void growth (see, e.g., ref. [14]) follows from the diffusion limit at $\beta \to 0$.

Thus, the interaction between cavities arising due to SIA-loop absorption or punching, can explain the formation and main properties of void and bubble lattices in irradiated metals, alloys and alkali earth halides, though in the latter case a quantitative analysis has not been performed as yet. According to our approach, void and bubble lattices are open dissipative structures, which can arise and exist only under specific irradiation conditions providing a cooperation of the dislocation and diffusion mechanisms of interaction between cavities in a crystal.

In conclusion, we should like to attract attention to the most important prediction of our theory, which could be tested by subsequent experiments. Namely, perfect SIA loops must form under irradiation in order to induce the void ordering. This argument could be verified by irradiating fcc metal samples, whose stacking fault energy (SFE) is increased by slight alloying additions which should stimulate the unfaulting of SIA loops (see section 8.7). In this view, it seems possible to produce void lattices, e.g., in stainless steel, where they are seldom seen because of a very low SFE. The known exception is the experiment by Fisher and Williams [28] who observed the void ordering in 20/25 stainless steel containing additions of Ti and a high concentration of nitrogen (see section 8.4). Unfortunately, they have not reported the SIA loop structure, so this point needs further investigations. Note that the loop analysis is most simple at an early stage of irradiation, preceding a substantial growth of voids which may reduce the stationary loop density and size beyond the TEM resolution limits.

Another consequence of the alloying additions would be a decrease of void swelling due to the annihilation of SIA loops by voids, which is, in our opinion, the reason of higher swelling resistance of bcc as compared to fcc metals.

References

[1] J.H. Evans, Nature 229 (1971) 403.
[2] S.L. Sass and B.L. Eyre, Philos. Mag. 27 (1973) 1447.
[3] K. Krishan, Radiat. Eff. 66 (1982) 121.
[4] A.M. Stoneham, in: Proc. Consultant Symposium, The Physics of Irradiation Produced Voids, Ed. R.S. Nelson AERE-R 7934 (1975) p. 319.
[5] E. Johnson and L.T. Chadderton, Radiat. Eff. 79 (1983) 183.
[6] C.H. Woo and W. Frank, J. Nucl. Mater. 137 (1985) 7.
[7] J.H. Evans, J. Nucl. Mater. 132 (1985) 147.
[8] V.I. Dubinko, V.V. Slezov, A.V. Tur and V.V. Yanovskij, Radiat. Eff. 100 (1986) 85.
[9] L.A. Maksimov and A.I. Ryazanov, Fiz. Met. Metalloved. 41 (1976) 284.
[10] P. Erhart et al., Physics of Radiation Effects in Crystals (Elsevier Science Publisher, Amsterdam, 1986) p. 3.
[11] V.I. Dubinko, A.V. Tur, V.V. Yanovskij and A.A. Turkin, Vopr. at. nauki i tekhniki. Ser.: Fiz. rad. povrezhdenij rad. materialoved., is. 1(39) (1987) p. 40.
[12] J.L. Brimhall and G.L. Kulcinski, Radiat. Eff. 20 (1972) 25.
[13] B.A. Loomis and S.B. Gerber, J. Nucl. Mater. 102 (1981) 154.
[14] W.G. Wolfer, J. Nucl. Mater. 122 & 123 (1984) 367.
[15] V.I. Dubinko, P.N. Ostapchuk and V.V. Slezov, Vopr. at. nauki i tekhniki. Ser.: Fiz. rad. povrezhdenij rad. materialoved., is. 1(39) (1987) p. 35.

[16] R. Bullough, S.M. Murphy, T.M. Qwigly and M.H. Wood, J. Nucl. Mater. 117 (1983) 78.
[17] I.M. Lifshits and V.V. Slezov, Zh. Ehksp. Teor. Fiz. 35 (1958) 479.
[18] A.N. Orlov, Vvedenie v Teoriyu Defektov v Kristallakh (Vysshaya shkola, Moscow, 1983) p. 144.
[19] B.L. Eyre and A.E. Bartlett, J. Nucl. Mater. 47 (1973) 143.
[20] V.K. Sikka and J. Moteff, J. Nucl. Mater. 54 (1974) 325.
[21] A.N. Orlov and Yu.V. Trushin, Ehnergii Tochechnykh Defektov v Metallakh (Ehnergoatomizdat, Moscow, 1983) p. 80.
[22] J.H. Evans, J. Nucl. Mater. 88 (1980) 31.
[23] J.H. Evans, S. Mahajan and B.L. Eyre, Philos. Mag. 26 (1972) 813.
[24] J. Friedel, Dislocations (In Russian, Mir, Moscow, 1967) p. 603.
[25] P.B. Johnson, D.J. Mazey and J.H. Evans, Radiat. Eff. 78 (1983) 147.
[26] B.A. Loomis, A. Taylor and S.B. Gerber, in: Proc. Int. Conf. on Fundamental Aspects of Radiation Damage in Metals, Eds. M.T. Robinson and F.W. Young, Jr., CONF-751006-P2 (1975) p. 1245.
[27] A.J.E. Foreman, Harwell Report AERE-R-7135.
[28] S.B. Fisher and K.R. Williams, Radiat. Eff. 32 (1977) 123.
[29] A. Horsewell, B.N. Singh, Radiat. Eff. 102 (1987) 1.
[30] J.H. Evans, Mater. Sci. Forum 15–18 (1987) 869.

Journal of Nuclear Materials 178 (1991) 108–113
North-Holland

The influence of dislocation structure and impurities on the void lattice formation in crystals under irradiation

V.I. Dubinko

Institute of Physics and Technology, The Ukrainian Academy of Sciences, Kharkov 310108, USSR

Received 2 February 1990; accepted 6 July 1990

The void ordering under irradiation in simple cubic, bcc, fcc and hcp crystals is considered within the framework of the dislocation model of void lattice formation based upon the absorption of perfect interstitial loops by voids. The ordering criterion is derived taking into account not only perfect loops but Frank sessile loops and straight dislocations as well. Analytical dependence of void lattice parameters on the concentration of the loop nucleation sites is derived. Impurities are shown to stimulate or prevent void ordering depending on their influence on the loop nature. Finally, a mechanism of loop punching from submicroscopic overpressurized gas bubbles is considered as a possible source of perfect loops which could induce the swelling saturation and void ordering in fcc metals with low stacking fault energy.

1. Introduction

Considerable progress in the theory of void lattice formation has been achieved recently in works by Evans [2], Woo and Frank [3] and Dubinko et al. [1,4], where a relation of the crystal structure to the anisotropy of self-interstitial atom (SIA) transfer has been taken into account. This relation is important for an explanation of the prominent feature of the void lattice, namely, that it usually has the same symmetry and alignment as the host matrix.

The main peculiarity of the model reported by Dubinko et al. [1,4] is the dislocation mechanism of anisotropic SIA transfer which assumes that the diffusion of isolated SIA is isotropic (contrary to the basic assumptions made in refs. [2,3]) but SIA clusters having converted into perfect dislocation loops, can glide along some crystallographic directions under elastic stress exceeding the Peierls stress σ_p. In the case of highly overpressurized gas bubbles, SIA-loops are formed at the bubble surfaces and are then punched out due to the bubble–loop repulsion induced by the gas pressure [4]. On the other hand, vacancy voids absorb SIA-loops from the matrix due to the void–loop attraction induced by the void surface tension [1]. Obviously, neighbouring cavities lying along the same loop-gliding direction punch out or absorb a smaller number of loops as compared to isolated ones. As a result, a dislocation interaction arises between cavities where SIA-loops rather than SIA play the role of quanta. This interaction was shown to influence both the size and position of cavities in the matrix and to lead under specific conditions to an ordering of the cavities.

In the present paper the dislocation model of void ordering is futher developed to include effects of impurities on the nucleation of SIA-loops. Special attention is paid to the mode of the ordering in different crystal structures and to the influence of Frank sessile loops and straight dislocations.

2. Dislocation model of the void ordering

The maximum distance of the loop–void annihilation l_p determines the length of loop-supply-cylinders (LSCs) which are extended from the void along loop gliding directions. l_p is given by the equilibrium between the void–loop attractive force and the Peierls force [1]: $l_p = (3\gamma r/\sigma_p)^{1/4} R^{1/2}$, where γ is the void surface energy, R is the void radius, r is the loop radius. At an early stage of nucleation and growth voids are randomly distributed since they do not interact by the dislocation mechanism until l_p is less than half the mean distance between voids l. At this stage the mean void size $\bar{R}$ grows along with $l_p \sim \bar{R}^{1/2}$. At $l_p \geq l$ LSCs overlap meaning that all perfect SIA-loops cannot

0022-3115/91/$03.50 © 1991 - Elsevier Science Publishers B.V. (North-Holland)

escape voids, and hence, are not able to form new crystal planes. Accordingly, a futher void swelling is possible only at the expense of straight dislocations and sessile Frank loops that absorb extra SIA irreversibly. If one assumes (as was done in ref. [1]) that all SIA-loops are perfect and their coalescence is the main source of new straight dislocations, then at $l_p \gtrsim l$ the straight dislocation density should fall drastically without a futher supply of growing loops and the void swelling should saturate. This is confirmed by experiments (see [1]). The mean void size $\bar{R}_s$ corresponding to the swelling saturation is given by the condition $l_{pl}(\bar{R}_s) = l$:

$$\bar{R}_s = \left(\frac{\sigma_p}{3\gamma}\right)^{1/3} \left(\frac{3}{4\pi N}\right)^{4/9}, \quad N = \frac{3}{4\pi l^3}, \tag{1}$$

where N is the void number density.

If voids are ordered, then the void lattice parameters a_s (which equals $4\bar{l}/\sqrt{3}$ for the bcc lattice) may be expressed by eq. (1) in terms of $\bar{R}_s$: $a_s = (10.7\gamma/\sigma_p)^{0.25}(2\bar{R}_s)^{0.75}$, that is very close to a relationship, experimentally found in niobium [10]: $a_s = 5.91(2\bar{R}_s)^{0.73}$. A comparison of the coefficients of the powers of $2\bar{R}_s$ gives a reasonable value of $\sigma_p = 5 \times 10^{-4}\,\mu$ [1], where μ is the shear modulus.

However, the SIA-loop absorption alone leading to the void growth saturation is not sufficient for a shrinkage of unfavourably placed voids [1]. At $l_p \gtrsim l$ the fate of each void depends on its size and the location of the void's immediate neighbours. Voids that have neighbours along gliding directions (locally ordered voids [1]) absorb fewer SIA-loops as compared to locally random voids which have immediate neighbours outside glide directions. On the other hand, larger voids ($R > \bar{R}$) absorb more extra vacancies than smaller ones ($R < \bar{R}$) due to the diffusion-induced coarsening mechanisms, that control void densities [5]. According to [5], without the loop absorption a steady-state void density under irradiation can not exceed the value $2N_\mu$, dependent on the dislocation density and material constants (N_μ will be formally defined in section 4). The loop absorption lowers the maximum steady-state void density by a factor of two [1]. At $N > N_\mu$ the diffusion coarsening was shown to dominate over the loop absorption resulting in the growth of larger voids at the expense of smaller ones, irrespectively of their positions in the matrix. Hence, N decreases with dose.

At $N < N_\mu$ the diffusion coarsening is too weak to make the voids shrink, and a random stationary state is established, where 'random' voids are smaller than 'ordered' ones but both neither shrink nor grow.

Finally, at $N = N_\mu$ only "random" voids shrink, while "ordered" voids form stable lattice with close-packed directions lying along loop gliding directions. Thus, the ordering is a process of coarsening where the dislocation mechanism points out "random" voids making them smaller than "ordered" ones, while the diffusion mechanism shrinks them out. That is why a critical void density parameter for ordering N_μ is determined by diffusion-induced coarsening.

In cubic crystals, where SIA-loops glide along the matrix close-packed directions, the void lattice copies the host lattice. In hcp crystals a planar or linear void ordering takes place depending on whether SIA-loops glide within the basal plane or along the c-direction, as will be shown in the following section.

3. Mode of ordering

Elementary cells of cubic void lattices are shown in fig. 1, where "random" voids are depicted in interstitial positions. It is seen that at $l/R > (l/R)_{pl}$ "ordered" voids do not shield the "random" one against SIA-loop influxes and the latter shrink at $N = N_\mu$ in agreement with ref. [1]. In this case voids may form linear strings along c.p.d. even at early stages of the ordering. In the opposite case of $l/R < (l/R)_{pl}$ an overlap of LSCs of "ordered" and "random" voids takes place within close-packed planes which helps the latter to survive. Consequently, at $N = N_\mu$ only those voids shrink that do not have enough immediate neighbours within the close-packed planes, and hence voids align first into planes (planar ordering) parallel to the close-packed planes. Later on a superposition of these planes results in the formation of void lattice copying the host matrix. Fig. 1 shows that $(l/R)_{pl}$ increases in the following sequence: simple cubic, bcc, fcc, and a tendency for the planar ordering increases respectively. However, experimental values of $\bar{l}/\bar{R}$ increase in the same sequence, which means that a fashion of ordering may be either planar or linear depending on the actual value of swelling $S = (\bar{R}/\bar{l})^3$. This conclusion is supported by Liou et al. [6] who observed that in Mo already at 2 dpa "some void ordering occurs, primarily in one- and two-dimensional arrays". On the other hand, it does not contradict Evan's view about a planar fashion of ordering in Mo [2]. In general, an increase of $S_{pl} = (R/l)^3_{pl}$ should favour the void lattice perfection which accordingly should increase in a sequence of fcc ($S_{pl} \approx 2\%$), bcc ($S_{pl} \approx 10\%$) and simple cubic lattice ($S_{pl} \approx 12\%$). Experimentally, there is a small difference in perfection of simple cubic anion void lattice [7] and bcc void lattice in niobium [10], and they both are substantially better than lattices found in fcc metals.

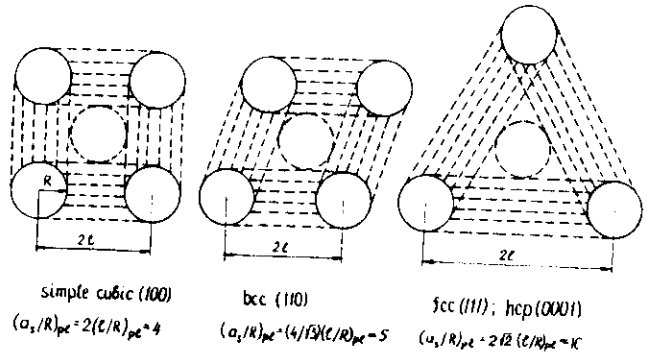

Fig. 1. Two-dimensional illustration of the void alignment at $l/R = (l/R)_{pl}$ within the close-packed planes: (100) plane for simple cubic lattice, (110) plane for bcc, (111) plane for fcc, (0001) plane for hcp. At $l/R < (l/R)_{pl}$ "ordered" voids start to shield "random" one (depicted in the middle of the cell) from the SIA fluxes along LSCs (dashed). a_s is the void spacing along ⟨100⟩, usually referred to as the void lattice parameter.

Although a mode of ordering may be variant, the final structure of the void lattice in all cubic crystals copies the host lattice or that sublattice which determines the loop gliding (the latter is the case with a simple cubic anion superlattice in CaF_2 [1,7]). On the other hand, in hcp crystals loops can glide either along 3 directions ⟨1120⟩ within the basal plane or along the c-direction depending on the crystal anisotropy.

In the first case a planar ordering is expected to arise parallel to the basal plane. If $S \gtrsim S_{pl} \approx 2\%$, this would occur without ordering along ⟨1120⟩ directions as was actually observed in neutron irradiated Mg [8] where S was measured to be between 0.7 and 0.9%.

In the second case the dislocation model predicts formation of linear strings of voids along the c-direction. They are observed in alumina (Al_2O_3) which is known to swell along the c-direction confirming that SIA-loops have Burgers vectors parallel to the c-direction [9]. Finally, one may expect the formation of an hcp void lattice in such hcp crystals where both loop glide systems operate simultaneously and the saturation level of swelling is sufficiently low so that $S \ll S_{pl}$. To our knowledge there is no experimental evidence confirming the last prediction so far.

4. Influence of the dislocation structure

The necessary condition of void ordering by the dislocation mechanism is the formation of sufficiently small perfect SIA-loops which could be absorbed b voids. The minimum size of perfect loops is determine by the unfaulting mechanism and is very small in bc and some other metals where the stacking fault energ γ_F is high. The maximum size is about the mean voi size, and such loops could be seen coexisting with th void lattices. There is some evidence for this. For exam ple, Gelles et al. [16] have found in TZM neutron-irradiated at 540 °C a lattice array of loops similar to that of the voids in the same region under similar tilt conditions but with different degrees of strain contrast. Loomis and Gerber [10] have observed in O-doped niobium a well-defined void lattice coexisting with a slightly lower concentration of black spots (i.e. loops or precipitates) similar in size to the voids. The critical parameters N_μ calculated using the observed loop density [1] (that was far greater than the density of straight dislocations) was very close to the observed void density N. On the other hand, in "pure" niobium it appeared that $N < N_\mu$, and a random stationary state was observed in agreement with the theory [1]. However, such a detailed quantitative analysis is inaccessible in cases where a majority of loops is absorbed by voids beyond the TEM resolution limit, and straight dislocations along with a few large loops are the main constituents of the visible dislocation structure [11,17]. Let us consider a general case, where straight dislocations and sessile Frank loops coexist with perfect SIA loops in order to find the minimum density of perfect loops that is sufficient for the ordering. Taking into account the straight

...cations and Frank loops void growth equations and (23) from ref. [1] take the following form:

$$= \frac{\Delta^* \rho_d \delta_d}{4\pi N R^2}(u - u_1)(u_2 - u), \quad u \equiv \frac{R}{\dot{R}}. \tag{2}$$

$$= \frac{1+\beta}{2\Psi}\left(1 \mp \sqrt{1 - \Psi\frac{4\beta}{(1+\beta)^2}}\right), \quad \beta = \frac{N}{N_v} \tag{3}$$

$$= \frac{\rho_d \delta_d}{4\pi\alpha_{iv}(1 + D^*\alpha/\Delta^*\alpha_{iv})},$$

$$_d \equiv \rho_p\delta_p + \rho_F\delta_F + \rho_s\delta_s, \tag{4}$$

$$= D_v c_v^e + D_i c_i^e, \quad \Delta^* = D_v(\bar{c}_v - \bar{c}_v^e), \tag{5}$$

$$= \begin{cases} \Psi_0 \equiv \rho_p\delta_p/\rho_d\delta_d & \text{for "ordered" voids,} \\ \Psi_r \equiv (l/\bar{l})\rho_p\delta_p/\rho_d\delta_d & \text{for "random" voids,} \end{cases} \tag{6}$$

...ere $\alpha = 2\gamma\omega/kT$, ω is the atomic volume, T the ...mperature, k the Boltzmann constant, D_n the diffu...ity of vacancies ($n = v$) and SIA ($n = i$), c_n^e are their ...uilibrium concentrations in perfect crystal, c_n^e and $\bar{c}_n$ ...e the mean point defect concentrations in a crystal ...ntaining voids and dislocations without and under ...adiation, respectively; α_{iv} is the constant of the void ...as factor $\delta_c = \alpha_{iv}/R$ [5]; δ_p, δ_F, δ_s are the bias factors ... perfect and Frank loops and straight dislocations, ...spectively, while ρ_p, ρ_F, ρ_s are their densities, so that ... is the mean dislocation interstitial bias and ρ_d the ...ean dislocation density.

At $\rho_F\delta_F + \rho_s\delta_s = 0$ we come to the equations from ...f. [1]. In this case $\Psi_0 = 1$, and at $\beta \to 1$ "ordered" ...ids get into a stationary state, $(dR/dt)_0 = 0$, whereas ...l "random" voids shrink, $(dR/dt)_r < 0$, since $\Psi_r > 1$ ... $l_p > \bar{l}$. This corresponds to the formation of void ...ttice and swelling saturation.

It is seen from the definition that the critical void ...ensity N_p, eq. (4), is determined by the interaction with ...oint defects. The ratio $D^*\alpha/\Delta^*\alpha_{iv}$ entering N_p, shows ...he relative strength of thermal coarsening to radiation-...nduced coarsening [5]. If $D^*\alpha/\Delta^*\alpha_{iv} \ll 1$, then the ...atter dominates (at low temperatures or high dose ...ates) and N_p does not depend on irradiation condi...ions. In this region void lattice parameters are de...ermined only by the mean loop density and material ...onstants, while in the thermal coarsening region $D^*\alpha/\Delta^*\alpha_{iv} \gg 1$) they depend on irradiation tempera...ure and dose rate as well [1].

At $\rho_F\delta_i + \rho_s\delta_s > 0$, $\Psi_0 < 1$ which corresponds at $\beta \to 1$ to a stable growth of "ordered" voids, $(dR/dt)_0 > 0$, while the condition of shrinkage of "random" voids, $\Psi_r > 1$, becomes less accessible: $l_p > \bar{l}(\rho_d\delta_d/\rho_p\delta_p)$. The ...atter determines the minimum density of perfect loops ρ_p^{th} that is sufficient for the ordering at a given swelling level S:

$$\rho_p > \rho_p^{th} \equiv \frac{3\alpha_{iv}^*}{\delta_p}\left(\frac{\sigma_p}{3\gamma S}\right)^3\left(\frac{\rho_s\delta_s}{\rho_p\delta_p}\right)^{11}.$$

$$\alpha_{iv}^* \equiv \alpha_{iv}\left(1 + \frac{D^*\alpha}{\Delta^*\alpha_{iv}}\right). \tag{7}$$

This criterion is easily met in bcc and some other crystals where the stacking fault energy γ_f is high enough for the nucleation of perfect rather than Frank loops so that $\rho_d\delta_d/\rho_p\delta_p \sim 1$. The low temperature limit for ρ_p^{th} when $\alpha_{iv}^* \to \alpha_{iv} - b\delta_p$ [1], $b = 2.5$ nm, $\sigma_p = 10^6$ J m^{-3}, $\gamma = 2$ J m^{-2}, $S = 10^{-2}$, is fairly low: $\rho_p^{th} \approx 10^{12}$ m^{-2}. If $\delta_s \ll \delta_p$ then ρ_s may be higher than ρ_p and still satisfy the criterion (7). In this case the void lattice forms while swelling increases at a rate $dS/dt \approx \Delta^*\rho_s\delta_s$ that is low as compared with the initial swelling rate at $l_p \ll \bar{l}$ when $dS/dt \approx \Delta^*(\rho_p\delta_p + \rho_s\delta_s)$.

The growth rate of a perfect SIA loop is given by

$$v_p = \frac{1}{b}\left[\Delta^*\delta_p - D^*(1 - e^{-\alpha_p/r})\right], \quad \alpha_p \equiv \mu b\omega/kT, \tag{8}$$

where r is the loop radius. At $\Delta^*\delta_p \gg D^*$ the radius dependence of v_p may be neglected and, hence, the loop nucleation rate J_p reaches its maximum value: $J_p = c_N r_N \times \Delta^*\delta_p\omega^{-2}$, where r_N is the SIA trapping radius of a loop nucleus, c_N is the concentration of the nuclei. A stationary density of loops is maintained by the balance between their nucleation and absorption by voids which does not allow the loops to grow beyond the maximum size r_{max}:

$$\rho_p = \pi r_{max}^2 J_p/v_p = \pi r_{max}^2 C_N r_N b\omega^{-2}, \tag{9}$$

where r_{max} lies between the loop unfaulting size and the mean stationary void size $\bar{R}_s$. If $r_{max} < \bar{R}_s$, then it explicitly determines $\bar{R}_s$:

$$\bar{R}_s = \left(\frac{\sigma_p}{3\gamma r_{max}}\right)^{1/2}\left(\frac{3}{4\pi\bar{N}}\right)^{2/3}. \tag{10}$$

The ordering condition, $N = N_p$, gives another relationship between $\bar{R}_s$ and N and leads to the following expressions for the void lattice parameters in terms of r_N and c_N at $\rho_d = \rho_p$:

$$\bar{R}_s = \left(\frac{3\alpha_{iv}^*\omega^2}{\pi\delta_p c_N r_N b}\right)^{2/3}\left(\frac{\sigma_p}{3\gamma}\right)^{1/2} r_{max}^{11/6},$$

$$a_s = m\left(\frac{3\alpha_{iv}^*\omega^2}{\pi\delta_p b c_N r_N}\right)^{1/3} r_{max}^{2/3} \tag{11}$$

$$m = \begin{cases} 2 & \text{for simple cubic,} \\ \dfrac{4}{\sqrt{3}} & \text{for bcc,} \\ 2\sqrt{2} & \text{for fcc,} \end{cases} \tag{12}$$

where $a_s = ml_p$ is the void spacing along ⟨100⟩. If $r_{max} \to \bar{R}_s$, then eq. (10) coincides with eq. (1), while the expressions for a_s and $\bar{R}_s$ take the following form:

$$\bar{R}_s = \left(\frac{\sigma_p}{3\gamma}\right)^{3/7}\left(\frac{3\alpha_{iv}^*\omega^2}{\pi\delta_p b c_N r_N}\right)^{4/7},$$

$$a_s = m\left(\frac{3\alpha_{iv}^*\omega^2}{\pi\delta_p b c_N r_N}\right)^{3/17}\left(\frac{3\gamma}{\sigma_p}\right)^{2/17}. \tag{13}$$

Note that α_{iv}^* is the only parameter in eqs. (11)–(13) which explicitly depends on temperature and dose rate via D^* and Δ^*. In the radiation coarsening region ($\alpha_{iv}^* \to \alpha_{iv}$) $\bar{R}_s$ and a_s may depend on the irradiation conditions only via characteristics of the loop nuclei c_N and r_N. At higher temperatures the loop nucleation becomes difficult and the dislocation network is sustained by the Bardeen–Herring sources. The $\rho_d\delta_d/\rho_p\delta_p$ ratio grows, drastically increasing ρ_p^{th} and preventing the void lattice formation (e.g. at $\rho_d\delta_d/\rho_p\delta_p = 5$, $\rho_p^{th} \sim b^{-2}$). According to eq. (8) a critical radius for the loop growth appears at $D^* > \Delta^*\delta_p$ which determines the upper temperature limit for the void ordering T_{up}: $D^*(T_{up}) \sim \delta_p\Delta^*$. At $T > T_{up}$ the dislocation network absorbs SIA irreversibly and swelling increases. Thus, T_{up} lies slightly below the maximum swelling temperature in agreement with experimental observations [18]. At the same time, $T_{up} > T_{RIC}$ (the temperature of transition from the radiation coarsening to the thermal coarsening region:

$$D^*(T_{RIC}) \sim \Delta^*\alpha_{iv}/\alpha \sim \Delta^*\delta_p b/\alpha < \Delta^*\delta_p.$$

At $T_{RIC} < T < T_{up}$ a_s and $\bar{R}_s$ increase with temperature, their ratio $a_s/\bar{R}_s$ slightly decreasing in agreement with experimental data [1,10,11].

The dependence of $a_s/\bar{R}_s$ on c_N at $T < T_{RIC}$ is shown in fig. 2 for niobium and molybdenum with the assumption that $r_N = 1$ nm, $\gamma = 2$ J m^{-2}, $\sigma_p = 10^7$ J m^{-3} (Nb), 10^6 J m^{-3} (Mo). A theoretical curve for niobium corresponds to eqs. (13) since in this case there is an experimental evidence of the presence of loops similar in concentration and size to voids [10]. On the other hand, in molybdenum the observed SIA-loops are substantially coarser than voids [11,17], which allows us to assume that the main loop constituent was beyond the TEM resolution limit. Accordingly, a theoretical curve for molybdenum is due to eq. (11) at $r_{max} = 1$ nm

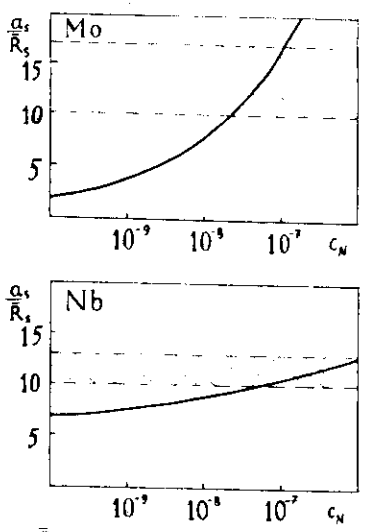

Fig. 2. $a_s/\bar{R}_s$ versus concentration of SIA-loop nucleation centers, c_N, in Mo and Nb according to eqs. (11) and (13), respectively, at $T < T_{RIC}$, i.e. in the radiation coarsening region. Shaded areas correspond to experimental $a_s/\bar{R}_s$ values in the region under consideration, according to refs. [10,11,17].

which is taken for the TEM limit. The loop density ρ_p calculated by eq. (9) at $c_N = 10^{-8}$–10^{-7} (deduced from a comparison of theoretical and experimental $a_s/\bar{R}_s$ ratios) is about 10^{14} to 10^{15} m^{-2} which is indeed substantially higher than the observed dislocation density, $\rho_d^{exp} \sim 10^{13}$ m^{-2} [11,17].

5. Effect of impurities

Fig. 2 shows that experimental $a_s/\bar{R}_s$ ratios correspond to $c_N \sim 10^{-8}$ to 10^{-6} which is far higher than the mean SIA concentration $\bar{c}_i < 10^{-12}$. Thus, a homogeneous loop nucleation (when $c_N = \bar{c}_i$) cannot provide the void ordering which shows the importance of impurities as loop nucleation centers *. However, the required c_N values are very low and, hence, are attainable even in so-called "pure" metals due to residual

* There is another possibility related with nucleation of SIA-loops in displacement cascades, since SIA group around the cascade depleted zone which favours their clustering. This may also explain the resistance to void ordering by electrons that do not produce cascades.

impurities and especially due to transmutation. That is why, if a substantial impurity concentration is a prerequisite for ordering, it is usually needed in order to increase the void density up to the critical N_p values (as was argued to be the case in Nb [1,10]). On the other hand, the void lattice data for Mo, as a rule, have no obvious correlation with purity [18] since the void density in pure Mo is sufficient for ordering. Yet, even in Mo the ordering may be affected by alloying components or impurities, if they impede the unfaulting process of SIA-loops or somewhat increase the Peierls stress. A characteristic example of the former effect is 14 MeV Cu ion irradiation of of a Mo-9.1 at% Zr alloy as compared with similar irradiation of pure Mo in the temperature range 700–900 °C [12].

In the alloy voids were randomly distributed and the swelling rate was substantially higher than in Mo at $T \geq 850$ °C. Analysis of the larger loops at 850 °C showed that they were faulted ($b = \frac{1}{2}\langle 110\rangle$) unlike the loops in pure Mo, so that Zr probably reduces the stacking fault energy γ_F. This experiment gives direct evidence of the close relation of the void ordering and swelling saturation to the loop nature. Besides it shows the main possibility of influencing the loop nature by alloying components. The latter aspect is of considerable importance in the case of fcc metals where SIA loops are usually faulted due to a relatively low stacking fault energy. Accordingly, the void lattice is rarely found in fcc metals. There is only one exception to this rule, namely stainless steel (to say nothing of Ni and Al which have abnormally high values of γ_F) irradiated by electrons [13]. However, a high concentration of nitrogen has been reported to be a prerequisite for void ordering in this case. The gas impurities are usually supposed to stabilize void nuclei against shrinkage. Here we would like to point out another effect concerning the nucleation of perfect SIA loops at gas bubbles and solid inclusions consisting of gas compounds with other elements. According to Wolfer and Ashkin [14], a gas bubble has the interstitial bias δ_b which depends on the bubble size and gas pressure p as

$$\delta_b = \frac{\alpha_{iv}}{R} + \frac{\alpha_\mu}{\mu^2}\left(p - \frac{2\gamma}{R}\right)^2, \quad \alpha_\mu = \frac{3}{56kT}\left(\alpha_i^\mu - \alpha_v^\mu\right). \tag{12}$$

where α_n^μ is the shear polarizability of the point defect. Owing to this dependence of $\delta_b(R, p)$ the gas nucleus under irradiation may develop into a void or a stable bubble, or a shrinking bubble depending on irradiation conditions. In the latter case p increases up to the limit p_{max} determined by stress relief mechanisms such as the ejection of gas atoms or SIAs or SIA-loops [4,15]. Thus, submicroscopic gas bubbles may become sources of perfect SIA-loops even at elevated temperatures in the low γ_F metals and, hence, to decrease the void growth rate and stimulate void ordering. The actual number density and size of these bubbles depends on various factors such as the gas solubility and concentration, the injection mode and irradiation conditions. These aspects will be considered in subsequent papers dealing with gas bubble evolution under irradiation.

6. Summary

(1) The dislocation model explains both the planar and linear ordering of voids observed in hcp crystals as well as a mode of the ordering process in cubic crystals.

(2) The ordering criterion is derived taking into account the loop nature and straight dislocations.

(3) Void lattice parameters are expressed in terms of the concentration of SIA loops nuclei.

(4) Impurities and alloying components are shown to stimulate or prevent void ordering and swelling saturation depending on their influence on the nature of SIA loops.

References

[1] V.I. Dubinko, A.V. Tur, A.A. Turkin and V.V. Yanovski, J. Nucl. Mater. 161 (1989) 57.

[2] J.H. Evans, J. Nucl. Mater. 119 (1983) 190; Mater. Sci. Forum 15–18 (1987) 869.

[3] C.H. Woo and W. Frank, J. Nucl. Mater. 137 (1985) 7; Mater. Sci. Forum 15–18 (1987) 875.

[4] V.I. Dubinko, V.V. Slezov, A.V. Tur and V.V. Yanovski, Radiat. Eff. 100 (1986) 85.

[5] V.I. Dubinko, P.N. Ostapchuk and V.V. Slezov, J. Nucl. Mater. 161 (1989) 239.

[6] K.Y. Liou, H.V. Smith, D. Wilkes and G.L. Kulcinski, J. Nucl. Mater. 83 (1979) 335.

[7] E. Johnson and L.T. Chadderton, Radiat. Eff. 79 (1983) 183.

[8] A. Jostson and K. Farrell, Radiat. Eff. 15 (1972) 217.

[9] F.W. Clinard, J. Nucl. Mater. 85/86 (1979) 393.

[10] B.A. Loomis and S.B. Gerber, J. Nucl. Mater. 102 (1981) 154.

[11] V.K. Sikka and J. Moteff, J. Nucl. Mater. 54 (1974) 325.

[12] K.Y. Liou, P. Wilkes, G.L. Kulcinski and J.M. Billen, J. Nucl. Mater. 85 & 86 (1979) 735.

[13] S.B. Fisher and K.R. Williams, Radiat. Eff. 32 (1977) 123.

[14] W.G. Wolfer and M. Ashkin, J. Appl. Phys. 46 (1975) 547.

[15] S.E. Donnelly, Radiat. Eff. 90 (1985) 1.

[16] D.S. Gelles, D.T. Peterson and J.F. Bates, J. Nucl. Mater. 103 & 104 (1981) 1141.

[17] B.L. Eyre and A.E. Bartlett, J. Nucl. Mater. 47 (1973) 143.

[18] K. Krishan, Radiat. Eff. 66 (1982) 121.

THE THEORY OF GAS BUBBLE LATTICE

V. I. DUBINKO, V. V. SLEZOV, A. V. TUR and V. V. YANOVSKY

Institute of Physics and Technology, The Academy of Sciences of Ukrainian SSR, Kharkov 310108, USSR

(Received November 28, 1985)

The theory of gas bubble lattice that is formed under irradiation by light gas ions is developed. To explain the ordering, a new mechanism of bubble interaction is proposed which is based on the loop-punching from growing bubbles. The symmetry and alignment of the bubble lattice are explained, its stability criteria are derived and characteristic parameters are estimated.

The theoretical results are in good agreement with experimental data.

1 INTRODUCTION

There is considerable interest in the formation of void and bubble lattices by irradiation, since this is a characteristic manifestation of fundamental properties of crystals in non-equilibrium conditions. Despite a large number of experimental and theoretical investigations of the phenomenon, the underlying mechanisms are still controversial.[1] The theoretical description of cavity-lattice formation has been concentrated on the void-lattice case,[1–4] while we are primarily concerned with the ordering of gas bubbles. The physical processes responsible for the formation of gas bubbles differ from those associated with void formation and we show in this paper that even the most successful known theories of void ordering are invalid in the bubble case.

In contrast to void development, bubble formation has been observed at room temperatures that are too low to initiate any significant vacancy migration. In such conditions the bubble formation generally begins with the trapping of gas atoms in radiation-induced vacancies and is followed by subsequent bubble growth initially by an athermal self-interstitial atom emission, followed afterwards by loop-punching.[4] Loop-punching has been observed experimentally.[4,5]

Loop-punching mechanism has been proposed by Greenwood *et al.* as an explanation of the bubble growth[6] and by Slezov[7] and Gegusin *et al.*[8] for description of the growth (or shrinkage) of voids under external stresses. However, the mechanism of bubble interaction which results in the adjustment to the superlattice, is not yet properly understood. The existence of such interaction follows from the fact that initially bubbles are formed randomly and ordering begins only subsequently. The "microstructure induced instability model" proposed by Krishan[1] is not valid in helium bubble lattice (the most perfect one) because of extremely low solubility of He in metals, which suppresses shrinkage of "unfavourably" placed bubbles.

The known mechanisms of elastic and diffusive interaction both result in mutual attraction of bubbles in isotropic materials. (Diffusive attraction of bubbles at low temperatures arises due to competition for self-interstitials, in contrast to diffusive repulsion of voids at high temperatures that is due to competition for vacancies.) It is evident, however, that the attraction alone is insufficient not only for formation,

but even for stability of an ordered structure. Thus, the main problem is to find a mechanism resulting in repulsion between bubbles. Moreover, an additional requirement must be satisfied, which is associated with the most striking feature of the bubble lattice, namely the coincidence of its symmetry and alignment with those of the host lattice. It means that the interaction in question must be directly related to the crystallographic structure of the host lattice. Note that neither the elastic nor diffusive interactions of bubbles in isotropic materials satisfy this requirement.

As it is shown in this paper, the loop-punching mechanism of the bubble growth is closely linked with the process of ordering. The point is that the loop-punching results not only in growth but also in the interaction of bubbles that satisfies all the requirements stated above. First, it is repulsive, and, second, it arises only between neighbouring bubbles lying along the same loop-punching direction. These directions are parallel to the minimum Burgers vectors of the host lattice, i.e. to its close-packed directions. Alignment of these directions depends on the type of host lattice, and their number is equal to the lattice coordinate number. For example, the number of loop-punching directions is 6 in a simple cubic lattice, 8 in bcc and 12 in fcc. That is why each bubble can be in equilibrium with its nearest neighbours only when they are arranged along the close-packed directions. The nearest bubbles lying in other directions diffusionally attract each other and coalesce. Consequently, a random distribution of bubbles is unstable and transforms into an ordered one, where bubbles are arranged in the same pattern as atoms in the host lattice.

Thus, the observed coping of the host lattice by bubble lattice receives a natural explanation: it is due to the coincidence of loop-punching directions with close-packed directions in the host lattice.

The dislocation-interaction mechanism explains not only the symmetry and stability of the bubble lattice, but also makes it possible to find out the region of its formation and evaluate the ratio of the superlattice scale to the bubble radius. As is shown in the last section, our calculations are in good agreement with experimental data.

2 EXPERIMENTAL OBSERVATIONS

Helium bubble lattice was first observed[11] in bcc molybdenum in 1973. Later, ordering of helium bubbles was observed in fcc metals Cu, Ni, Au, stainless steel and in hcp Ti.[12] The irradiation of Mo and Cu with Ne and H ions respectively, was also found to result in bubble lattice formations.[1]

The main properties of the bubble lattice that follow from available experimental data are as follows:

1) A random distribution of bubbles is first formed, which then orders with the growth of the radiation dose in local regions, subsequently spreading to adjacent areas.[1]

2) The bubble lattice always has the same symmetry and alignment as the host matrix.[1,13]

3) The average bubble radius is typically 10 Å and the lattice constant lies in the range 40–80 Å.[1]

4) The gas bubble ordering begins at room temperature, which is too low for any significant vacancy migration. The upper temperature limit for bubble ordering is

0.35 *Tm* (*Tm* is the melting point). Bubble lattice parameters are essentially temperature independent.[3,12–14]

5) The bubble lattice is stable against the annealing at temperatures up to 0.4 *Tm*; at higher temperatures bubbles coalesce and produce blisters.[1]

6) Number density of gas atoms in a bubble is about 2–3 atoms per vacancy.[3,13]

According to the first two of the above cited features, a close parallel can be found between bubble lattice formation and the ordering of voids produced in metals and alloys by neutron or ion bombardment.[1] Yet there are significant differences between the void and bubble lattices in scale, temperature dependence and region of formation. Void density is 10^2 times smaller and the void size is nearly 10 times greater than those for bubbles and both show a strong temperature dependence. Voids are produced only at sufficiently high temperatures when vacancies are mobile. Hence, the growth mechanisms should be different for voids and bubbles. Voids grow absorbing extra vacancies, whereas bubbles, if overpressured, gain vacancies by punching out interstitial dislocation loops.

The loop-punching mechanism proposed by Greenwood *et al.* in 1959[6] recently received experimental confirmation: loop-punching from growing helium clusters in molybdenum was observed *in situ* in TEM.[4] The loops with Burgers vector $1/2\ a\langle 111\rangle$ were aligned along glide directions $\langle 111\rangle$ parallel to the close-packed directions of the bcc matrix. A similar effect was observed in tritium-charged vanadium.[5]

Thus, the available experimental data give evidence that bubbles grow at low temperatures by punching out interstitial dislocation loops along close-packed directions of the host matrix.

3 ELASTIC AND DIFFUSIVE INTERACTION MECHANISMS

According to the experimental data, bubbles are initially randomly distributed and, subsequently, begin ordering, i.e. the ordering proceeds with adjustments in bubble positions. At the present time, there is only one known mechanism of bubble (or void) motion, namely the diffusive mechanism. Diffusive fluxes that control bubble motion are induced either by elastic or purely diffusive interaction.

The elastic interaction of two bubbles (or voids) in isotropic materials is attractive at all distances.[9] The elastic attractive force between two bubbles of radius R separated by a distance $2l \gg R$ is given by

$$F_e = \frac{3}{16}\,\frac{\left(P-\dfrac{2\gamma}{R}\right)^2 R^9}{\mu l^7}, \tag{1}$$

where P is the gas pressure in bubbles, γ the surface energy and μ the shear modulus. For bubbles of the size of interest, surface diffusion controls the velocity of motion under the force F_e[14]:

$$\frac{dl}{dt} = -\frac{3}{2}\,\frac{raD_s}{\pi kTR^4}F_e, \tag{2}$$

where r is the atomic volume, a the lattice constant, D_s the surface diffusion constant, T the temperature and k the Boltzmann constant.

As can be seen from Eqs (1) and (2) the elastic interaction between bubbles increases exponentially with the temperature and does not depend on the point defect production rate.

Another mechanism of bubble interaction is purely kinetic. It arises as a result of competition between neighbouring bubbles for point defects. Vacancy flux is directed so that neighbouring bubbles grow preferentially in the opposite directions, i.e. effectively repulse one another. On the other hand, the self-interstitial diffusion and absorption by the bubbles introduce an "attraction force."

Generally, variation in the distance between two bubbles (or voids) with time due to the diffusive interaction is given by[15]

$$\frac{dl}{dt} = \frac{3}{4} \cdot \frac{v}{4\pi l^2}(\mathcal{F}_1 - \mathcal{F}_i), \tag{3}$$

where $\mathcal{F}_1$ and $\mathcal{F}_i$ are the total fluxes of vacancies and self-interstitials on each bubble, respectively:

$$\mathcal{F}_v = \frac{4\pi R D_v}{v}\left(\bar{C}_v - C_v^0 \exp\left\{-\frac{Pv}{kT} + \frac{2\gamma v}{kTR}\right\}\right), \tag{4}$$

$$\mathcal{F}_i = \frac{4\pi R D_i}{v}\left(\bar{C}_i - C_i^0 \exp\left\{\frac{Pv}{kT} - \frac{2\gamma v}{kTR}\right\}\right), \tag{5}$$

where D_i and D_v are the point defect diffusivities in the lattice. The mean volume concentrations of point defects $\bar{C}_i$ and $\bar{C}_v$ obey the balance equations[16]:

$$\frac{d\bar{C}_i}{dt} = G - 2\pi D_i\left\{\rho Z_i(\bar{C}_i - C_i^0) - \frac{v}{2\pi} N\mathcal{F}_i\right\} - \beta_i D_i \bar{C}_i C_v, \tag{6}$$

$$\frac{d\bar{C}_v}{dt} = G - 2\pi D_v\left\{\rho Z_v(\bar{C}_v - C_v^0) - \frac{v}{2\pi} N\mathcal{F}_v\right\} - \beta_i D_i \bar{C}_i \bar{C}_v, \tag{7}$$

$$(Z_{i,v})^{-1} = \ln\left(\frac{2l_{i,v}}{L_{i,v}}\right), \tag{8}$$

$$l_{i,v} = \left(\frac{2Z_{i,v} D_{i,v} \bar{C}_{i,v}}{G}\right)^{1/2}, \tag{9}$$

where G is the point defect production rate, ρ the dislocation density, N the bubble density, $\mathcal{F}_{i,v}$ the mean point defect fluxes on a bubble, $l_{i,v}$ the effective radius of dislocation influence, $L_{i,v}$ the effective radius of the point defect capture by dislocation[16]; C_v^0 and C_i^0 are, respectively, the equilibrium concentrations of vacancies and self-interstitials in a perfect crystal, β_i is the recombination constant. C_i^0 is extremely low in metals, so that the thermal emission of interstitials from dislocations may be neglected, but the interstitial emission from bubbles is promoted by the gas pressure and will be shown to play an important role at high temperatures.

At low temperatures, vacancies are practically immobile ($\mathcal{F}_v \ll \mathcal{F}_i$) and self-interstitial diffusion leads to the mutual attraction of the bubbles.

Since a repulsive interaction is required to stabilize the bubble lattice, we may conclude that formation of the latter in an isotropic crystal cannot be explained within the framework of the known interaction mechanisms.

4 DISLOCATION MECHANISM OF CAVITY INTERACTION

Following the energy considerations of Greenwood *et al.*[6] it can be easily shown that the condition for a bubble of radius R to produce an interstitial dislocation loop of radius r_l is

$$P \geq \frac{\mu b}{(1-\nu)2\pi r_c} \ln\left\{\frac{8r_c}{er_0}\right\} - \frac{2\gamma}{R}, \tag{10}$$

where r_0 is the dislocation core radius. If $r_l = R$, the condition (10) coincides with the criterion of Greenwood *et al.* But, apart from the energy considerations, one should take into account the shear stresses at the bubble surface, which punch the loop out. They vanish at the equatorial circle and reach the maximum value $3/4\,P$ at the circle of radius $R/\sqrt{2}$. Therefore, $R/\sqrt{2}$ is the most probable radius of punching loops.[7,8] Though the exact value of the loop radius is of no particular importance, we shall take here $r_l = R/\sqrt{2}$, whence the threshold value P is given by

$$P_0 = \frac{\mu b}{\sqrt{(2)}\pi(1-\nu)R} \ln\left\{\frac{8R}{\sqrt{(2)}er_0}\right\} - \frac{2\gamma}{R}. \tag{11}$$

The punching out of an interstitial loop leads to the bubble growth, but it grows preferentially in the direction of punched-out loop. This is easily shown in the case of a simple cubic lattice (Figure 1), but the effect is qualitatively independent of the matrix structure. An equilibrium shape of a sufficiently large bubble is usually spherical, and it is restored due to the surface diffusion, after punching out a loop, but around a new "gravity centre" of the bubble. Thus, the bubble, as a whole, moves in the direction of the punched-out loop.

The increase in bubble radius is given by

$$\Delta R = \sqrt[3]{\left(R^3 + \frac{3}{8}bR^2\right)} - R \approx \frac{b}{8}, \quad R \gg b. \tag{12}$$

A shift in bubble position can be estimated after choosing the reference point in the bubble centre before the loop-punching. Then the coordinate of the bubble "gravity centre" just after the loop-punching but before the relaxation to a spherical shape will give us the maximum shift in bubble position, ΔX (see Figure 1).

$$\Delta X = \frac{\frac{1}{2}\pi R^3 \cdot \frac{4\pi}{3} R^3 \cdot 0}{\frac{4\pi}{3} R^3 + \frac{1}{2}\pi b R^2} \approx \frac{3}{8} b. \tag{13}$$

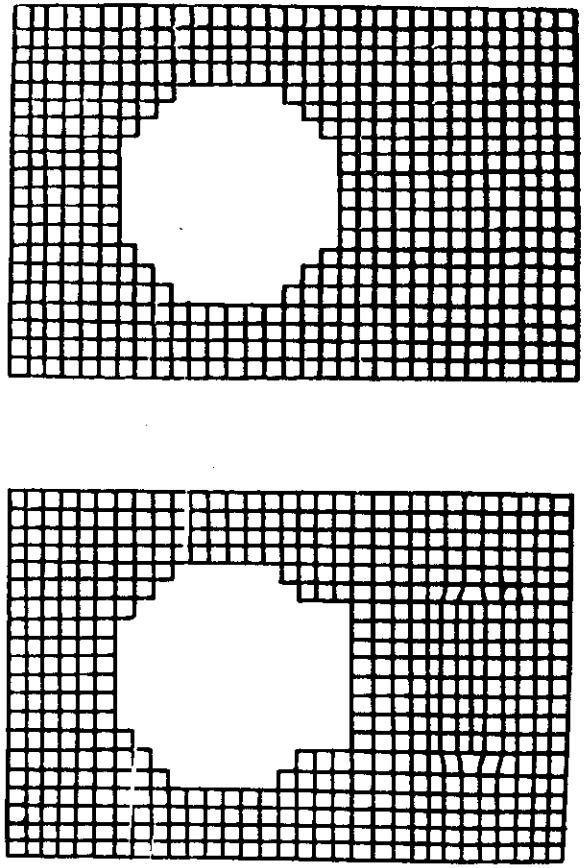

FIGURE 1 Illustration of consequences of loop-punching. A number of additional vacancies in the bubble due to loop-punching is equal to the number of interstitials in the loop. The "centre of gravity" of the bubble has been shifted by the value

$$\Delta x = \frac{(4\pi/3)R^3 \cdot 0 + \pi(R/2)^2 b \times R}{(4\pi/3)R^3 + \pi(R/2)^2 b} \approx \frac{3}{8} b.$$

This mechanism of bubble motion is somewhat analogous to the mechanism of bubble (or void) motion in the inhomogeneous diffusion field.[15] But in the case under consideration the fluxes of material are due to the dislocation loop punching and gliding, but not to the diffusive processes. This fact introduces two important differences between the "dislocation" and diffusion mechanisms of cavity motion.

First, the loop-punching is the athermal process and, hence, can lead to the bubble motion even at very low temperatures when the vacancy diffusion in the matrix is suppressed. Second, in real crystals loop-punching occurs along the glide directions which depend on the crystallographic structure of the host matrix. Therefore, dislocation mechanism of bubble motion is anisotropic even in elastically and diffusionally isotropic crystals. The last point is of particular importance because it is the clue to understanding macrodefect ordering processes in crystals.

The dislocation mechanism of bubble interaction is based on an elastic repulsion between loops that are already punched out and on a back stress exerted by the loops on the bubble. In consequence, further loop punching is prevented, when local shear stresses at the bubble surface fall below the threshold value $3/4\,P_0$. At a given gas pressure, $P \geq P_0$, an equilibrium number of loops at the line connecting two neighbouring bubbles is smaller than elsewhere, where the loop gliding is limited only by the Peierls force. It means that neighbouring bubbles grow preferentially in the opposite directions, i.e. effectively repulse each other.

Consider two bubbles of initial radii $R(0)$, with centres lying on the same glide direction and separated by the distance $2l(0)$ before the loop punching. When, at $P > P_0 \gg 2\gamma/R$, the loop punching is accomplished, two qualitatively differing distributions of loops are formed with linear loop densities d_j and d_0: d_j is the loop density between the bubbles, that act as stoppers for the loops; d_0 is the loop density along each of the $(n-1)$ "free" directions, where n is the total number of loop-punching directions. Let R and $2l$ be, respectively, the equilibrium radius and distance between bubbles. We shall be interested in the case where l is smaller than the distance between a bubble and the first loop punched out from it in a "free" direction l_0. In this case the bubble interaction is considerable and can be described by introducing an effective loop stopper between the bubbles at a distance l from any of them. In this approximation, the set of equations describing the equilibrium state of bubbles and loops is as follows.[25]

Equations for equilibrium loop densities describe the elastic equilibrium of each loop with the bubble and other loops in the same row:

$$\frac{bPR^4}{X^4} - \sigma_s b = -\frac{\mu b^2}{2\pi(1-\nu)} \int_{l_R'}^{l_0} \frac{d_0(\xi)}{\xi - X}\, d\xi, \tag{14}$$

$$d_0(l_0) = 0, \tag{15}$$

$$\frac{bPR^4}{X^4} - \sigma_s b = \frac{\mu b^2}{2\pi(1-\nu)} \int_{l_R'}^{l} \frac{d_j(\xi)}{\xi - X}\, d\xi, \tag{16}$$

where $PR^4 b/X^4$ is the repulsive force produced by the bubble per unit length of a loop lying at a distance X along the respective glide direction, $b\sigma_s$ is the Peierls force. Equation (15) determines the upper boundary of the loop distribution along a free direction, l_0; l_j and l_R' are the lower boundaries of loop rows in free and occupied directions, respectively. $\mu b^2/2\pi(1-\nu)(\xi - X)$ is the repulsive force between two loops in the same row separated by a distance $|X - \xi| \ll R'/2$. This expression has been chosen for estimation of resulting force acting upon a loop from its neighbours.[7]

The loop punching is stopped when the pulling-off force acting upon the loop at the bubble surface is compensated by the repulsion from the loops punched out earlier:

$$\frac{3}{4}\,b(P - P_0) = \frac{\mu b^2}{2\pi(1-\nu)} \int_{l_R}^{l_0} \frac{d_0(\xi)}{\xi - R}\,d\xi, \tag{17}$$

$$\frac{3}{4}\,b(P - P_0) = \frac{\mu b^2}{2\pi(1-\nu)} \int_{l_{R'}}^{l} \frac{d_l(\xi)}{\xi - R}\,d\xi. \tag{18}$$

The variation in bubble radius is equal to the total number of punching loops multiplied by the change due to punching-out one loop, $b/8$:

$$R - R(0) = \frac{b}{8}\left[(n-1)\int_{l_R}^{l_0} d_0(\xi)d\xi + \int_{l_{R'}}^{l} d_l(\xi)d\xi\right]. \tag{19}$$

Similarly, the variation in bubble position is equal to the difference between numbers of loops punched in opposite directions multiplied by the shift due to the punching of one loop, $3b/8$. Due to the symmetry of the problem, bubbles move only along the glide direction, which connects their centres, so that

$$l - l(0) = \frac{3b}{8}\left[\int_{l_R}^{l_0} d_0(\xi)d\xi - \int_{l_{R'}}^{l} d_l(\xi)d\xi\right]. \tag{20}$$

Thus, we have derived the complete set of equations, (14)–(20), that describes the dependence of equilibrium state of bubbles and loops on the gas pressure P and initial bubble parameters ($R(0)$ and $l(0)$). This set is analogous to that derived in Refs. 7 and 17 for voids under stress, where the motion of voids has not been taken into account.

One can see that the set has an approximate character, but even in this form it can be reduced only to a rather complicated set of algebraic transcendental equations (see Appendix). Here we consider the most interesting limits of short and long distances between the bubbles for $P \gg P_0 \geq \sigma_s$.

1) In the "short distance" approximation, $R \sim l_R \sim l_{R'} \sim l \ll l_0$ we find that

$$R - R(0) = -\frac{\pi(1-\nu)}{8\mu}\left[\left(\frac{3}{5}\right)^{7/8}\frac{5}{8}(n-1)P\sqrt{(Rl_0)} + P(l-R)\right], \tag{21}$$

$$l - l(0) = \frac{3\pi(1-\nu)}{8\mu}\left[\left(\frac{3}{5}\right)^{7/8}\frac{5}{8}P\sqrt{(Rl_0)} - P(l-R)\right]. \tag{22}$$

2) In the "long distance" approximation, $R \sim l_R \sim l_{R'} \ll l, l_0$, the result is given by

$$R - R(0) = -\frac{\pi(1-\nu)}{8\mu}\left[\frac{3}{5}\right]^{7/8}\frac{5}{8}P[(n-1)\sqrt{(Rl_0)} + \sqrt{(Rl)}]. \tag{23}$$

$$l - l(0) = \frac{3\pi(1-\nu)}{8\mu}\left(\frac{3}{5}\right)^{7/8}\frac{5}{8}P[\sqrt{(Rl_0)} - \sqrt{(Rl)}]. \tag{24}$$

As follows from Eqs. (21)–(24), the dislocation interaction results in repulsion of bubbles, since $l - l(0)$, and suppression of bubble growth, since the radius variation

$\Delta R \equiv R - R(0)$ of a "free" bubble ΔR_0 exceeds that of a bubble having k neighbours, ΔR_k:

$$\frac{\Delta R_k}{\Delta R_0} = \frac{n-k}{n} + \begin{cases} \dfrac{k}{n}\,\dfrac{8}{5}\left(\dfrac{5}{3}\right)^{7/8}\dfrac{l-R}{\sqrt{(l_0)R}}, & l \sim R, \\ \dfrac{k}{n}\sqrt{\dfrac{l}{l_0}}, & l \gg R. \end{cases} \tag{25}$$

In particular, if $k = n$ (which is the case in bubble lattice), the bubble growth is strongly suppressed and cannot be correctly described without account for the dislocation interaction.

If P varies with time, the distance between two bubbles and their radii also vary at the rates connected by the following equation:

$$\frac{dl}{dt} = \frac{3}{n-1}\left(\frac{dR}{dt}\right)[1 - F(l, l_0)], \tag{26}$$

where

$$F(l, l_0) = \begin{cases} \dfrac{n(l-R)}{(n-1)\dfrac{5}{8}\left(\dfrac{3}{5}\right)^{7/8}\sqrt{(Rl_0)} + l - R}, & l \sim R, \\ \dfrac{n\sqrt{l}}{(n-1)\sqrt{l_0} + \sqrt{l}}, & l \gg R, \end{cases} \tag{27}$$

$$l_0 = \left(\frac{3}{5}\right)^{7/4}\left(\frac{5P}{16\sigma_s}\right)^2 R. \tag{28}$$

One can see that l_0 is the range of the dislocation interaction of bubbles, so that interaction of bubbles separated by the distance $2l > 2l_0$ can be neglected.

Note that the dislocation interaction occurs not only between gas bubbles, but also between vacancy voids in solids under stress. Although above P was associated with the gas pressure, in the general case P is equal to the sum of gas pressure and the hydrostatic part of external stresses. In the absence of gas, the character of the external load determines the type of punching loops and the sign of dislocation interaction between vacancy voids. In particular, tensile stresses act in the same way as the gas pressure in bubbles. But compressive stresses result in punching of vacancy loops from voids, which causes a decrease both in void size and distance between them, i.e. the dislocation interaction becomes attractive. The set of equations (14)–(20) is valid in this case also after changing signs on the left-hand sides of Eqs. (19) and (20).

5 FORMATION AND SYMMETRY OF THE BUBBLE LATTICE

In this section we shall show how formation and symmetry of bubble lattice can be explained with the help of the dislocation, diffusive and elastic interaction mech-

anisms. For this purpose consider physical processes that occur in metals under irradiation with gas ions insoluble in the crystal matrix.

The formation of bubbles at low temperatures generally starts with the trapping of gas atoms in radiation-induced vacancies and is followed by their subsequent growth by athermal self-interstitial atom emission. Since the emission is isotropic, the bubbles at this stage are non-interactive, and, hence, are randomly distributed. At most a short-range isotropic order occurs as a result of competition for gas atoms, and the bubble distribution is similar to that in the "hard-sphere" gas model, as was argued by Stoneham.[3] The loop-punching from small bubbles is unfavourable because of a high threshold pressure $P_0 \sim \mu b/R$. As bubble size increases, P_0 drops and loop-punching begins at $P \geq P_0$, resulting in the dislocation repulsion between neighbouring bubbles lying along the same loop-punching directions at distances $2l \leq 2l_0$. Moreover, gas pressure falls owing to the bubble growth and the interstitial emission from bubbles is replaced by its absorption, and diffusive attraction between bubbles is thus developed. Thus, the evolution of bubble structure is determined at low temperatures, by the dislocation repulsion and diffusive mutual attraction of bubbles. Diffusive attraction at $l < l_0$ is substantially weaker than the dislocation repulsion, and is essential only for neighbouring bubbles which do not interact by dislocation mechanism. Such bubbles coalesce. At the same time, bubbles are stabilized equidistantly along the loop-punching directions by dislocation repulsion. In this way a random distribution of bubbles becomes unstable and transforms to an ordered one, wherein each bubble has its nearest neighbours along the loop-punching directions.

It is hardly possible to give a detailed description of the transient state, but it should be noted that motions over only small distances are needed for ordering because of some short-range order already present. Although bubbles cannot travel over distances exceeding their size, these small adjustments are sufficient for the lattice formation.

The most important property of the bubble lattice formed through this mechanism is the fact that symmetry and alignment of the lattice are determined by loop-punching directions of the host matrix. It is known that, as a rule, these are the matrix close-packed directions, along which the Burgers vector has minimal length. This explains why the bubble lattice copies the host matrix. For example, in bcc crystals each atom has 8 nearest neighbours along ⟨111⟩ directions, which are parallel to loop-punching directions.[4,5,19] Therefore, each bubble has, in the stable configuration, 8 nearest neighbours along the same ⟨111⟩ directions, i.e. the bubble lattice copies the host matrix, as shown in Figure 2.

In fcc crystals each atom has 12 nearest neighbours along ⟨110⟩ directions which coincide with loop-punching directions.[20,21] Consequently, an fcc bubble lattice must have the form of an fcc crystal.

Naturally, the type of bubble lattice would be different for any other set of loop-punching directions. For example, in the case of ⟨110⟩ loop-punching directions the simple cubic bubble lattice would arise, wherein each bubble would have 6 nearest neighbours.

We come to the conclusion that observed copying of the host matrix by the bubble lattice is due to coincidence of the loop-punching directions with close-packed directions of the matrix.

Our theory predicts that bubbles in the superlattice are surrounded by rows of interstitial loops aligned along the matrix close-packed directions. Unfortunately, the density of images in microcopies of such structures is too high to obtain easily

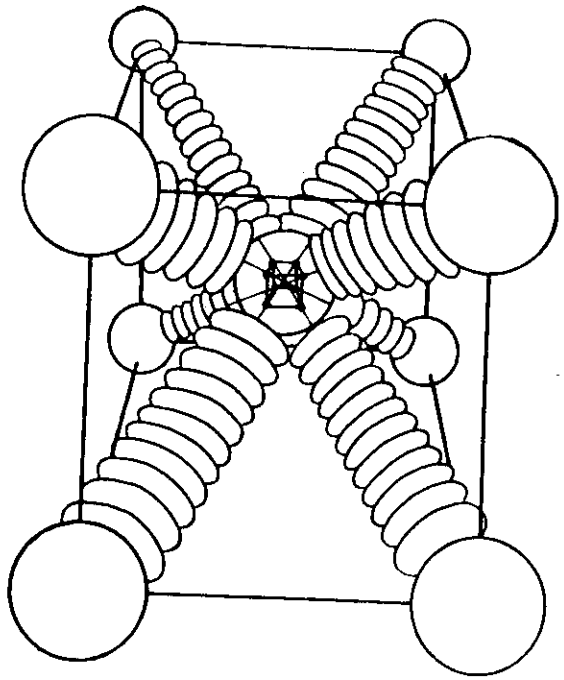

FIGURE 2 Elementary cell of the bubble lattice in bcc material. To compare with the host lattice, its elementary cell is depicted in the central bubble. Rows of loops are aligned along ⟨111⟩ directions, which coincide with close-packed directions of the host matrix.

detailed information on the dislocation arrangement.[4] But using a special helium filling technique, which limits the nucleation of helium bubbles to low values, direct evidence was obtained that bubbles in bcc Mo and V are surrounded by rows of loops aligned along ⟨111⟩ directions.[4,5]

6 REGION OF BUBBLE LATTICE FORMATION

It follows from the above that bubble ordering starts when the range of dislocation interaction l_0 exceeds a half of the average distance between bubbles l. At this stage the gas pressure only slightly exceeds P_0 because an excess pressure in non-interactive bubbles is easily released by loop-punching. Then, by Eq. (3.6)

$$\frac{l}{\hat{R}} \sim \frac{l_0}{\hat{R}} \sim \left(\frac{P_0}{\sigma_s}\right)^{1/3}. \tag{29}$$

Supposing that all the gas is contained in bubbles wherein there are k gas atoms per vacancy, we obtain a simple expression for swelling due to gas bubbles S:

$$S \approx \left(\frac{\hat{R}}{l}\right)^3 \approx \frac{G^g t}{k}, \tag{30}$$

where G^g is the gas implantation rate per atom.

At constant $P \sim P_0$ the gas density in bubble k is also constant which gives, by Eqs. (29) and (30), the following estimate of the threshold dose at which the ordering commences:

$$G^g t_0 \sim k\left(\frac{\sigma_s}{P_0}\right)^{3/2}. \tag{31}$$

Above we have described bubble ordering at low temperatures, whereas it is observed experimentally up to $0.35\,T_m$, when vacancy and interstitial fluxes are nearly equalized in a short time so that the diffusive attraction of bubbles disappears. It can be shown[22] that in this case the elastic attraction increasing with temperature substitutes for the diffusive one, and results in coalescence of "unfavourable" bubbles. Therefore, the necessary and sufficient condition for bubble ordering is the loop-punching resulting in the dislocation repulsion between bubbles. The loop-punching occurs if the increase in P due to absorption of gas atoms exceeds the decrease in P due to diffusive bubble growth. At high temperatures, the latter dominates, so that P does not reach the critical ordering value P_L and distribution of bubbles remains random.

As has been shown in Ref. 25, it is not the absorption of vacancies, but the thermal emission of self-interstitials that determines the upper temperature limit of bubble ordering T_{up} which is given by

$$T_{up} = \frac{E_i^m + E_i^f - P_L\Omega}{\ln[4\pi Z_{ip}\Lambda\hat{R}D_i^0 G^g(Z_{ip} + 2\Lambda\hat{R})]}, \tag{32}$$

where E_i^m and E_i^f are respectively the migration and formation of self-interstitial energies. The value P_L will be estimated below.

7 STABILITY CRITERIA AND PARAMETERS OF BUBBLE LATTICE

According to our scheme, the ordering is a result of both the dislocation repulsion and diffusion (or elastic) attraction between bubbles, operating simultaneously. Subsequently, however, the dislocation repulsion becomes dominant, because the diffusive attraction weakens with time due to a steady increase in the point defect recombination rate which diminishes self-interstitial flux to bubbles. In its turn, the elastic attraction between nearest bubbles in the superlattice is much weaker than the repulsion from loop rows. Thus, the question arises whether the dislocation repulsion alone can stabilize bubble lattice. To answer it, consider the imperfect superlattice wherein each bubble has n nearest neighbours at different distances $2l_j (j = 1, \ldots, n) \geq 2R$. An absence of "free" loop-punching directions leads to a substantial increase in the gas pressure. Consequently, the approximation (21), $P \gg P_0$, $l_j \sim R$, may be used for a mathematical description of the superlattice. Furthermore, the initial bubble radius $R(0)$ is small compared to R and may be neglected. And what is more, Eq. (21) was derived for two bubbles, each having $n-1$ free directions (the first term in brackets) and one occupied by another bubble (the second term in brackets). For the superlattice, obviously, the summation must be taken over all n directions occupied by neighbouring bubbles:

$$R = \frac{\pi(1-\nu)}{8\mu}\sum_{j=1}^{n} P(l_j - R). \tag{33}$$

After introducing the following notations

$$P^* \equiv \frac{8\mu}{\pi(1-\nu)n}, \quad l \equiv \frac{1}{n}\sum_{j=1}^{n} l_j, \tag{34}$$

the expression (33) takes the simple form:

$$R = \frac{Pl}{P + P^*}. \tag{35}$$

The change in l_j is proportional to the difference between numbers of loops punched out in opposite directions j and j', and is given by

$$l_j - l_j(0) = \frac{3P}{P^* n}(l_j - l_{j'}) \tag{36}$$

in the same approximation. It follows from this expression that bubble deviation from the position, symmetric with respect to any opposite neighbours, $\delta l \equiv l_j - l_{j'}$, decreases with an increase in gas pressure within the bubble:

$$\delta l = \frac{\delta l(0)}{1 + \dfrac{6P}{nP^*}}, \quad \delta l(0) \equiv l_j(0) - l_{j'}(0). \tag{37}$$

In other words, the bubble lattice is stable in the coordinate space, when P increases with time.

The radiation stability of the superlattice in the bubble size space is physically obvious owing to the fact that the gas pressure in smaller bubbles is higher than in larger ones:

$$P = P\left(\frac{3G^g t}{4\pi\Lambda\hat{R}R^2}\right), \tag{38}$$

where $P = P(k)$ is the monotonously increasing function of the gas density k. The bubble size, in its turn, is a monotonously increasing function of the gas pressure, Eq. (35). This leads to a decrease in the bubble size dispersion with time.

Thus, the dislocation interaction alone is sufficient to stabilize the bubble superlattice under ion irradiation.

By Eq. (35) the l/R ratio (where $2l$ is the distance between neighbouring bubbles in the superlattice) is dependent on the gas pressure and elastic constants of the material only:

$$\frac{l}{R} = 1 + \frac{P^*}{P}. \tag{39}$$

The number of loops punched out from a single bubble is equal to $8R/b$, so that the mean equilibrium distance between neighbouring loops is given by

$$\lambda = b\frac{nl}{8R} = b\frac{n}{8}\left(1 + \frac{P^*}{P}\right). \tag{40}$$

8 COMPARISON WITH EXPERIMENTAL DATA

Above we have explained the experimentally observed character of the bubble ordering and two main properties of the bubble lattice, namely its symmetry and stability. To calculate the l/R ratio, we need an equation of state for the gas in bubbles. We use the equation derived by Evans[22] for helium because it is sufficiently simple and proves to be in good agreement with experimental data:

$$P = P_1 \exp\left\{\left(\frac{k}{k_1}\right)^3\right\}, \tag{41}$$

where $P_1 = 4.85 \cdot 10^5$ dyne/cm^2; $k_1 = 1 \cdot 1.94 \cdot 10^{22}$.

Take the relation between the helium density k and the implantation dose D from Ref. 20:

$$k = \frac{0.53 \cdot f \cdot \alpha \cdot D}{\frac{3}{2}\sigma \cdot N \cdot \frac{4\pi}{3}R^3}, \tag{42}$$

where σ is the range straggling and f the fraction of the implantation dose D precipitated into visible bubbles; $f = \alpha\beta$ with α the helium retention coefficient and β the percentage of helium atoms precipitated into visible bubbles.

Substitution of (41) and (42) into (39) gives the dependence of l/R ratio on the implantation dose:

$$\frac{l}{R} = 1 + \frac{P^*}{P_1}\exp\left\{-\frac{\alpha\beta f D}{3\sigma\eta k_1}\left(\frac{l}{R}\right)^3\right\}, \tag{43}$$

where

$$\eta = \frac{4\pi}{3}N^3 = \begin{cases} 0.74 \text{ for fcc lattice,} \\ 0.68 \text{ for bcc lattice.} \end{cases}$$

The superlattice constant a_s is related to l by

$$a_s = \begin{cases} 2\sqrt{(2)}l, & \text{for fcc lattice,} \\ 4l/\sqrt{3}, & \text{for bcc lattice.} \end{cases} \tag{44}$$

Comparison of ratios a_s/R derived from experiments and calculated from Eqs. (43) and (44) is shown in Table I. Parameters of Eq. (43) are taken from references indicated in Table I. The value σ for 30 keV He^+ ion-irradiated molybdenum has not been reported in Ref. 14 and thus was chosen to be equal to that for 30 keV He ion-irradiated Cu. The parameter β has been reported to be within the range from 0.15 up to 0.55. In Ref. 20, β has been assumed to vary with dose in order to obtain an agreement with experimental data. But the dislocation interaction suppressing the bubble growth has not been taken into account in Ref. 20. We choose the intermediate value $\beta = 0.25$ for all doses, temperatures and materials considered. It can be seen from Table I that our calculations are in good agreement with experimental data, notably with that from Ref. 20.

TABLE I

Experimental and theoretical values of a_s/R. References are indicated in brackets

Material	Lattice type	T, °C	Dose, He^+/cm^2	σ, nm	α	Experimental a_s/R	Theoretical a_s/R
Ni	fcc	0	$5 \cdot 10^{16}$	18	1–0.8	6.8–8.9 [20]	7.2–7.5
Ni	fcc	0	$2 \cdot 10^{17}$	18	0.8–0.6	5.4–6.1 [20]	5.5–5.9
Ni	fcc	0	10^{18}	18	0.16–0.12	5.3–7.2 [20]	5.5–5.9
Ni	fcc	20	$4 \cdot 10^{17}$	56	1	6.1–7.1 [12]	5.8
Cu	fcc	20	$4 \cdot 10^{17}$	56	1	7.2–8.2 [12]	5.6
321 steel	fcc	20	$4 \cdot 10^{17}$	56	1	5.9–6.9 [12]	5.8
Mo	bcc	20	10^{17}	56	1	4.4–5 [14]	5.4
Mo	bcc	300	$2 \cdot 10^{17}$	56	1	3.7–4.3 [14]	4.3
Mo	bcc	700	$2 \cdot 10^{17}$	56	1	3.8–4.4 [14]	4.3

A good approximation for the l/R ratio according to both calculated and experimental data, is $l/R = 2$, which gives, through Eq. (40), the following estimate of λ, the mean distance between loops in a row:

$$\lambda = \begin{cases} 3b, & \text{for fcc lattice,} \\ 2b, & \text{for bcc lattice} \end{cases} \tag{45}$$

Substituting $l_0/R = 2$ into Eq. (39) we obtain $P \geq P^*$ in the superlattice. Thus, the critical ordering gas pressure P_L lies within the range $P_0 \leq P_L \leq P^*$, which is consistent with an estimate of P_L from Eq. (32). Substituting in Eq. (32) the experimental values $T_{\alpha\beta} \approx 0.35\,Tm$, and $G^\theta = 10^{-3}$ He$^+$/c,

$$NR = 10^{12}\,\mathrm{cm}^{-2} \ll \rho = NR \frac{16\pi R}{\sqrt{(2)b}},$$

$D_i^0 = 1$, $E_i^m + E_i^f = 3.5$ eV (in nickel[23]), 2.9 eV (in copper[23]), we obtain $P_L = 0.75\,P^*$ in nickel and $P_L = P^*$ in copper.

By Eq. (41) at $P = P^*$ helium density in bubbles is between 1 and 2 helium atoms per vacancy, which is in good agreement with experimental data: 2-3 helium atoms per vacancy.[4,13]

The threshold dose $G^\theta t_0$ at which the ordering commences, according to Eq. (30), is given by

$$Gt_0 = \frac{3\sigma k}{\nu f}\left(\frac{\sigma_s}{P_0}\right)^{3/4} = 1.2 \cdot 10^{17} - 3.8 \cdot 10^{18}\ \frac{\mathrm{He}^+}{\mathrm{cm}^2} \tag{46}$$

for σ_s lying within the range $10^{-4} < \sigma_s < 10^{-2}\,\mu$.

The experimental value $Gt_0 = 1\text{–}4 \cdot 10^{17}$ He$^+$/cm^2, confirms the calculations.

The following is worth noting about the bubble lattice behaviour in the absence of further gas deposition. Johnson and Mazey[24] found that the average bubble radius increased from 10 Å to 14 Å and the spacing from 70 Å to 90 Å during subsequent electron irradiation of Cu. The increase in spacing without disordering suggests that the superlattice expands as a whole, which is consistent with our conclusion that the dislocation repulsion between bubbles in the superlattice is dominant.

The loss of order during post-irradiation heating is also easy to explain. At high temperatures the gas pressure in bubbles falls due to diffusion growth, which, by Eq. (37), results in an increase in bubble deviations from the perfect superlattice sites.

9 SUMMARY

1) A new mechanism of interaction of cavities is proposed, which is based on dislocation loop-punching induced by either internal or external pressure.

2) The main peculiarity of the dislocation interaction is its rigid relation to the crystallographic structure of material, namely, it arises only between cavities lying along the same loop punching directions, which are determined by the type of host matrix.

3) Tensile stresses and gas pressure in cavities result in the dislocation repulsion between growing cavities, whereas compressive stresses cause shrinkage and attraction between cavities by the dislocation mechanism.

4) Bubble ordering commences as a result of dislocation repulsion and diffusion attraction between bubbles operating simultaneously.

5) Symmetry and alignment of the bubble lattice are determined by orientations of loop-punching directions. Observed copying of the host lattice by the bubble lattice is due to the coincidence of the loop-punching directions with close-packed directions of the matrix.

6) The dislocation interaction between bubbles becomes dominant when the ordering is accomplished and provides stability of the bubble lattice, if gas pressure increases with time.

7) Our calculations of the σ_s/R ratio, dose and temperature region of bubble lattice formation are in good agreement with the experimental data available.

In conclusion, we should like to note that a rigorous description of various physical processes involved in the formation of bubble lattice has not been attempted here. Our aim was rather to evolve a consistent physical picture of the ordering and to attract attention to the dislocation interaction mechanism, which, in our opinion, plays an important role in the evolution of microstructure in solids.

Appendix

Equations (14)-(16) are of the Cauchy type and have exact solutions[7,17]:

$$d_0(x) = -\frac{2(1-\nu)}{\pi\mu b}\sqrt{\left(\frac{x-l_R}{l_0-x}\right)}\int_{l_R}^{l_0}\sqrt{\left(\frac{l_0-\xi}{\xi-l_R}\right)}\frac{P\dfrac{R^4}{\xi^4}-\sigma_s}{\xi-x}\,d\xi, \tag{A1}$$

$$d_0(l_0) = 0, \tag{A2}$$

$$d_i(x) = -\frac{2(1-\nu)}{\pi\mu b}\sqrt{\left(\frac{x-l_R'}{l-x}\right)}\int_{l_R'}^{l}\sqrt{\left(\frac{l-\xi}{\xi-l_R'}\right)}\frac{P\dfrac{R^4}{\xi^4}-\sigma_s}{\xi-x}\,d\xi \tag{A3}$$

Condition $d_0(l_0) = 0$, as was shown in Ref. 17, is identical to the integral condition

$$\int_{l_R}^{l_0}\frac{PR^4/\xi^4-\sigma_s}{\sqrt{[(l_0-\xi)(\xi-l_R)]}}\,d\xi = 0,$$

which is necessary for the existence of the solution to the Cauchy equation with a free boundary. Physically, (A2) means that loop density at the free boundary vanishes, which determines l_0, the free path length of the first punched loop. Evaluating the integral over ξ one obtains d_0 and d_i and condition (A2) in the form:

$$d_0(x) = -\frac{2\pi(1-\nu)\sigma_s}{\mu b}[\psi(x, l_0, l_R) - 1]\sqrt{\left(\frac{x-l_R}{l_0-x}\right)}. \tag{A4}$$

$$B(l_0, l_R) = \sigma_s. \tag{A5}$$

$$d_j(x) = \frac{2\pi(1-\nu)}{\mu b}\int_{l_R'}^{l} [\psi(x, l, l_R')B(l, l_R') - \sigma_s]\sqrt{\left(\frac{x-l_R'}{l-x}\right)}, \tag{A6}$$

with the following notations:

$$B(l_0, l_R) = \frac{PR^4}{\sqrt{(l_0 l_R)}}\left(\frac{l_0+l_R}{2l_0 l_R}\right)^3\left(1+\frac{3}{2a^2(l_0, l_R)}\right),$$

$$a(l_0, l_R) = \frac{l_0+l_R}{l_0-l_R},$$

$$\psi(x, l_0, l_R) = \frac{l_0}{x} + \frac{l_0-x}{x^2}\left(\frac{2l_0 l_R}{l_0+l_R}\right)\frac{1+0.5a^{-2}}{1+1.5a^{-2}} + \frac{l_0-x}{x^3}\left(\frac{2l_0 l_R}{l_0+l_R}\right)^2\frac{1}{1+1.5a^{-2}} + \frac{l_0-x}{x^4}\left(\frac{2l_0 l_R}{l_0+l_R}\right)^3\frac{1}{1+1.5a^{-2}},$$

Substituting d_0 and d_j into Eqs. (17)–(20) and using Eq. (A5), reduces the set of integral equations to the set of transcendental ones, which describes the equilibrium state of bubbles and loops after the loop-punching is over.

$$\frac{3}{4}(P-P_0) = B(l_0, l_R)T(l_0, l_R) - \sigma_s\left[1-\sqrt{\left(\frac{l_R(l_R-R)}{l_0(l_0-R)}\right)}\right], \tag{A7}$$

$$\frac{3}{4}(P-P_i) = B(l, l_R')T(l, l_R') - \sigma_s\left[1-\sqrt{\left(\frac{l_R'(l_R'-R)}{l(l-R)}\right)}\right], \tag{A8}$$

$$R-R(0) = \frac{\pi(1-\nu)(n-1)}{4\mu}\sigma_s\left[\chi(l_0, l_R) - \frac{l_0-l_R}{2}\right] + \frac{\pi(1-\nu)}{4\mu}\left[B(l, l_R')\chi(l, l_R') - \sigma_s\frac{l-l_R'}{2}\right], \tag{A9}$$

$$l-l(0) = \frac{3\pi(1-\nu)}{4\mu}\left[B(l_0, l_R)\chi(l_0, l_R) - B(l, l_R')\chi(l, l_R') + \frac{\sigma_s}{2}(l+l_R-l_R'-l_0)\right], \tag{A10}$$

$$l(l_0, l_R) = \sigma_s, \tag{A11}$$

$$\chi(l_0, l_R) = l_0\left\{1-\sqrt{y}+\frac{2l_R}{l_0+l_R}\frac{1}{1+1.5a^{-2}}\left[\left(1+\frac{1}{2a^2}\right)\left(\frac{l_0+l_R}{2\sqrt{(l_0 l_R)}}-1\right)+\frac{l_0-l_R}{2\sqrt{(l_0 l_R)}(l_0+l_R)}\right]\right\}, \tag{A12}$$

$$T(l_0, l_R) = \frac{l_0}{l_R}\sqrt{y}\left[1-\sqrt{\left(\frac{1-R/l_R}{1-R/l_0}\right)}\right] + \frac{2l_0^2 l_R}{(l_0+l_R)^2}\frac{1+0.5a^{-2}}{1+1.5a^{-2}}\left\{\sqrt{y}\left(1-\frac{R}{2l_R}-\frac{R}{2l_0}\right)-\sqrt{\left[\left(1-\frac{R}{l_0}\right)\left(y-\frac{R}{l_0}\right)\right]}\right\} + \left(\frac{2l_0 l_R}{l_0+l_R}\right)^2\frac{l_0}{(1+1.5a^{-2})R^3}\left\{\sqrt{y}\left(1-\frac{R}{2l_R}-\frac{R}{2l_0}\right)-\frac{R^2(1-y)^2}{16l_0^2 y\sqrt{y}}-\sqrt{\left[\left(1-\frac{R}{l_0}\right)\left(y-\frac{R}{l_0}\right)\right]}\right\} + \left(\frac{2l_0 l_R}{l_0+l_R}\right)^3\frac{l_0}{(1+1.5a^{-2})R^4}\left\{\left[\sqrt{y}\left(1-\frac{R}{2l_R}-\frac{R}{2l_0}\right) - \frac{R^2(1-y)^2}{16l_0^2 y\sqrt{y}}\left(2+\frac{R}{l_0}-\frac{R}{l_R}\right)-\sqrt{\left[\left(1-\frac{R}{l_0}\right)\left(y-\frac{R}{l_0}\right)\right]}\right\}, \tag{A13}$$

$$y(l_0, l_R) = \frac{l_R}{l_0}. \tag{A14}$$

This set determines l_0, l_R, R, and l. It is rather complicated but takes the simple form in the limits of interest (see the text).

Here we write down the general expression for the velocity of the relative motion of two bubbles if P varies slowly with time:

$$\frac{dl}{dt} = \frac{3}{n-1}\left(\frac{dR}{dt}\right)[1-F(l, l_0)],$$

$$F(l, l_0) = \frac{n[B(l, l_R')\chi(l, l_R') - \sigma_s(l-l_R')/2]}{(n-1)\sigma_s\left[\chi(l_0, l_R) - \frac{l_0-l_R}{2}\right] + B(l, l_R')\chi(l, l_R') - \frac{l-l_R'}{2}\sigma_s}. \tag{A15}$$

$$l_0 \approx \begin{cases} \left(\frac{3}{5}\right)^{7/4}\left(\frac{5}{16}\right)^2\frac{P^2}{\sigma_s^2}R, & P \gg P_0, \\ \left(\frac{P_0}{\sigma_s}\right)^{1/4}R, & \sigma_s \ll P-P_0 \ll P_0. \end{cases} \tag{A16}$$

$$F(l, l_0) \to \begin{cases} 1, & l \to l_0, \\ 0, & l \to R. \end{cases} \tag{A17}$$

REFERENCES

1. K. Krishan, *Rad. Effects* **66**, 121 (1982).
2. A. M. Stoneham, *Harwell Voids Symposium*, P. S. Nelson (Ed.) (AERE—R 7934, 1974), p. 319.
3. A. M. Stoneham, in *Proc. Int. Conf. on Fundamental Aspects of Radiation Damage in Metals*, vol. 2, M. T. Robinson and R. W. Young, Jr. (Eds.) (CONF—751006, 1975), p. 222.
4. J. H. Evans, A. Van Veen, and L. M. Caspers, *Rad. Effects* **78**, 105 (1983).

5. W. Jager, R. Lässer, T. Shober, and G. J. Thomas, *Rad. Effects* **78**, 165 (1983).
6. G. W. Greenwood, A. J. E. Foreman, and D. E. Rummer, *J. Nucl. Mater.* **4**, 305 (1959).
7. V. V. Slezov, *Fiz. Tverd. Tela* **16**, 785 (1974).
8. Ya. E. Geguzin and V. G. Kononenko, *Fiz. Tverd. Tela* **15**, 3550 (1973).
9. J. R. Willis and R. Bullough, *J. Nucl. Mater.* **32**, 76 (1969).
10. L. A. Maksimov and A. I. Ryazanov, *Fiz. Met. Metalloved* **41**, 284 (1976).
11. S. L. Sass and B. L. Eyre, *Phil. Mag.* **27**, 1447 (1973).
12. P. B. Johnson and D. J. Mazey, *J. Nucl. Mater.* **93,94**, 721 (1980).
13. P. B. Johnson, D. J. Mazey, and J. H. Evans, *Rad. Effects* **78**, 147 (1983).
14. D. J. Mazey, B. L. Eyre, J. H. Evans, S. K. Erents, and G. M. McCracken, *J. Nucl. Mater.* **69**, 145 (1977).
15. Ya. E. Geguzin and M. A. Krivoglaz, *Dvizhenie makroskopicheskikh vklyuchenij v tverdykh telakh* (in Russian) (M.: Metallurgiya, 1971).
16. V. I. Dubinko and V. V. Slezov, *Fiz. Met. Metalloved.* **53**, 456 (1982).
17. V. V. Slezov and V. V. Yanovskij, *Fiz. Met. Metalloved.* **44**, 698 (1977).
18. J. Hirth and I. Lothe, *Teoriya dislokatsij* (M.: Atomizdat, 1972).
19. B. L. Eyre and R. Bullough, *Phil. Mag.* **12**, 31 (1965).
20. N. Van Swygenhoven, G. Knuyt, J. Vanoppen, and L. M. Stals, *J. Nucl. Mater.* **114**, 157 (1982).
21. K. Shiraishi, A. Hishinuma, and Y. Katano, *Rad. Effects* **21**, 161 (1974).
22. J. H. Evans, *J. Nucl. Mater.* **66**, 129 (1977).
23. A. N. Orlov, *Vvedenie v teoriyu defektov v kristallakh.* (in Russian) (M.: Visshaya Shkola, 1983).
24. B. P. Johnson and D. J. Mazey, *Nature* **281**, 359 (1979).
25. V. I. Dubinko, V. V. Slezov, A. V. Tur, and V. V. Yanovskij, Preprint. Space Research Institute N 922, Moscow (1984).

Proc. Int. Conf. on Radiation Materials Science, Alushta, 1990, v. 2, Kharkov-1990, pp. 149-155.

UDC 539.2I9.2

DISLOCATION MECHANISM OF THE VOID ORDERING AND SATURATION OF IRRADIATION SWELLING OF METALS

V.I.Dubinko

(Kharkov Institute of Physics & Technology)

1. Introduction

Previous papers by Dubinko et al.[1-3] have proposed that the formation of void and bubble lattices in irradiated metals is a consequence of the dislocation mechanism of interaction between cavities, which is based upon their absorption (voids) or emission (buttles) of self-interstitial dislocation loops (SIA-loops). The void lattice forms at elevated temperatures mainly in bcc metals, while the bubble lattice forms at low gas implantation temperatures irrespectively of the crystal structure. In the present paper a brief summary of the dislocation model of cavity ordering will be given and besides, bubbles will be shown to punch out perfect SIA-loops even at elevated temperatures due to their bias for SIA absorption. At such conditions vacancy voids, if present, absorb SIA-loops created at bubbles which results in saturation of swelling, observed in st. steel containing helium[4,5].

2. Diffusion and dislocation mechanisms of cavity growth and interaction

Generally, a cavity can emit or absorb point defects (PD) and dislocation loops depending on its bias factor, gas pressure and irradiation conditions. Variation of the cavity size and position in the matrix is determined by the total balance of PD and loop fluxes. The growth rate of a cavity of radius R can be expressed as:

$$\frac{dR}{dt} = \left(\frac{dR}{dt}\right)_D + \left(\frac{dR}{dt}\right)_L , \qquad (1)$$

where indexes D and L designate the diffusion and the loop-induced constituents, respectively. In the diffusion-limited approximation with account of the image and modulus interaction of PD with a cavity $(dR/dt)_D$ is given by [6,7]:

$$\left(\frac{dR}{dt}\right)_D = Z_v^c \mathcal{D}_v \left(\bar{C}_v - C_v^R\right) - Z_i^c \mathcal{D}_i \left(\bar{C}_i - C_i^R\right), \qquad (2)$$

$$Z_n^c = 1 + \frac{\alpha_n}{R} - \frac{3}{56}\frac{\alpha_n^\mu}{T}\left(\frac{p^*}{\mu}\right)^2, \quad \alpha_n \approx 6\left(\frac{\Omega_n}{\omega}\right)^{\frac{2}{3}}, \qquad (3)$$

$$C_n^R = C_n^e \exp\left(\pm \frac{\omega}{T} p^*\right), \quad p^* = p - \frac{2\gamma}{R}, \qquad (4)$$

where D_n is the PD diffusivity (index n=v designates vacancies, while n=i-SIA), C_n^e the equilibrium concentration of PD in a perfect crystal, $\bar{C}_n$ the mean PD concentration under irradiation, Ω_n, α_n^μ are the PD relaxation volume and shear polarizability, respectively, w is the atomic volume, b the interatomic spacing, μ the shear modulus, γ the surface energy, p is the gas pressure within a cavity, T the temperature.

The loop-induced part $(dR/dt)_L$ is determined by the type, size r_L and flux J_L of loops absorbed or emitted by a cavity. Overpressurized gas bubbles ($p^* > \mu b/R \gg 2\gamma/R$) punch out SIA-loops while voids ($p^* \approx -2\gamma/R$) absorb SIA-loops from the matrix. Accordingly we have

$$\left(\frac{dR}{dt}\right)_L = -J_L \frac{r_L b}{4R^2}. \qquad (5)$$

A cavity produces the force $F_L(x)$ per unit length of a SIA-loop lying at a distance x from its centre in the direction parallel to the loop Burgers vector, where

$$F_L(x) = \frac{3}{2}\frac{b r_L R^3 x}{(r_L^2 + x^2)^{5/2}} p^* \xrightarrow[x \gg r_L]{} \frac{3}{2}\frac{b r_L R^3 p^*}{x^4}. \qquad (6)$$

The condition $F_L(\ell_p) = b\sigma_p$ determines maximum distance of absorption or emission of a loop, where σ_p is the Peierls stress. Obviously, neighbouring cavities lying along the same loop-gliding direction at a distance $2\ell < 2\ell_p$ punch out or absorb a smaller number of loops than isolated cavities ($\ell > \ell_p$) do. This dislocation-induced interaction influences both the size and position of cavities and may lead under specific conditions to ordering of the cavities.

3. The void ordering [2].

The maximum distance of the loop-void annihilation $\ell_p|_{r_L = R} = (3\gamma/\sigma_p)^{\frac{1}{2}} R^{\frac{1}{2}}$ determines the length of the loop-supply-cylinders (LSCs) which are extended from the void along loop gliding directions.

As long as voids are small they are randomly distributed untill the range of dislocation interaction $\ell_p \sim R^{3/4}$ is less than half the mean void spacing $\bar{l}$. At this stage the mean void size $\bar{R}$ grows along with $\bar{\ell}_p(\bar{R})$. At $\bar{\ell}_p \geq \bar{\ell}$ LSCs overlep meaning that no perfect SIA-loop can escape getting into the voids. If all SIA-loops are perfect and their coalescence is the main source of new crystal planes and straight dislocations, then at $\bar{\ell}_p \geq \bar{\ell}$ the void swelling should saturate. The mean void size $\bar{R}_s$ corresponding to the swelling saturation is given by the condition $\ell_p(\bar{R}_s) = \bar{\ell}$:

$$\bar{R}_s = \left(\frac{\sigma_p}{3\gamma}\right)^{\frac{1}{3}}\left(\frac{3}{4\pi N}\right)^{\frac{4}{9}}, \qquad N = \frac{3}{4\pi\bar{\ell}^3}. \qquad (7)$$

At this stage the fate of each void depends on its size and location of the void's immediate neighbours. Voids that have neighbours along gliding directions (locally ordered voids [2]) absorb less SIA-loops as compared to locally random voids which have immediate neighbours outside glide directions. On the other hand, larger voids ($R > \bar{R}$) absorb more extra vacancies than smaller ones ($R < \bar{R}$) due to the diffusion-induced coarsening [7]. At $N > N_\rho$ the diffusion coarsening was shown to dominate resulting in the growth of larger voids at the expence of shrinkage of smaller ones, where

$$N_\rho = \frac{\rho_\omega \delta_d}{4\pi(\alpha_{iv}\Delta^* + \alpha\mathcal{D}^*)}, \quad \alpha_{iv} = \alpha_i - \alpha_v, \quad \alpha = \frac{2\gamma\omega}{T}, \qquad (8)$$

$\rho_d \delta_d = \rho_L \delta_L + \rho_S \delta_S$, $\mathcal{D}^* = \mathcal{D}_v C_v^e + \mathcal{D}_i C_i^e$, $\Delta^* = \mathcal{D}_{iv}(\bar{C}_v - \bar{C}_v^e)$, $\bar{C}_v^e$ is the mean concentration of thermal PD, δ_L, δ_S are the bias factors of loops and straight dislocations, respectively, while ρ_L, ρ_S are their densities, $\rho_d = \rho_L + \rho_S$.

At $N < N_\rho$ the diffusion coarsening is too week to make the voids shrink, and a random stationary state is established, where voids of different sizes and positions neither grow nor shrink.

At $N = N_\rho$ only locally random voids shrink, while locally ordered ones form stable lattice with close-packed directions lying along loop gliding directions. In cubic crystals, where the loops glide along the matrix close-packed directions, the void lattice copies the host lattice. In hcp crystals a planar or linear void ordering takes place depending on whether SIA-loops glide within the basal plane or along the c-direction [3]. The void lattice

parameters are fully determined by the eqs. $\bar{R} = R_g$ and $N = N_\rho$.

The necessary condition of the void ordering and saturation of their growth is the nucleation of perfect SIA-loops which is characteristic of bcc metals where the stacking fault energy γ_f is high. In fcc metals SIA -loops are usually faulted due to low γ_f. Accordingly, in fcc metals voids grow larger and do not form lattices as readily as in bcc metals. However, there is a possibility of the perfect SIA-loop formation at the gas bubbles which does not depend on the crystal structure. It will be discussed in the following section.

4. Bimodal size distribution of cavities

The diffusion growth rate $(dR/dt)_D$ can be expressed with account of the rate equations [7] in the following form:

$$\left(\frac{dR}{dt}\right)_D = \frac{\Delta^*}{R}\left(\bar{\delta} - \delta_c(R)\right) + \frac{\mathcal{D}_v}{R}\left(\bar{C}_v^e - C_v^R\right) + \frac{\mathcal{D}_i}{R}\left(C_i^R - \bar{C}_i^e\right), \qquad (9)$$

$$\delta_c(R) = \frac{\alpha_{iv}}{R} + \frac{\alpha_\mu}{\mu^2}\rho^{*2}, \quad \alpha_\mu = -\frac{3}{56T}\left(\alpha_i^\mu - \alpha_v^\mu\right) > 0, \qquad (10)$$

$$\bar{\delta} = \frac{\rho_d \delta_d + 4\pi\int_0^\infty f(R) R \delta_c dR}{\rho_d + 4\pi\int_0^\infty f(R) dR}, \quad \bar{C}_n^e = \frac{C_n^e \rho_d + 4\pi\int_0^\infty f(R) R C_n^R dR}{\rho_d + 4\pi\int_0^\infty f(R) dR} \qquad (11)$$

where $\delta_c(R) = Z_i^C - Z_v^C$ is the bias factor of a cavity, $f(R)$ the size distribution function of cavities, $\bar{\delta}$ is the mean bias factor of the dislocation and cavity ensemble. The first term in eq. (9) corresponds to the radiation-induced PD fluxes, while the last two describe thermally activated PD fluxes, which are directed so that to diminish the over-or-underpressure p*. Without irradiation $(\Delta^* = 0)(dR/dt)_D \to 0$ at $p^* \to 0$ and this equilibrium is stable. However, under irradiation the equilibrium gas bubbles lose stability which can be seen from eqs. (9)-(11) at p*=o (See Fig.1)

$$\left(\frac{dR}{dt}\right)_D = \frac{\Delta^* \alpha_{iv}}{R}\left(\frac{1}{R_c} - \frac{1}{R}\right), \quad R_c = \frac{\bar{R} + R_c^\circ N_\rho^*/N}{1 + N_\rho^*/N}, \qquad (12)$$

$$N_\rho^* = N_\rho|_{\Delta^*=0} = \frac{\rho_d \delta_d}{4\pi\alpha_{iv}}, \quad R_c^\circ = R_c|_{N=0} = \frac{\alpha_{iv}}{\delta_d} \qquad (13)$$

Bubbles with $R > R_c$ start to grow whereas those with $R < R_c$ to shrink. The critical radius R_c is determined by the N/N_ρ^* ratio. If $N/N_\rho^* \gg 1$, then $R_c \simeq \bar{R}$ meaning that division of bubbles into

growing and shrinking ones is inevitable. The former convert into voids ($p^* \to -2\gamma/R$) while the latter became overpressurized, and hence their preference towards SIA increases, which in its turn enhances the bubble shrinkage. As a result of this radiation-induced collapse p* increases up to the limit p^*_{MAX} determined by stress relief mechanisms such as the ejection of gas atoms, SIA's or SIA-loops [8]. In the case of helium bubbles the first mechanism can be neglected, the second one requires $p^* \sim \mu/2$ and the last one operates at $p^* \sim \mu b/R$. The stable bubble size R_g is determined by the number of gas atoms for a bubble n_g, the gas law $p(n_g, R_g)$ and the loop-punching condition $p^*(n_g) = \mu b/R_g < \mu/2$, whence the minimum loop-punching bubble size $R_g^{min} = 2b$. On the other hand, the R_g^{max} is determined by the equality of bias factors of bubbles and loops: $\delta_c(R^{max}) = \delta_i = \alpha_{iv}/b$ [7] whence $R_g^{max} \simeq (\alpha_\mu b^3/\alpha_{iv}) b = 12b$, if $\alpha_\mu = 10^2$ [6], $\alpha_{iv} = 0{,}6b$ [7].

The minimum concentration of gas atoms in matrix C_g which is necessary for the generation of SIA loops by bubbles can be estimated taking into account that: 1) $N > N_\rho^* \sim 10^{22} \ldots 10^{23} m^{-3}$; 2) $n_g > n_g(R_g^{min}) \sim 10^2$ whence $C_g > N n_g/\omega > 10^{-4}$.

As the irradiation temperature increases, thermally activated PD fluxes became important in stabilization of bubbles against the radiation-induced shrinkage and growth. This stabilization is the core of the conventional approach to the bubble-void transition (see, e.g., ref. [9]) which, however, does not take into account the size and pressure dependence of the cavity bias for SIA. The thermal stabilization may be neglected below T_{up} which is determined by the comparison of maximum thermally activated PD fluxes (at $p^*_{MAX} \sim \mu b/R_g$) with radiation-induced PD fluxes into a cavity:

$$\Delta^* \delta_c > \mathcal{D}_v C_v^e + \mathcal{D}_i C_i^e \exp\left(\frac{p^* \omega}{T}\right),$$

$$\delta_c^{min} = \frac{\alpha_{iv}}{R_g^*}, \quad \delta_c^{max} = \frac{\alpha_{iv}}{R_g} + \alpha_\mu \left(\frac{b}{R_g}\right)^2 \qquad (14)$$

where R_g^* is the size of an equilibrium bubble (p*=o). See Fig.2.

At $R_g \simeq R_g^{max} = 12b$ $p^* \omega = \mu\omega/12 = E_i^f/6$ [8] Since E_i^f, the SIA formation energy is substantially higher than the self-diffusion energy E_v^s, thermal SIA may be neglected. Taking $E_v^s = 2{,}85$ eV (as in nickel) we obtain T = 560°C - 630°C for reactor irradiation

(dose rate $\sim 10^{-6}$ dpa/s) and T=740°C-850°C for ion irradiation (10^{-3} dpa/s). Below this temperature overpressurized bubbles become the sources of perfect SIA-loops irrespectively of the crystal structure. Vacancy voids, if present, absorb SIA-loops which compensate for their diffusive growth resulting in a saturation of swelling, as has been observed experimentally [4,5] (Fig.5).

5. The bubble ordering [1].

At low temperature implantation of gas ions voids do not form while the bubble number density reaches as high as $10^{25} m^{-3}$. Consequently, SIA-loop punched out by the bubbles interact loading to the repulsion between neighbouring bubbles lying along the same loop gliding directions. As a result of the dislocation repulsion and an isotropic diffusive attraction (due to absorption of SIA) a random distribution of bubbles became unstable and transforms into a lattice which copies the host lattice in cubic crystals. The dislocation interaction results also in the increase of the loop-punching pressure up to $P^*_{MAX} = 8\mu/\pi(1-\nu)z$, where z is the coordination number, ν the Poisson ratio. This P^*_{MAX} is close to the pressure for SIA emission, $\mu/2$ [8], which limits the upper temperature of bubble ordering $T_{up} \sim 0{,}35\, T_m$, where T is the melting point.

6. Conclusions

The most important prediction of the present theory is that perfect SIA-loops must form under irradiation in order to induce the cavity ordering and swelling saturation. Apart from the explanation of higher swelling resistance of bcc as compared to fcc metals, this offers a recomendation for improvement of fcc metals by adding impurities stimulating the formation of perfect SIA-loops. This paper has considered the effect of gas impurities and proposed a mechanism of SIA-loop generation by the bubbles due to their bias for SIA's, which can operate at elevated temperatures irrespectively of the crystal structure. This mechanism may induce swelling saturation in such fcc metals as st. steel [4,5], where SIA-loops are faulted without gas and swelling rate is high. At the same time, the large bias of bubbles for SIA's δ_g enhances the diffusive stability of voids increasing the critical void density N_p, necessary for the ordering by the value $N_g \bar{R}_g \bar{\delta}_g / \alpha_{iv} \sim 10 N_g$. Here N_g is the bubble density which is usually higher than the void density. Thus, a possibility of the gas-induced void ordering needs futher experimental investigations.

REFERENCES

1. Dubinko V.I., Slezov V.V., Tur A.V., Yanovski V.V. The theory of gas bubble lattice // Radiat. Eff. 1986. Vol. 100. P.85-104.
2. Dubinko V.I., Tur A.V., Turkin A.A., Yanovski V.V. A mechanism of formation and properties of the void lattice in metals under irradiation // J.Nucl.Mater. 1989. Vol. 161. P.57-71.
3. Dubinko V.I. Influence of dislocation structure and impurities on the void lattice formation in irradiated crystals (in Russian): Preprint KhFTI 89-51. Kharkov: KhFTI AN UkrSSR, 1989.-8c.
4. Farrell K. Experimental effects of helium on cavity formation during irradiation - a review // Radiat. Effects. 1980. Vol.53. P. 175-194.
5. Loomis B.A. Comparison of swelling for structural materials on neutron and ion irradiation // J.Nucl.Mater. 1986. Vol. 141-143. P. 690-694.
6. Wolfer W.G., Ashkin M. Stress-induced diffusion of point defects to spherical sinks // J.Appl.Phys. 1975. Vol. 46. P. 547-557.
7. Dubinko V.I., Ostapchuk P.N., Slezov V.V. Theory of radiation-induced and thermal coarsening of the void ensemble in metals under irradiation // J.Nucl.Mater. 1989. Vol. P.239-260.
8. Donnelly S.E. The density and pressure of helium in bubbles in implanted metals: a critical review // Radiat. Eff. 1985. Vol. 90. P. 1-47.
9. Hishinuma A., Mansur L.K. Critical radius for bias-driven swelling: a further analysis and its application to bimodal cavity size distributions // J.Nucl. Mater. 1983. Vol. 118. P.91-98.

DIFFUSION STABILITY: $T > T_{up}$

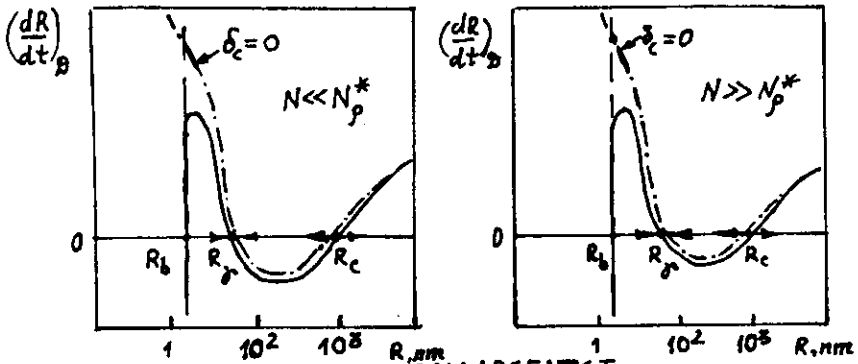

DIFFUSION COLLAPSE: $T < T_{up}$

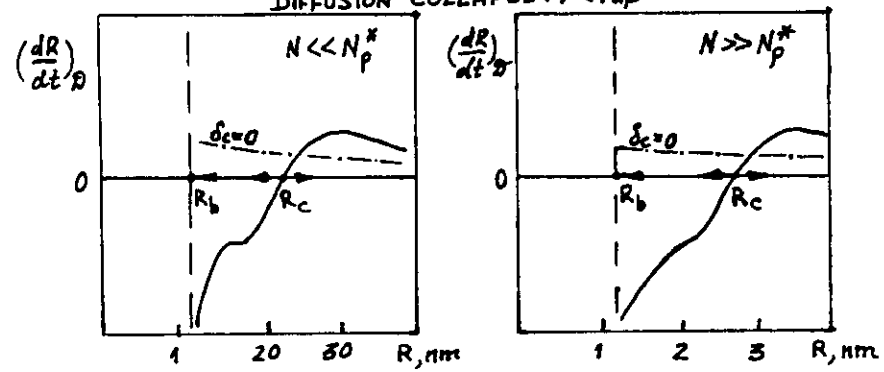

Fig.1: $\Omega_i = 1.2\omega$, $\delta_d = 10^{-2}$, $\alpha_i^M = -150\,eV$, $\alpha_v^M = -15\,eV$, $\Omega_v = -0.5\omega$, $a_{lv} = 1.8\,Å$, $\boxed{n = 10^3}$, $\rho_d = 10^{14}\,m^{-2}$, $\Rightarrow N_\rho^* = 5\cdot 10^{21}\,m^{-3}$

T_{up}: $\delta_c \Delta^* = D_v C_v^e(T_{up})$; $\delta_c = \frac{a_{lv}}{R} + \alpha_\mu \left(\frac{\rho^*}{\mu}\right)^2$

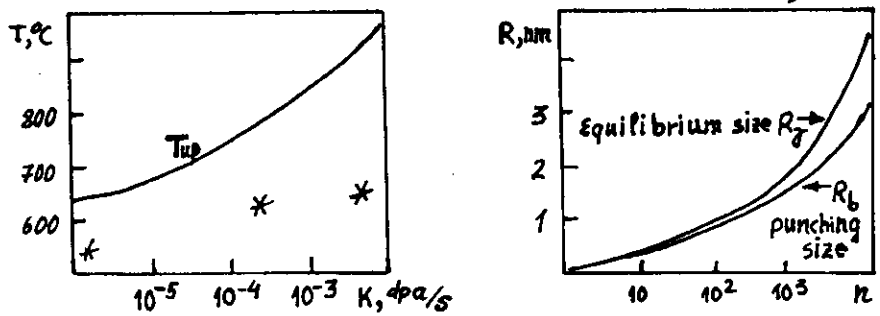

Fig.2: $R_\gamma = 2\gamma/P(n, R_\gamma)$; $R_b = (2\gamma + \mu b)/P(n, R_b)$

n = number of gas atoms in a bubble

GAS-INDUSED (He) SWELLING SATURATION

EXPERIMENT [Pacan, Farrell, J. Nucl. Mater. 85/86 (1979) 677]

316 St. Steel, Irradiated with 4 MeV Ni ions

$K = 6\cdot 10^{-3}\,\frac{dpa}{s}$, $T = 625\,°C$

- ● No Helium
- ■ Coimplanted: $\frac{He}{dpa} = 20$
- ◆ 625 °C PREIMPLANTED 1400 appm He
- ◇ 25 °C

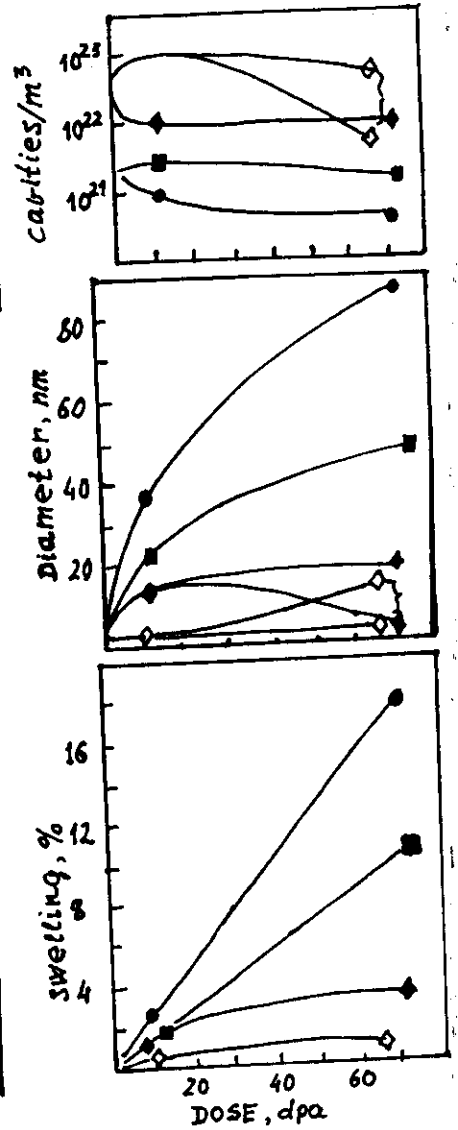

Fig.3

THEORY

$\frac{dR}{dt} = \left(\frac{dR}{dt}\right)_D - \left|\left(\frac{dR}{dt}\right)_L\right| \to 0$

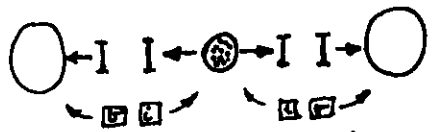

DISLOCATION–DIFFUSION EQUILIBRIUM

$V(t) \to V_S = \frac{Z}{2}\left(\frac{b}{R_b}\right)^{\frac{3}{\mu}}\left(\frac{\sigma_p}{3\mu}\right)^{\frac{1}{\mu}} \sim 6\%, \quad \frac{R_b^2 N_b}{R_v^2 N_v} \gg 1$

$\to V_S = V_b^{\frac{1}{2}}(Z/20)^{1/2} \sim 1\%, \quad \frac{R_b^2 N_b}{R_v^2 N_v} \ll 1$

CRITERION FOR VOID ORDERING

$N_v \geq N_\rho^* + N_b \frac{R_b \delta_b}{a_{lv}} > N_b$

N_v – VOID DENSITY

N_b – BUBBLE DENSITY